

NAS 12-15

N68-34881

AMT File Copy

NASA CR-86047

SPACE CABIN ATMOSPHERE CONTAMINANT
DETECTION TECHNIQUES

Douglas Report SM-48446-F

By Norman R. Byrd, Ph. D.

July 1968

Distribution of this report is provided in the interest of information exchange and should not be construed as endorsement by NASA of the material presented. Responsibility for the contents resides in the organization that prepared it.

Prepared under Contract No. NAS 12-15 by
ASTROPOWER LABORATORY
DOUGLAS MISSILE & SPACE SYSTEMS DIVISION
MCDONNELL DOUGLAS CORPORATION
Newport Beach, California

Electronics Research Center
NATIONAL AERONAUTICS AND SPACE ADMINISTRATION

NASA CR-86047

SPACE CABIN ATMOSPHERE CONTAMINANT
DETECTION TECHNIQUES

Douglas Report SM-48446-F

By Norman R. Byrd, Ph. D.

July 1968

Prepared under Contract No. NAS 12-15 by
ASTROPOWER LABORATORY
DOUGLAS MISSILE & SPACE SYSTEMS DIVISION
MCDONNELL DOUGLAS CORPORATION
Newport Beach, California

Electronics Research Center
NATIONAL AERONAUTICS AND SPACE ADMINISTRATION

FOREWORD

This is a final report prepared under Contract NAS 12-15, covering the period 15 June 1965 to 31 January 1968. The work on this contract was carried out at Astropower Laboratory, Advance Systems and Technology, Missile and Space Systems Division, Douglas Aircraft Company, under the supervision of Dr. N. R. Byrd, Section Chief, Organic-polymers and Principal Investigator on this program. Experiments and analysis were conducted at various times by Dr. T. L. Mackay, Dr. S. Asunmaa, F. D. Kleist, R. Silvestri, G. I. Chandler, and J. L. Lister. Additional assistance was provided by R. Zuleeg. The program was administered by the NASA Electronics Research Center, Cambridge, Massachusetts, with Dr. W. Leavitt as Project Scientist.

This report was prepared by Dr. N. R. Byrd, with the assistance of G. I. Chandler and R. Zuleeg.

CONTENTS

Section 1	INTRODUCTION AND SUMMARY	1
Section 2	TECHNICAL DISCUSSION	9
	2.1 Literature Survey	9
	2.1.1 Adsorption Methods	10
	2.1.2 Mass Spectrometry	11
	2.1.3 Spectrophotometry	11
	2.1.4 Electronic Systems	12
	2.1.5 Miscellaneous Systems	15
	2.2 Solid State Gas Detector	16
	2.2.1 Organic Semiconductors	16
	2.2.1.1 Preparation of Poly(phenylacetylene)	18
	2.2.1.2 Derivatives of Poly(phenylacetylene)	27
	2.2.2 Electrical Properties of Polymers	35
	2.2.2.1 Effect of Structure and Morphology on Electrical Characteristics of Polymers	35
	2.2.2.2 Electrical Response of Organic Semiconductors	42
	2.2.2.3 Charge-Transfer Complexes	56
	2.2.3 Sensor Preparation	63
	2.2.4 Gas-Polymer Interactions	68
	2.2.4.1 Finter Electrode Geometry	68
	2.2.4.2 Lock-and Key Electrode Geometry	89
	2.3 Combination Organic-Inorganic Devices	138
	2.4 Prototype Portable Gas Detector	148
Section 3	CONCLUSIONS	157
	REFERENCES	159
Appendix A	CHARGE-TRANSFER COMPLEXES	

- Appendix B ORGANIC SEMICONDUCTORS WITH PN-JUNCTION
 DEVICES FOR GAS DETECTION
- Appendix C ANALYSIS OF THE PORTABLE GAS DETECTOR
- Appendix D NEW TECHNOLOGY DISCLOSURE – GAS
 DETECTION DEVICES

FIGURES

1	Reaction Sequence Used in Preparation of Some Poly(phenylacetylenes)	17
2	Random Dehydrohalogenation	20
3	Poly(phenylacetylene) from Dehydrohalogenation of Poly(alpha chlorostyrene) with Zinc Chloride	22
4	Poly(phenylacetylene) from Thermal Polymerization of Phenylacetylene)	23
5	Infrared Spectrum of Chromatographed AlCl ₃ -Catalyzed Solution-Polymerized Poly(phenylacetylene)	24
6	Relation of Lim η_{sp}/C to Softening Point of Poly(phenylacetylene)	25
7	pH Titration Curve of Poly(p-aminophenylacetylene) Prepared by Lithium Chloride Dehydrohalogenation of Poly(alpha chloro p-nitrostyrene)	30
8	pH Titration Curve of Poly(p-aminophenylacetylene) From Polymerization of Phenylacetylene Followed by Nitration and Reduction	31
9	pH Titration Curve of Poly(p-aminophenylacetylene) Prepared by ZnCl ₂ Dehydrohalogenation of Poly(alpha chloro-styrene) Followed by Nitration and Reduction	32
10	pH Titration Curve of Poly(p-aminophenylacetylene) Prepared Six Months Previously by Lithium Chloride Dehydrohalogenation Technique	33
11	pH Titration Curve for Aniline	34
12	Electron Photomicrograph of Poly(phenylacetylene) Illustrating a Distinct Preferred Molecular Lamination	37
13	Poly(phenylacetylene) Low Energy State Trans Configuration (Highest Alignment)	38
14	Poly(phenylacetylene) Trans Configuration Unaligned Form	39
15	Poly(phenylacetylene) Low Energy State Cis Configuration (Highest Alignment)	40
16	Poly(phenylacetylene) Cis Configuration Unaligned Form	41
17	Current-Voltage Plot on Pressed Pellet of Poly(p-formamidophenylacetylene)	45

18	Conductivity – Temperature Plots on Pressed Pellets	46
19	Poly(p-nitrophenylacetylene), Aligned and Unaligned, and the Conduction Path for Each	48
20	Poly(p-formamidophenylacetylene), Aligned and Unaligned, and the Conduction Path for Each	51
21	Conduction Path Through Hydrogen-Bonded Proteins	52
22	Current-Voltage Plot of Poly(p-nitrophenylacetylene) Film	57
23	UV – Visible Spectrum of Poly(phenylacetylene) (0.0025% in CHCl ₃)	58
24	UV – Visible Spectra of Charge-Transfer Complexes (I ₂ Plus Poly(phenylacetylene))	60
25	Maximum Absorbance (Δ) Versus Mole Ratio of I ₂ /Poly(phenylacetylene)	61
26	Resistivity Versus Composition of I ₂ /Poly(phenylacetylene)	62
27	Finger Electrode Gas Detector	64
28	Major Breakdown Point of Sensor	65
29	Minor Breakdown Point of Sensor	66
30	Five Mil Spacing, 43-Line Lock-and-Key Electrode on a Glass Surface	69
31	Bell-jar for Maintaining Constant Atmosphere on Sensor	70
32	Constant Atmosphere Chamber Connected to Vacuum Rack	71
33	Measurement Circuitry	72
34	Response of Poly(phenylacetylene) to 16 mm Ammonia (in Dark); Top Electrode (-0.5 Volt)	73
35	Response of Poly(phenylacetylene) to 80 mm Ammonia (in Dark); Top Electrode (-0.5 Volt)	74
36	Response of Polyphenylacetylene to 760 mm Ammonia (in Dark); Top Electrode (-0.5 Volt)	75
37	Energy Bands at Surface with Adsorbed Molecules Giving (a) Donor Type Surface States, and (b) Acceptor Type Surface States	78
38	Response of Poly(phenylacetylene) Finger Electrode Sensor to 19 mm Oxygen (in Dark); Top Electrode (-0.5 Volt)	79
39	Response of Sensors to 13 mm Ammonia (in Dark)	81
40	Response of Sensor to 16 mm CO ₂ (in Dark); Top Electrode (-0.5 Volt)	82
41	Response of Poly(phenylacetylene) Sensor to 16 mm Trimethylamine (in Dark); Top Electrode (-0.5 Volt)	86
42	Response of Poly(phenylacetylene) Sensor to 25 mm Triethylamine (in Dark); Top Electrode (-0.5 Volt)	87

43	Profile of 5 Mil Sensor Coated with 4% Solution of Poly(p-nitrophenylacetylene)	90
44	Schematic Drawing of Measurement Circuitry	93
45	Modified Vacuum Chamber for Gas Measurements	95
46	Variation in Polymer Film Thickness with Decreasing Solution Concentration	96
47	Current/Thickness Correlation for Poly(p-nitrophenylacetylene) on the 5 Mil Sensor	97
48	Relative Plot of Effect of NH ₃ on Varying Film Thicknesses on the 5 Mil Sensor	99
49	Ratio of I_p/I_{p_0} at Varying Pressures of NH ₃ for Different Film Thicknesses	
50	I_p/I_{p_0} Ratio for 4% Film on 5 Mil Sensor at High Pressure Level	101
51	Rise Time Versus Pressure for 4% Poly(p-nitrophenylacetylene) Film on 5 Mil Sensor	103
52	Reversal Time Upon Evacuation After Exposure to NH ₃ for a 4% Film on 5 Mil Sensor	104
53	Strip Chart Recording of 4% Poly(p-nitrophenylacetylene) Film Exposed to Different Pressures of NH ₃	105
54	Various Pathways and Equilibria for a Gas/Polymer Interaction	106
55	Reproduction of Strip Chart Recording of 1% Nitro Polymer Film on 1 Mil Sensor Exposed to Different Pressures of NH ₃	107
56	Poly(phenylacetylene) with Different Pressures of Ammonia	110
57	Response of Poly(phenylacetylene) to Various Gases	111
58	Response of Poly(p-nitrophenylacetylene) to Gases Below 100 Torr	113
59	Response of Poly(p-nitrophenylacetylene) to Gases Above One Torr	114
60	Response of Poly(p-formamidophenylacetylene) to Gases	115
61	Response of Poly(p-aminophenylacetylene) to Various Gases	116
62	Resonance Form of Polarized Poly(p-aminophenylacetylene)	117
63	Effect of Pressure on Conductance of Poly(p-aminophenylacetylene)	122
64	Effect Pressure in Conductance of Poly(p-nitrophenylacetylene)	123
65	Relation Between Permittivity and Conductance of Poly(p-aminophenylacetylene)	128

66	Relation Between Permittivity and Conductance of Poly(p-formamidophenylacetylene) in Presence of NH ₃	129
67	Relation Between Permittivity and Conductance of Poly(p-formamidophenylacetylene) in Presence of (CH ₃) ₃ N	130
68	MOS Device but with a Thin Aluminum Gate	139
69	MOS-FET (P ⁺ -n-p ⁺) Device Used Without the Gate	141
70	Circuitry for Measuring the Characteristics of P ⁺ N P ⁺	142
71	Gas Response of Uncoated Planar p ⁺ n p ⁺ Device	143
72	Leakage Current Through p ⁺ n p ⁺ Silicon Sensor Coated With Poly(phenylacetylene) and Exposed to Ammonia Followed by Regeneration and Re-exposure (9 Volts Applied)	144
73	The p ⁺ n p ⁺ Sensor Coated with Poly(phenylacetylene) and Left Standing for One Week	145
74	Response of a p ⁺ n p ⁺ Sensor Coated with Poly(p-nitrophenylacetylene) and Exposed to Ammonia	147
75	Astropower Gas Detector Showing Detector Chamber and Attached Electronic Gear	149
76	Detector Chamber with Sensors Partly Pulled Out	150
77	Detector Sensors	151
78	Circuit Schematic, Portable Gas Detector Differential Amplifier	152
79	Block Diagram of Differential Gas Detector (Prototype)	153

TABLES

I	Relation of Softening Point, $\text{Lim } \eta_{sp}/C$ and Molecular Weight of Poly(phenylacetylene)	26
II	Activation Energies for D. C. Electrical Conductivities	44
III	Dielectric Properties of Poly(phenylacetylene)	55
IV	Effect of I_2 on Resistivity of Poly(phenylacetylene)	59
V	Response of Poly(p-nitrophenylacetylene) to 13 mm of SO_2 with 75 mv Applied Potential	84
VI	Response of Poly(p-aminophenylacetylene) to 13 mm of SO_2 with 75 mv Applied Potential	85
VII	Gas Effects on Poly(phenylacetylene) (Amphoteric)	131
VIII	Gas Effects on Poly(p-nitrophenylacetylene) (Acid-Type)	132
IX	Gas Effects on Poly(p-formamidophenylacetylene) Weak Acid-Type)	133
X	Gas Effects on Poly(p-aminophenylacetylene) (Basic-Type)	134
XI	Qualitative Response Behavior of Astropower Gas Detector	155

Section 1
INTRODUCTION AND SUMMARY

In any closed ecological system, such as a spacecraft, there is the constant problem of atmosphere control. This is normally effected by metering the vital gases into the system and exhausting the spent atmosphere through a series of scrubbers, adsorbents and other means for waste product removal. The calculations governing the removal of an expected quantity of waste product by a known amount of adsorbent would adequately control the enclosed atmosphere, barring any major build-up of a particular contaminant, or of any unforeseen decomposition product. What is needed, however, is a sensor capable of monitoring a closed atmosphere and rapidly detecting the presence of any contaminant build-up. For this purpose, a solid-state sensor has been considered as the most feasible system. It is low weight, has no moving parts, and requires very little power for its operation.

The use of polymeric, film-forming organic semiconductors, e. g., substituted polyacetylenes (poly(phenylacetylene) and its derivatives), have been suggested as film materials for the solid-state sensor. They can act as semiconductors, and can also be chemically modified so that the effects of substituents on their conduction and complexing capability can be observed. To date, no synthetic polymeric organic semiconductor has been proposed elsewhere for use as a contaminant detector, although reference has been made to the use of plastics, paper and other organics as a surface for adsorption of vapors, and which undergo a change in surface potential. The basic principle upon which the polymeric organic semiconductors depend for their detection capability is a relationship between their electronegativity, their adsorption characteristics, their complexing behavior, and a change in some one of their electrical parameters.

The objectives of this program were (1) to obtain or synthesize a number of promising semiconducting polymers having as high a degree of unsaturation as possible and having film-forming capability, (2) to prepare single sensors with candidate polymers, (3) to evaluate and establish parameters related to the sensor preparation and response characteristics to various contaminants under dark and light conditions and at low and high temperatures, and (4) to analyze the characteristics of a multiple sensor that may be used in a space cabin.

During the first phase of the project, performed during the period 1 July 1965 to 31 December 1966, the program was concerned with five major problem areas. Initially, there was a literature search to determine the state-of-the-art on gas detection techniques and to point out which areas to explore in depth. This was followed by the synthetic portion of the program, where the effort was to prepare and characterize the necessary polymers for use in the sensors. Another problem was actually preparing the sensor, while a related area of interest was the electrical response characteristics of these sensors. Finally, the gas-detection capability of the sensor was considered.

In the literature survey, which was a continuing effort throughout the program, a number of systems presently under consideration by various investigators were detailed and evaluated. There appears to be no other system developed to date that is as versatile as gas chromatography in conjunction with mass spectrometry. However, due to possible limitations of these systems for long-term use on a spacecraft, such as maintenance, need for a carrier gas and control of temperature and pressure, it is necessary to consider developing an alternative method which would have none of the limitations of the systems now in use. For this reason, the organic semiconductor solid state sensor was proposed.

Since the polymers (poly(phenylacetylene) and some of its derivatives) necessary for this study were not readily available materials, a major aspect of the program has been to synthesize and characterize the polymers that were used as the detectors for the various gases tested. Although the preparation of poly(phenylacetylene) has been reported in the literature, the majority of the methods described resulted in low molecular weight materials, i. e. ,

700-1000. Since molecular weight, as well as extent of conjugation, was critical, two methods were investigated that could presumably result in a high molecular weight polymer: (1) preparation of poly(alpha chlorostyrene) followed by dehydrohalogenation, and (2) AlCl_3 -catalyzed polymerization of phenylacetylene.

It subsequently developed that the dehydrohalogenation procedure also resulted in a lowered molecular weight, i. e., 1800-2000. This is somewhat higher, though, than the polymer obtained by the literature reported methods. Furthermore, although the dehydrohalogenation technique gave a polymer that was only 87-90% conjugated (due to a statistical removal of HCl), its electrical properties appeared to be little different from that which was obtained by the AlCl_3 -catalyzed polymerization of phenylacetylene. Therefore, since the latter method gave a poorer yield of polymer, albeit somewhat higher in molecular weight, i. e., 3000, the higher yield of polymer by the dehydrohalogenation method governed its choice as the preparative method for poly(phenylacetylene).

The adopted procedure was to chlorinate polystyrene and dehydrohalogenate the product with zinc chloride in nitrobenzene solution. When the infrared spectrum of this material was compared to that obtained from the polymerization of phenylacetylene (either thermally or aluminum chloride-catalyzed), they were found to be almost identical except for an increased absorption at 3.45μ (the aliphatic CH_2 group) found in the dehydrohalogenated polymer. This fits in with the concept of random dehydrohalogenation. In addition, a correlation was obtained between the intrinsic viscosity (molecular weight) and the softening point so that it was only necessary to determine the softening point in order to get an approximate idea of the molecular weight.

In the course of preparing the various derivatives, it was found that the nitro derivative could be obtained by two routes. Poly(alpha chlorostyrene) could be nitrated followed by dehydrohalogenation with LiCl in dimethylformamide (DMF) solution or poly(phenylacetylene) could be nitrated. In either case, the products were essentially identical. In view of the limited solubility of the poly(p-nitrophenylacetylene) in many solvents, it was found necessary to effect its reduction with stannous chloride and HCl in DMF solution. However,

a byproduct in this reaction was the formation of formyl chloride which readily formylates the poly(p-aminophenylacetylene). The first product obtained in the reduction process, then, was the poly(p-formamidophenylacetylene). This was effectively hydrolyzed in concentrated HCl to the poly(p-aminophenylacetylene).

Titration of the poly(p-aminophenylacetylene) established the fact that the amino polymer was a weaker base than aniline. In addition, it proved that one amino group per phenyl moiety existed in the polymer.

If we assume that the thermodynamically stable form is the trans configuration, and construct a model of the polymer, we find its structure to be in what we call the trans-aligned form. However, if we consider free rotation possible around the single bonds, and rotate every other phenyl group with its double-bonded backbone almost 120° , we get the trans-unaligned form. In the trans-aligned form, the phenyl groups are 90° out of coplanarity with the backbone and there is presumed to be little resonance interaction between the backbone and the appendage. In the trans-unaligned form, though, the phenyl group can rotate about 45° into coplanarity. If, therefore, an amino group were on the para position of the phenyl group, there could be proton interactions between the hydrogen of one amino group and the nitrogen of the next to sterically interfere with an incoming proton from an acidic species. Alternatively, if the polymer were in the trans-unaligned form and some resonance interaction were possible between the appendage and the backbone, there would be a positive charge on the nitrogen, thereby decreasing the base strength.

An electron micrograph of poly(phenylacetylene) indicates a distinctly preferred molecular lamination. This orientation is most likely if we have a trans polymer which is extended on a rod-like shape and close packing can occur between the chains. Thus, we have further evidence for the trans structure.

Subsequent to the preparation of the various polymers, a study was made of their electrical properties. On a priori basis, it would be expected that poly(p-aminophenylacetylene) would be most conductive since it could feed

electrons into the backbone; that poly(p-nitrophenylacetylene) and poly(p-formamidophenylacetylene) would be least conductive since they would be carrier traps (electron-withdrawing) and that poly(phenylacetylene) would be intermediate. In actuality, poly(phenylacetylene) had the highest room temperature resistivity (above 10^{17} ohm-cm) while the formamido polymer appeared to have the lowest resistivity (about 3×10^{16} ohm-cm) and the nitro and amino polymer were slightly poorer, but close to this value.

If we consider the possibility of the polymer being in the trans-aligned configuration, it can be seen that the phenyl groups in poly(phenylacetylene) are very closely aligned and that it is possible for a large amount of pi-pi overlap to occur between the benzene rings. Thus, if a carrier got into the phenyl group through some interaction between the appendage and the backbone, it would be in a very low energy well.

In the case of the nitro and formamido polymer, however, a different situation prevails. If we assume the normal polarization tendency of the nitro moiety, we can get either an electron unpairing and redistribution or an ionic charge distribution. It is possible that interchain interactions can occur such that hopping or tunneling from chain-to-chain is enhanced, thereby reducing the number of high impedance regions. Thus, the number of trapping sites would be minimal, and charge migration can occur along the backbone, as well as through the appendage. In the formamido case, an additional conduction mechanism is operative, namely, through a hydrogen bonded amide linkage analogous to that presumed for proteins and other polyamides.

Since the operating principle upon which the gas detector developed in this program involved an interaction between electron donor gases and electron acceptor polymers, and conversely, i. e., analogous to the formation of charge-transfer complexes, an investigation was undertaken to study the actual interaction of an electron acceptor with a conjugated polymer. The intent was to get some basic information of spectral response versus electrical conductivity for these complexes. In view of the fact that gas/polymer complexes could not be prepared and isolated for study, a model system consisting of varying mixtures of poly(phenylacetylene) (as electron donor)

and iodine (acceptor) were prepared and the ultraviolet absorption spectra obtained. It was observed that the spectrum for pure poly(phenylacetylene) had no maximum above 250 $m\mu$. With the I_2 present, two new peaks appeared (295 $m\mu$ and 360 $m\mu$), and the ratio of 2:1 I_2 /poly(phenylacetylene) gave the greatest absorbance. In addition, the resistivity of the polymer decreased sharply with increasing I_2 concentration and a ratio of 1.5-2/1 of I_2 /poly(phenylacetylene) leveled off to a constant value of about ten orders of magnitude lower than the zero mole concentration of iodine.

Once the polymers, and some of their basic electrical properties were evaluated, the actual development of the gas detector followed. The most critical problem was the preparation of the sensor. This involved the combination of the polymer with the proper electrode geometry and electrical circuitry so that a maximum response, in the shortest time and with the greatest sensitivity could be accomplished. The ultimate design was the lock-and-key geometry, i. e., the two electrodes on one surface, and a coating of the polymer over them. This gave the greatest surface area exposure to the incoming gas as well as exposing the gas most directly to the field between the electrodes.

Another matter of concern was whether a bulk or surface interaction was being observed in this system. By using poly(p-nitrophenylacetylene) as the representative polymer and varying the film thickness above the electrodes from as much as 0.24 microns (2400 Å) to as low as a monomolecular film, it was found that the lowest resistivity (at 10^{-4} torr) was obtained with the monomolecular film and that it increased sharply to a value over two orders of magnitude higher for the 0.24 micron film. However, in the presence of ammonia, the most responsive (greatest sensitivity) was the 0.24 micron film and the least responsive was the monomolecular film. Thus, it was unequivocally proven that the gas/polymer interaction was a bulk, not a surface, effect.

The response/recovery times and sensitivity of the system was also of concern. It was readily shown that the response and recovery time, after exposure to a gas, was in the order of seconds, and the sensitivity was shown

to be excellent, i. e. , showing varying degrees of responsiveness when a poly(p-nitrophenylacetylene) coated sensor was exposed to partial pressures of ammonia ranging from 5 microns to 500 microns. In each instance, the response spike was proportional to the partial pressure of gas introduced.

The next question resolved was the degree of specificity inherent in the system of polymers under evaluation. As was anticipated, under vacuum conditions, the nitro polymer (an electron seeking substance) showed the greatest response to varying partial pressures of ammonia (to as low as 2 ppm); and little response with BF_3 (an electron seeking gas) the poly(p-aminophenylacetylene) (an electron donating polymer) had an experimental sensitivity of 8 ppm with BF_3 and a projected sensitivity in the ppb range, while poly(phenylacetylene) had less sensitivity to either of these gases. This was excellent substantiation of the concept of electronegativity with respect to gas/polymer interactions, i. e. , the more electron donating gas showing the greater response with an electronegative polymer, and vice versa.

On the basis of these data, a prototype portable bisensor device was developed that utilized the nitro polymer as one sensor and the amino polymer as the other. When exposed to laboratory atmosphere conditions and introducing either NH_3 or SO_2 , separately, into the atmosphere, the device responded accurately. The nitro polymer only responded to the NH_3 from a lower level of 5-10 ppm and the amino polymer only to the SO_2 from a lower level of 10-20 ppm. In no instance, out of about 20 reliability tests, did the other sensor respond to the gas to which it was not sensitive. Thus, this first prototype gas detector proved the feasibility of ultimately developing a portable detector applicable to other gases.

Finally, in seeking out a method of ultimately being able to reduce the hardware to a microminiaturized package, it was found that a combination of the organic polymer with an MOS (metal-oxide-silicon field effect transistor) device resulted in good response characteristics. Thus, treating an MOS device with ammonia resulted in a passivated system. However, on first coating the device with the nitro polymer and then exposing it to NH_3 , there resulted a rapid and reversible response behavior; and it only required 9

volts to operate as opposed to the 100 volts needed for the polymer on the lock-and-key metal electrode system. Thus, the original concept of developing a solid state gas detector based upon electronegativity effects has been proven feasible. Further exploitation of this combination organic/inorganic device concept should result in a smaller and more sensitive system.

Section 2 TECHNICAL DISCUSSION

2.1 LITERATURE SURVEY

A first, and continuing, task in the performance of this program has been a literature survey to evaluate proposed methods of gas detection, and to determine which may be used as a point of departure for the experimental program. The detection of minute traces of substances has become of major importance to a number of different government agencies, and around the early part of July 1964, a Conference on Surface Effects in Detection was held in Washington, D. C. Most of the newly evolved detection principles were based on surface effects. ⁽¹⁾

Freons, human flatus and respiratory products, structural material degradation, electrical insulation decomposition, and a host of other gaseous contaminants could become serious problems in a closed ecological system if these are not adequately removed. ⁽²⁾ Although the method of removing them is not germane to the program, a knowledge of their presence and composition is. In this regard their detection has to be considered. As sensitive and adequate as the human olfactory sense is for many odoriferous materials, it can become insensitive by a massive array of many odors assailing it simultaneously. In addition, it is of little value for nonodorous substances, such as Freons, CO₂ and others. Therefore, one must rely on adjuncts to the human capability.

In culling the literature for information pertinent to detection devices, it was found that the systems being evaluated were in the following categories:

- a. Adsorption methods
- b. Mass spectroscopy as a detection technique
- c. Spectrophotometry for detection purposes

- d. Electronic systems used as detectors
- e. Miscellaneous detection devices

An earlier report⁽³⁾ had a lengthy discussion of each of the above methods. However, for the sake of review, the following will be a brief explanation of each category.

2.1.1 Adsorption Methods

Gas chromatography has been considered the most versatile tool for monitoring a space cabin atmosphere.⁽⁴⁻¹²⁾ However, in exploring the advantages and disadvantages of the gas chromatograph, it is well to consider that the detector in a gas chromatograph is probably the most critical component of the system. The detector determines which gases can be analyzed, and also determines the sensitivity of the instrument. The best detector developed, to date, is the Karmen glow discharge unit which is sensitive to the light permanent gases as well as the organics, and is potentially capable of analyzing all gases that are separated in the column. The gas chromatograph, therefore, appears to have many advantages; namely, low weight and small size (15 to 20 lb and 1000 in.³), low power requirement (one watt),⁽⁵⁾ and versatility and sensitivity, if the Karmen glow discharge unit proves feasible.⁽¹¹⁾ However, certain major disadvantages exist for space cabin conditions, i. e., that it requires a carrier gas, control of the temperature and pressure and the fact that an analysis would take about 10 minutes.^(5, 11)

Other systems were also found which relied upon adsorption techniques for detection, but they were not of the gas chromatograph type, nor were they applicable to a broad spectrum of gases. In addition, they were too specific and limited to scope as well as being unwieldy for space cabin confines. Representative examples are systems that involve changes in the work function of a metal,⁽¹³⁾ differentiation of species by analysis of physical adsorption versus chemisorption phenomena^(14, 15) and contact potential differences of metal electrodes.^(14, 16)

2.1.2 Mass Spectrometry

Another device considered for measuring major atmospheric contaminants, either by itself or in conjunction with a gas chromatograph, is the mass spectrometer. Presently, the only instruments that have been packaged for space flights have been the magnetic deflection type and the time-of-flight type. They generally weigh about 17 to 20 pounds, are about 1200 in.³ in volume, and require 15 watts of power. However, each requires a high gauss magnetic field for its operation, and this can pose a serious problem in spacecraft since interaction of a strong magnet with the Earth's field produces torques on the vehicle sufficient to disturb its attitude.⁽¹¹⁾ Furthermore, many vehicles carry magnetometers to read interplanetary magnetic fields, and this could be interfered with by a ship-board magnet.

Two important advantages of the mass spectrometer are the small sample size required (approximately 0.2 cc/min. at 0.2 mm pressure), and the capacity to "see" an unknown gas by its molecular weight. One disadvantage of this system is that it must have exceedingly high resolution for it to distinguish between constituents that have similar mass numbers. For example, carbon monoxide and nitrogen have atomic masses of 28.004 and 28.015, respectively, and are difficult to resolve in a compact, flight-weight unit. Furthermore, any mass spectrometer, when used alone, is an instrument for analyzing gaseous mixtures at near normal room temperatures and pressures, and does not possess a sensitivity higher than about one part per million under ideal laboratory conditions. Rapid scan mass spectrometers, such as the time-of-flight type, cannot be depended upon consistently to detect better than about ten parts per million. When packaged for space flight, this will be further degraded. Thus, an unaided mass spectrometer will fail to "see" a great many peaks of interest due to the low sensitivity and interference for the high concentration fixed gases such as oxygen and nitrogen.⁽¹¹⁾ In addition, they require a vacuum source for operation, and when on an extended space flight, they may require maintenance.

2.1.3 Spectrophotometry

Two types of spectrophotometers are used quite extensively in the laboratory for all types of analyses, and have been found to be particularly good for gas

and vapor analysis. One type is the visible and ultraviolet light spectrophotometer and the other is the infrared spectrophotometer. Between the two instruments, practically all gases and vapors can be detected, provided they are of sufficient concentration. For organic gaseous forms, only the infrared spectrophotometer is of value, due to the difficulty in handling gases in the U. V. instrument; sensitivities between 20 and 100 parts per million are feasible. ⁽¹¹⁾

Infrared spectroscopy has been used, and considered for use, mostly as an adjunct to chromatography in order to employ the specificity of infrared spectroscopy to aid in the identification of at least the major chromatographic peaks. ^(5, 7, 9, 10, 11) It has a major advantage in that it can be used for identification of almost any gaseous, liquid or solid substance. One of the major disadvantages for space applications is the weight and power factor. It weighs around 100 lb, is 10,000 in.³ in size, and requires about 100 watts of power for its operation. Furthermore, in order to achieve a reasonable sensitivity (better than 100 parts per million), complex, long optical path-lengths are needed. ⁽¹¹⁾ These long path lengths make instrument volume reduction difficult.

2.1.4 Electronic Systems

Recently, there has been a tendency to seek out systems other than the chromatographic, mass spectroscopic or infrared spectroscopic methods due, primarily, to their bulk and power requirements. A growing interest has been developing in electronic devices which could simulate the human olfactory process, as well as being a dry sensor with little or no moving parts. One area receiving considerable study for this purpose has been the semiconductors — both inorganic and organic.

In most instances, semiconductors have crystal imperfections giving them their unique properties. Thus, the introduction of foreign atoms into the crystal lattice (doping), lattice defects (hole or conduction electron trapping), and deviations from stoichiometry, and the control of these conditions, are the factors allowing a substance to show semiconducting behavior. In the case of organic semiconductors, the concepts of charge-transfer complexes and

polyconjugation are uniquely applicable. For either the inorganic or organic semiconductors, the introduction of a contaminant has a similar effect. In the case of the inorganic semiconductor, this might be considered equivalent to doping, and for the organic, it is related to the formation of a charge-transfer complex. In either instance, there will be a change in the conductivity or rectification properties. It is on the basis of this phenomenon that semiconductors have been considered for use in detection devices.

In the light of the behavior of aromatic organic compounds with substances capable of acting as electron donors or electron acceptors, it was recognized that there existed the possibility for making a contaminant detection device. Labes, et al.,⁽¹⁷⁾ and Reucroft, et al.,⁽¹⁸⁾ investigated the behavior of anthracene with iodine, on the one hand, and p-chloranil with amines, on the other. In the former case, it was found that the bulk dark conductivity of anthracene was increased when exposed to iodine vapor and was dependent upon the pressure of iodine (a change in pressure of 30 mm caused an increase by one order of magnitude). In the latter system, the p-chloranil, in the presence of amine vapors, also showed an increase in its bulk dark conductivity. In each instance, a charge-transfer complex was being formed in situ.

Thus, although the simple organics as charge-transfer complex are found to be highly conductive, they lack many properties for application as detection devices. They cannot be fabricated into any shape, they are too soluble and they do not have long-term stability. It appears, therefore, that aside from the work of Labes, et al.,^(17, 18) the observations of Terenin⁽¹⁹⁾ (that an ambient gas atmosphere produces a marked effect on the photoconduction of organic solids), and the work of Weiss and Bolto,⁽²⁰⁾ little more information appears to be in the literature pertaining to the use of organic semiconductors as gaseous contaminant detectors. The evidence exists that they are feasible for this purpose, but no device has, as yet, been developed.

Numerous other electronic systems have been evaluated, but they have not led to a workable device. However, two reported methods using inorganic semiconductors bear further discussion.

In a series of patents, ⁽²¹⁻²⁴⁾ Jacobsen takes advantage of the fact that the electrical properties of semiconductors are changed when they are exposed to gases or vapors. It is claimed that the most practical method for utilizing the effect of gases on semiconductors is to employ a device having one or more rectifying junctions between a semiconductor and a metal, or between a semiconductor and another semiconductor of different conductivity, where one is an n-type and the other a p-type semiconductor. Then, by first passing a high forward current to stabilize the system, followed by reverse biasing the diodes, the system is ready for measurement. The current is made to flow through the junction rather than along the surface. The reasons for this are (a) the current must cross a barrier layer; (b) the semiconductor surface in the vicinity of the contact or junction exposes the barrier layer to the ambient; (c) the ambient to be detected has to influence only a relatively small area adjacent to the diode junction; and (d) the measurement of the ambient gas is always performed with the current in the reverse direction using the change in number and mobility of the minority carriers. One thing that is absolutely necessary in this device is that there be a hole through the semiconductors to act as a conduit for the vapors to come into direct contact with the p-n junction, and that the p and n semiconductors be inorganic, i. e., silicon, germanium, doped silicon, etc.

Because inorganic semiconductors will most readily adsorb gases on a surface, the need for a conduit or series of conduits becomes important. This could pose fabrication problems with minute probes. Furthermore, the system's specificity is somewhat restricted. For example, in order to detect a nerve gas, the sample is first hydrolyzed and the resultant HF is then analyzed for; or, it is pyrolyzed to generate the same species before it can be detected. However, if one wishes to forego size and specificity, this system has very good possibilities for a highly sensitive detection system.

Another method is that reported by Buck, et al. ⁽²⁵⁾ They chose the change in surface conductivity of a semiconductor as detected by the reverse leakage current of a p-n junction diode because of its sensitivity and simplicity. Thus, adsorbed atoms or molecules can act as electron donors or acceptors and make the surface more strongly n-type or more strongly p-type. If the bulk material

is quite pure, then the relative conductance changes may be quite large, and electrically active adsorbed atoms may be detected with considerable sensitivity. With a system of this sort, using a p-n junction rectifier, Buck, et al., were able to detect NO_2 and NH_3 in N_2 , and in air, at concentrations as low as $1/10^8$.

2.1.5 Miscellaneous Systems

Many other gas detection devices have been considered or developed, but they may be specific for a particular gas, or do not fit entirely into one of the above-described methods. Among such systems may be found ellipsometry, where one measures the shift in the relative phase angle between the components of a polarized light beam polarized parallel and perpendicular to a reflecting surface. This shift is sensitive to small fractions of a monolayer of an adsorbed film, but is not very specific at a given wave length. Another method, multiple internal reflection of infrared light has been used and shows promise of good specificity, but it cannot detect less than a monolayer. Electron spin resonance is quite sensitive, but the equipment is elaborate and cumbersome.

Other systems, such as a condensation nuclei gas analyzer,⁽¹¹⁾ a catalytic combustor,⁽¹²⁾ and gas sampling and analysis kits,⁽¹¹⁾ are among many that have been proposed. It is obvious that a tremendous amount of effort is being expended in the direction of detection. Many of the techniques reported have excellent possibilities for development into useful detectors, although it is questionable that they would be useful for space cabin operation.

2.2 SOLID STATE GAS DETECTOR

2.2.1 Organic Semiconductors

There are many organic polymers that have been shown to possess a semi-conducting capability, but they are generally intractable substances having no capability for being fabricated other than in the form of pressed discs. However, during the course of this program intrinsic polymeric semiconductors of the polyacetylene type having film-forming capability with varying electronegativities have been developed. In particular, they have been polymers of phenylacetylene and some of its derivatives. Thus, poly(phenylacetylene) (I), poly(p-nitrophenylacetylene) (II), poly(p-formamidophenylacetylene) (III), and poly(p-aminophenylacetylene) (IV) have been synthesized, with the greatest emphasis being placed on I, since it is easiest to prepare, and the derivatives follow from it. Figure 1 is a schematic of the various preparative routes to the desired polymers. The basic principle upon which these materials depend for their detecting capability is a relationship between their adsorption properties, their electronegativity, and a change in some physical parameter. This study has not heretofore been made on conducting polymers. The majority of other programs concerned with the effects of gases on conducting substances have dealt with simple organics, ^(17, 18) dyes, ⁽¹⁹⁾ and metals, ^(14, 16) and the parameter most studied was the change in resistivity.

Although the polymers chosen for the first phase of this work have been limited to derivatives of poly(phenylacetylene), many other electrically-conducting polymers may be used. The major criterion for choice is that they show differences in electronegativity. To date, no synthetic polymeric organic semiconductor has been used as a contaminant detector, although plastics, paper and organics have been used as surfaces for adsorption of vapors, and have been found to undergo a change in surface potential.

The theoretical aspects of signal generation involve either formation of a charge-carrier at the polymer-electrode interface in the space-charge region with a subsequent migration through the bulk of the polymer to the opposite electrode interface or formation of a charge-transfer complex throughout the bulk of the polymer with a consequent change in the bulk resistivity. The

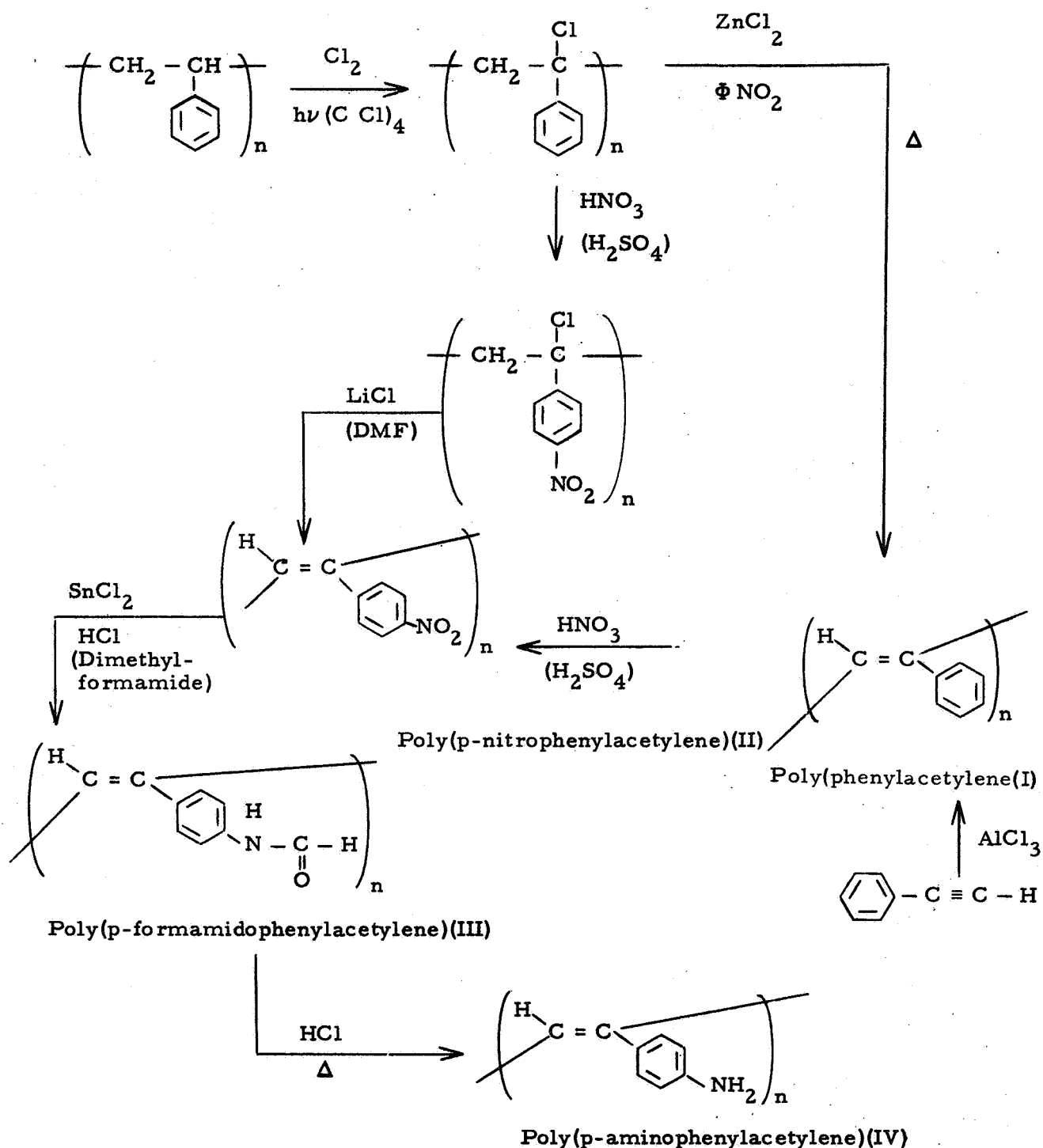


Figure 1. Reaction Sequence Used in Preparation of Some Poly(phenylacetylenes)

literature is not clear on this point, and it still has to be resolved. However, it is agreed that either mechanism will have a similar effect, i. e., generation of a signal.

Considering polymers I-IV, it will be observed that they have varying degrees of electronegativity. Thus, a highly electronegative polymer, such as II, will form a stronger complex with an electron-donating gas, e. g., an amine, than will polymer IV, an electropositive type of polymer; while polymer I should show intermediary behavior. Of necessity, though, adsorption characteristics also have to be considered, since the rates of adsorption and sorption (complex formation) will influence the speed with which a signal is generated. However, since physical adsorption of contaminant species is almost instantaneous, the major governing factor is the electronegativities of the sensor and the contaminant; and a signal will be generated only if they are of the proper magnitude and intensity. Although adsorption is important, its measurement is not of immediate consequence since no signal will be generated if no complex is formed.

In view of the fact that good film forming characteristics, e. g., flexibility, are needed, other derivatives of poly(phenylacetylene) were also prepared, and some of their physical properties evaluated. However, since they showed no major improvement in flexibility over poly(phenylacetylene), they were discarded. It cannot be emphasized enough that the concern with flexibility, conjugation, and molecular weight is quite important. This fact has been of concern to others, as well. Dewar and Talati⁽²⁶⁾ have stated that although conjugated organic molecules are known to act as semiconductors, the carrier mobilities in them are usually low. This is due to the difficulty electrons experience in jumping from one molecule to another, and so the carrier mobilities in compounds of this kind increase with increasing molecular size.

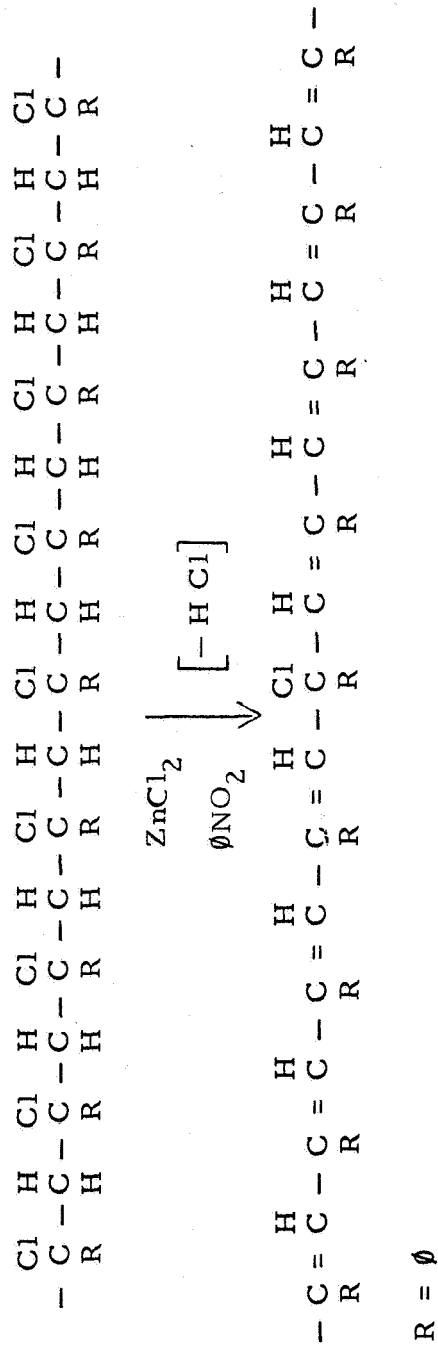
2.2.1.1 Preparation of Poly(phenylacetylene)

Since poly(phenylacetylene) was the parent compound of the program, with the other derivatives following from it, its synthesis was thoroughly investigated. Two synthetic routes available for its preparation — (1) halogenation of polystyrene followed by dehydrohalogenation, and (2) preparation and polymerization of phenylacetylene are shown in Figure 1.

In route (1), commercial polystyrene (Dow PS-2) was chlorinated at a low temperature, in the presence of UV light, to yield poly(alpha-chlorostyrene). This was dissolved in nitrobenzene and dehydrohalogenated with a catalytic amount of zinc chloride at reflux temperature. The resultant poly(phenylacetylene) was about 90% unsaturated as shown by chlorine analysis.

Zinc chloride was used for the dehydrohalogenation reaction because it can form a complex with the chlorine on the backbone, analogous to that which occurs in the Friedel-Crafts reaction, and a carbonium ion is generated before the adjacent trans-hydrogen is split off. However, only small amounts of zinc chloride were used since it acted as a true catalyst. Thus, if the rate-determining step for HCl removal was the formation of the carbonium ion, and if only trace amounts of $ZnCl_2$ were present, the dehydrohalogenation could, of course, be random. If, however, an equivalent amount of $ZnCl_2$ could be added, and it all complexed simultaneously, then all the HCl could be split off almost simultaneously for the generation of total conjugation. Unfortunately, this could not be tried since the zinc chloride is not too soluble in the nitrobenzene. Furthermore, it was observed that use of zinc chloride in the hot nitrobenzene always resulted in an appreciable depolymerization.

It had been shown by Bohrer⁽²⁷⁾ that the dehydrohalogenation of polyvinylidene chloride resulted in about 87% unsaturation. This invariably seemed to be a limiting condition and was corroborated by others^(28, 29) for the dehalogenation of poly(vinylchloride). In each instance, only 87% of the chlorine was removed. This was found to be equally true in our dehydrohalogenation of the poly(alpha-chlorostyrene). The reason for this can be seen in Figure 2. The dehydrohalogenation, being random rather than an unzipping reaction from the end of the chain, can go in two directions simultaneously and ultimately lead to an isolated chlorine. The resultant isolated chlorine is adjacent to two vinyl groups, and the vinyl hydrogens are not readily removed. Thus, there results about a 13% break in the chain conjugation leading to high-resistance sites for the electron flow along the backbone.



c-2807

Figure 2. Random Dehydrohalogenation

Another way of obtaining poly(phenylacetylene) is by polymerization of phenylacetylene. The major advantage of this method is that it should theoretically lead to a totally conjugated polymer rather than the 87 to 90% conjugation of the dehydrohalogenation technique. Phenylacetylene has been polymerized thermally, ^(30, 31) cationically, ^(32, 33) anionically, ⁽³⁴⁾ and with organometallic compounds, ⁽³³⁻³⁵⁾ among others. In almost every instance, the molecular weight was quite low — ranging from about 600 to about 1900.

We have investigated a number of ways of preparing poly(phenylacetylene) from the phenylacetylene monomer. Among these was the thermal polymerization, ⁽³⁰⁾ the Ziegler-catalyst system, ⁽³³⁾ a boron trifluoride catalyst, ⁽³⁶⁾ and an aluminum-chloride catalyzed system. ⁽³⁶⁾ This latter method appeared to be best.

Under vacuum, there was sublimed 0.75 g AlCl_3 into an ampoule kept at liquid nitrogen temperature. This was followed by distillation of 25 ml CS_2 and then 25 ml of phenylacetylene (from storage over MgSO_4). The ampoule was sealed off at 0.1 micron, warmed to room temperature and allowed to stand for six days. The dark brown solution was precipitated into isopropanol, and the polymer washed with alcohol to yield 15 g of a yellow-brown powder with a softening point of 228°C . Figures 3, 4, and 5 are the infrared spectra for the dehydrohalogenated polymer, the thermally polymerized phenylacetylene and the AlCl_3 polymerized phenylacetylene, respectively. As is to be expected, Figure 3 shows the greatest amount of CH_2 groups (3.45μ), but aside from solvent absorption peaks (CHCl_3) they are almost identical.

An interesting relationship was found to exist between the intrinsic viscosity of the poly(phenylacetylene) and its softening point. Figure 6 depicts this relationship for poly(phenylacetylene) prepared by different techniques. From this relationship, and the data in Table I, it is possible to roughly approximate the molecular weight of this class of polymers from the softening point.

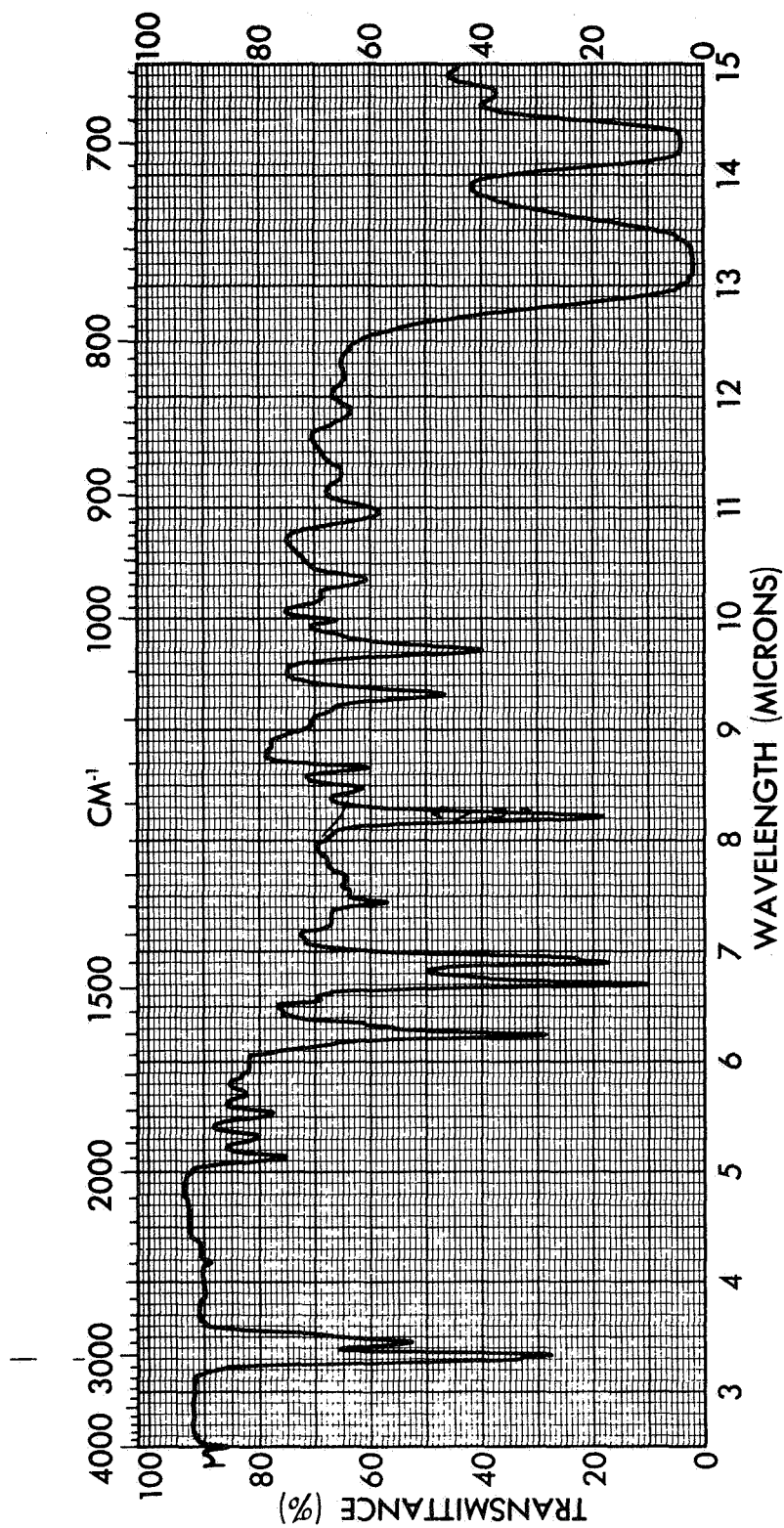
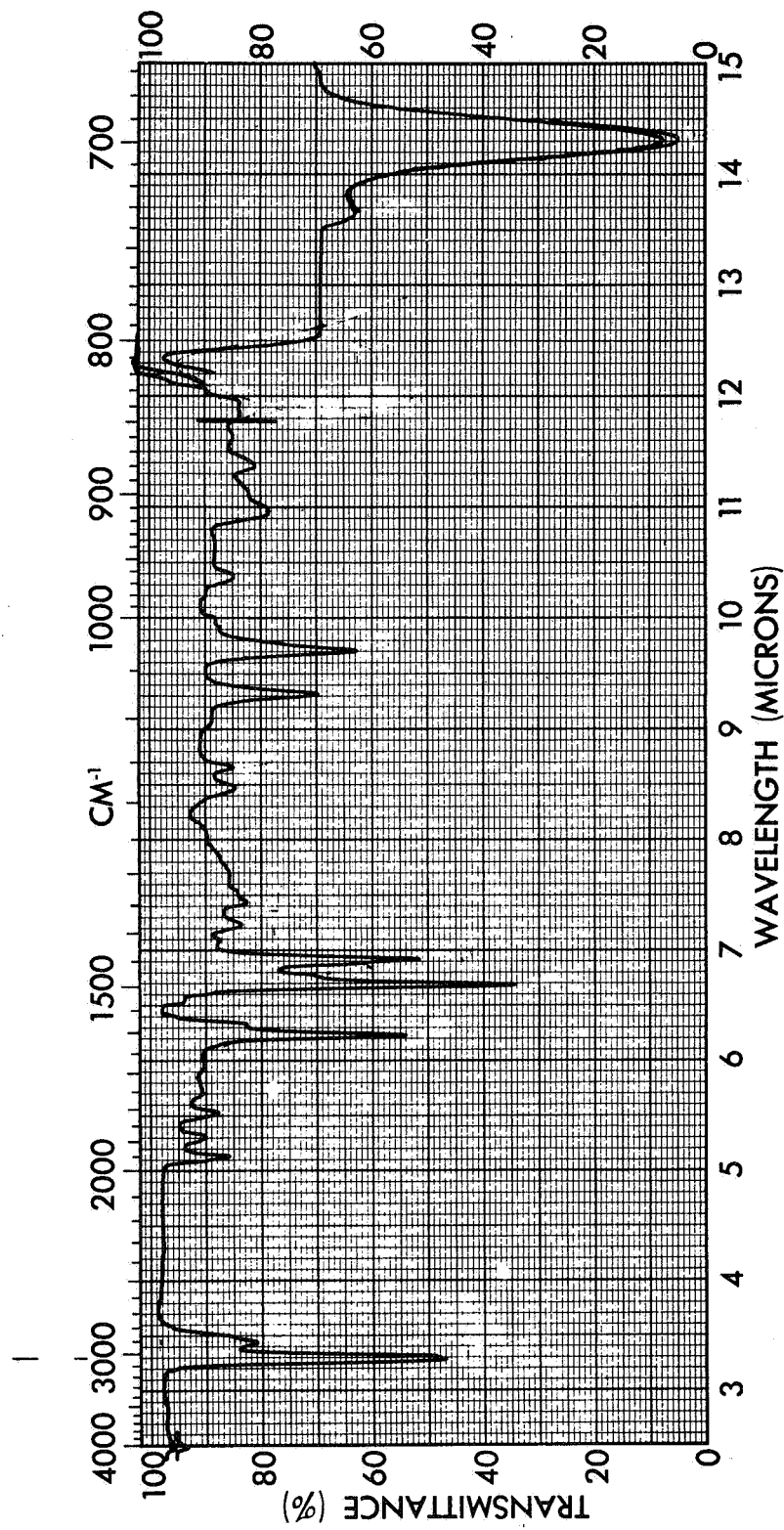
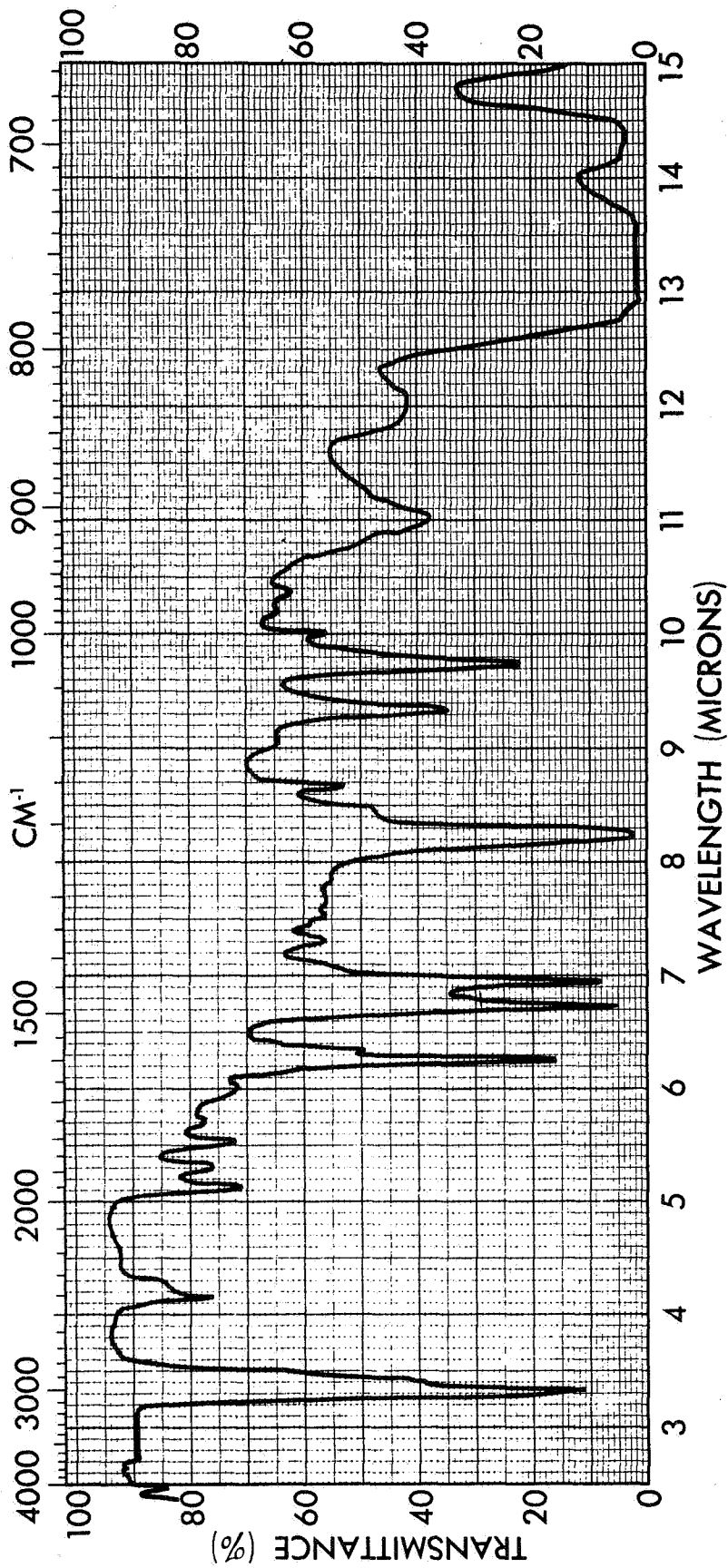


Figure 3. Poly(phenylacetylene) from Dehydrohalogenation of Poly-
(alpha chlorostyrene) with Zinc Chloride



0/1821

Figure 4. Poly(phenylacetylene) from Thermal Polymerization of Phenylacetylene



c/889

Figure 5. Infrared Spectrum of Chromatographed $AlCl_3$ -Catalyzed Solution-Polymerized Poly(phenylacetylene)

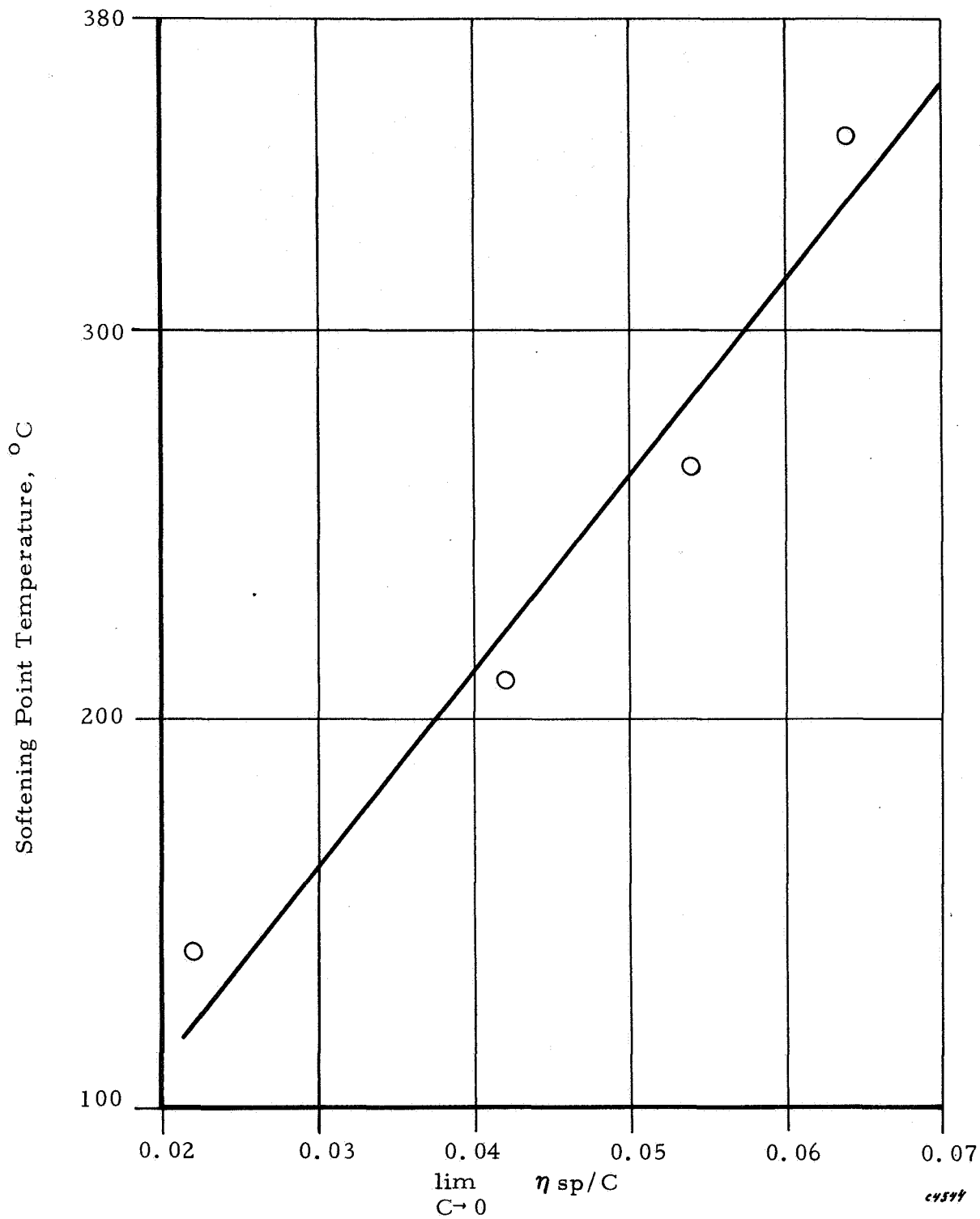


Figure 6. Relation of $\lim_{C \rightarrow 0} \eta_{sp}/C$ to Softening Point of Poly(phenylacetylene)

TABLE I
RELATION OF SOFTENING POINT, LIM η_{sp}/C AND
MOLECULAR WEIGHT OF POLY(PHENYLACETYLENE)

<u>Method of Obtaining Polymer</u>	<u>Softening Point °C</u>	<u>Visc. lim η_{sp}/C C→0</u>	<u>Molecular Weight</u>
AlBr ₃ Polymerized	140	0.022	—
ZnCl ₂ Dehydrohalogenated	210	0.042	1790
AlCl ₃ Polymerized	215	—	1810
AlCl ₃ Polymerized	265	0.054	3200
FeCl ₃ Dehydrohalogenated	350	0.064	4400

2.2.1.2 Derivatives of Poly(phenylacetylene)

Poly(p-nitrophenylacetylene)

Two synthetic approaches were taken for the preparation of the nitro polymer. The first utilized the poly(alpha-chlorostyrene) used for the dehydrohalogenation reaction (2.2.1.1 above).

One mole (138.5 g) of poly(alpha-chlorostyrene) was dissolved in 800 ml of carbon tetrachloride and cooled to 10°C. To this was added dropwise and with vigorous stirring a mixture of 520 ml 90% nitric acid and 130 ml 98% sulphuric acid. The mixture was kept at, or below, 10°C. As the nitration proceeded the reaction mixture became viscous, and the nitrated product came out of solution. After the addition of the acid mixture was completed, the reaction mixture was poured into two liters of water and vigorously stirred. It was decanted and washed several times with water then filtered and washed with water. The solid was ground with a mortar and pestle to release trapped acid in the particles and then washed with water, filtered and washed until washings were neutral. A final wash was made with acetone and the product dried. The product, poly(alpha-chloro-p-nitrostyrene), was obtained in 93.5% yield.

Dimethylformamide (500 ml) was added to a flask containing 91.75 g (0.5 mole) poly(alpha-chloro-p-nitrostyrene) plus 90 g lithium chloride. The polymer and salt were dissolved and the mixture heated to reflux for 48 hours. (This is analogous to a dehydrohalogenation procedure reported by Roth, et al. ⁽³⁷⁾ for dehydrohalogenation of poly(vinylchloride).) (Caution: CO is evolved.) The mixture was cooled and poured into two liters of water, filtered and washed with water. It was dried in a vacuum oven at 50°C.

Analysis: Found: C = 65.53%, H = 4.04%, N = 8.68%, Cl = 2.58%
 Theoretical: C = 65.30%, H = 3.04%, N = 10.50%, Cl = 0.0%

The product is predominantly poly(p-nitrophenylacetylene) with a small amount of chlorine left, just as in the dehydrohalogenation of poly(alpha-chlorostyrene) to yield poly(phenylacetylene).

The second method starts with poly(phenylacetylene) and involves a direct nitration of the unsaturated polymer.

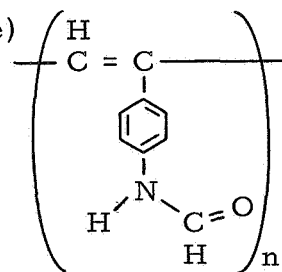
One gram of poly(phenylacetylene) was dissolved in 25 ml of 90% nitric acid at 0°C and allowed to react at this temperature for one hour. Ice was added to the solution to precipitate the polymer. It was filtered, washed with water until the washings were neutral, washed with alcohol and dried in a vacuum oven at 50°C. The yield of poly(p-nitrophenylacetylene) was 1.25 g.

Analysis: Found: C = 61.20%, H = 3.47%, N = 10.80%
 Theoretical: C = 65.30%, H = 3.40%, N = 9.53%

It appears that this product is very slightly over-nitrated, but it is the easiest method. It has a further advantage in that we do not have to restrict ourselves to the dehydrohalogenation process, but we can go directly from the polymerization of phenylacetylene monomer.

Poly(p-formamidophenylacetylene)

This is the third of our major polymers for this program. Ten grams of poly(p-nitrophenylacetylene) were dissolved in 50 ml dimethylformamide (DMF), followed by a solution of 35 g anhydrous stannous chloride in 75 ml DMF plus 25 ml concentrated HCl. The mixture was heated to 100°C for five hours, cooled and poured into 500 ml of H₂O made basic with concentrated NH₄OH. The precipitate was filtered, washed with water and dried. The mixture of polymer and tin salts was extracted with DMF, the extract filtered and then precipitated into water made basic with ammonium hydroxide. The precipitate was filtered, washed with water and dried to yield 6.90 g of a dark brown powder which proved, by means of infrared spectroscopy and chemical analysis, to be poly(p-formamidophenylacetylene)



Analysis: Found: C = 72.28%, H = 5.68%, N = 10.40%, Cl = 2.65%
 Theory: C = 74.48%, H = 4.83%, N = 9.65%, Cl = 0.0%

Preparation and Characterization of Poly(p-aminophenylacetylene)

The poly(p-formamidophenylacetylene) was hydrolyzed to the free amino derivative by the following procedure. Ten grams of poly(p-formamidophenylacetylene) were dissolved in 100 ml concentrated HCl and heated at 100°C for one hour. It was diluted with 500 ml of water and made basic with ammonium hydroxide. The resultant precipitate was filtered, washed with NH₄OH and finally with water. The product, dried in vacuum, was poly(p-aminophenylacetylene), as shown by infrared spectroscopy and chemical analysis.

Analysis: Found: C = 77.26%, H - 6.19%, N = 11.42%, Cl = 2.75%

Theory: C = 82.05%, H - 5.98%, N = 11.96%, Cl = 0.0%

In characterizing the amino polymer, a number of samples of poly(p-aminophenylacetylene), which had been prepared by different methods and left standing for different periods of time, were analyzed by titration by first adding an excess of HCl and back-titrating. Figures 7 through 11 are the pH titration curves for variously prepared poly(p-aminophenylacetylene) plus a comparison curve (Figure 11) for aniline. Figure 7 is that for the LiCl dehydrohalogenation of poly(alpha-chloro-p-nitrostyrene) followed by reduction to the amino polymer. Figure 8 is for the amino polymer prepared by nitration then reduction of the poly(phenylacetylene) from the polymerization of phenylacetylene monomer. Figure 9 is for the poly(p-aminophenylacetylene) prepared by zinc chloride dehydrohalogenation of poly(alpha chlorostyrene) then nitration and reduction. Figure 10 is the same material but prepared six months previous.

As is evident, the curves for the amino polymer indicate a much weaker base than aniline. This could be due to either a steric factor, i. e., the electrons on the nitrogen are blocked by protons from an adjacent nitrogen, whose proximity is related to the arrangement of the phenyl groups, or to the fact that the backbone is interacting with the phenyl groups and electrons are being drawn out of the phenyl group to the backbone.

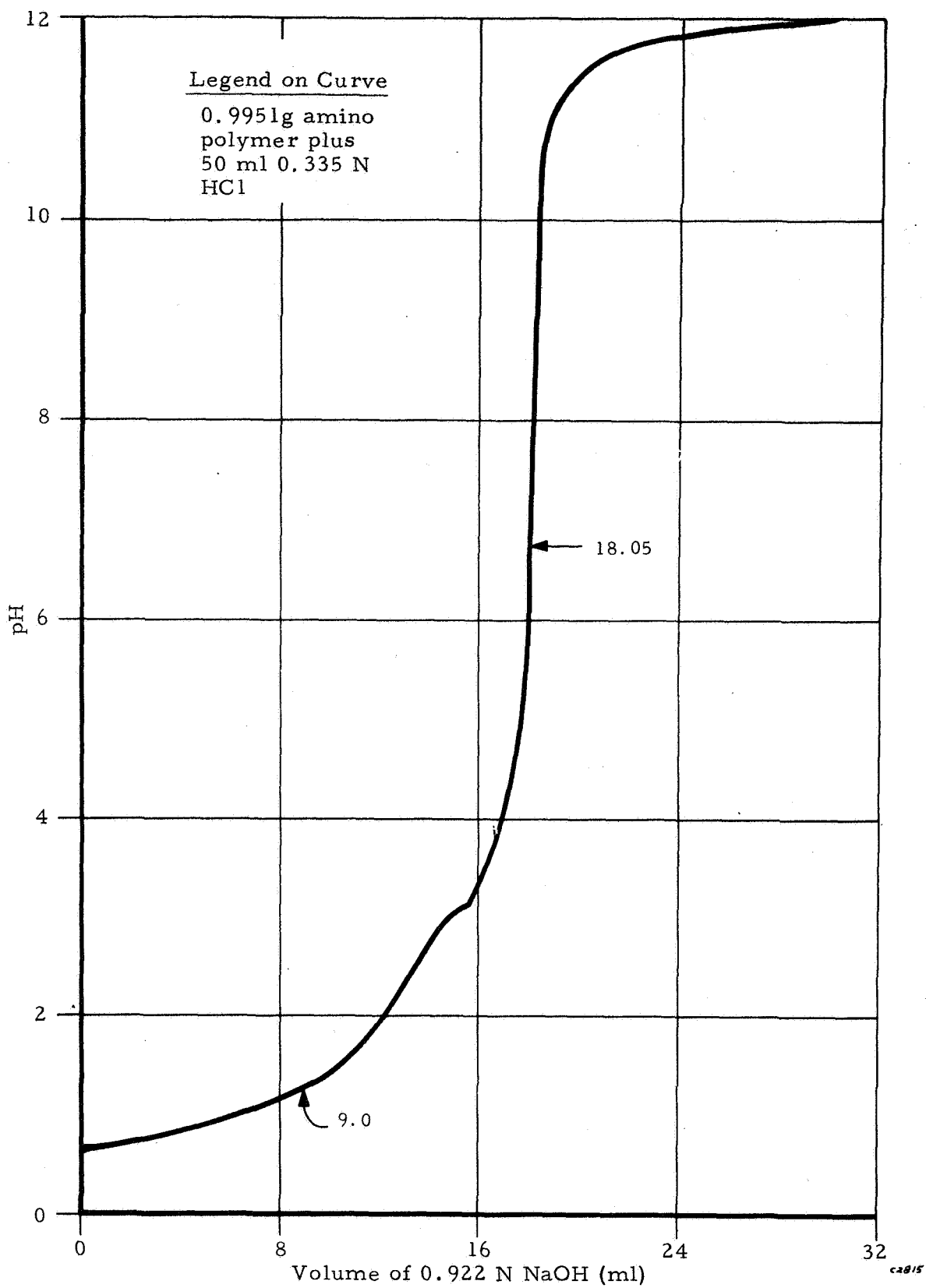


Figure 7. pH Titration Curve of Poly(p-aminophenylacetylene) Prepared by Lithium Chloride Dehydrohalogenation of Poly(alpha chloro p-nitrostyrene)

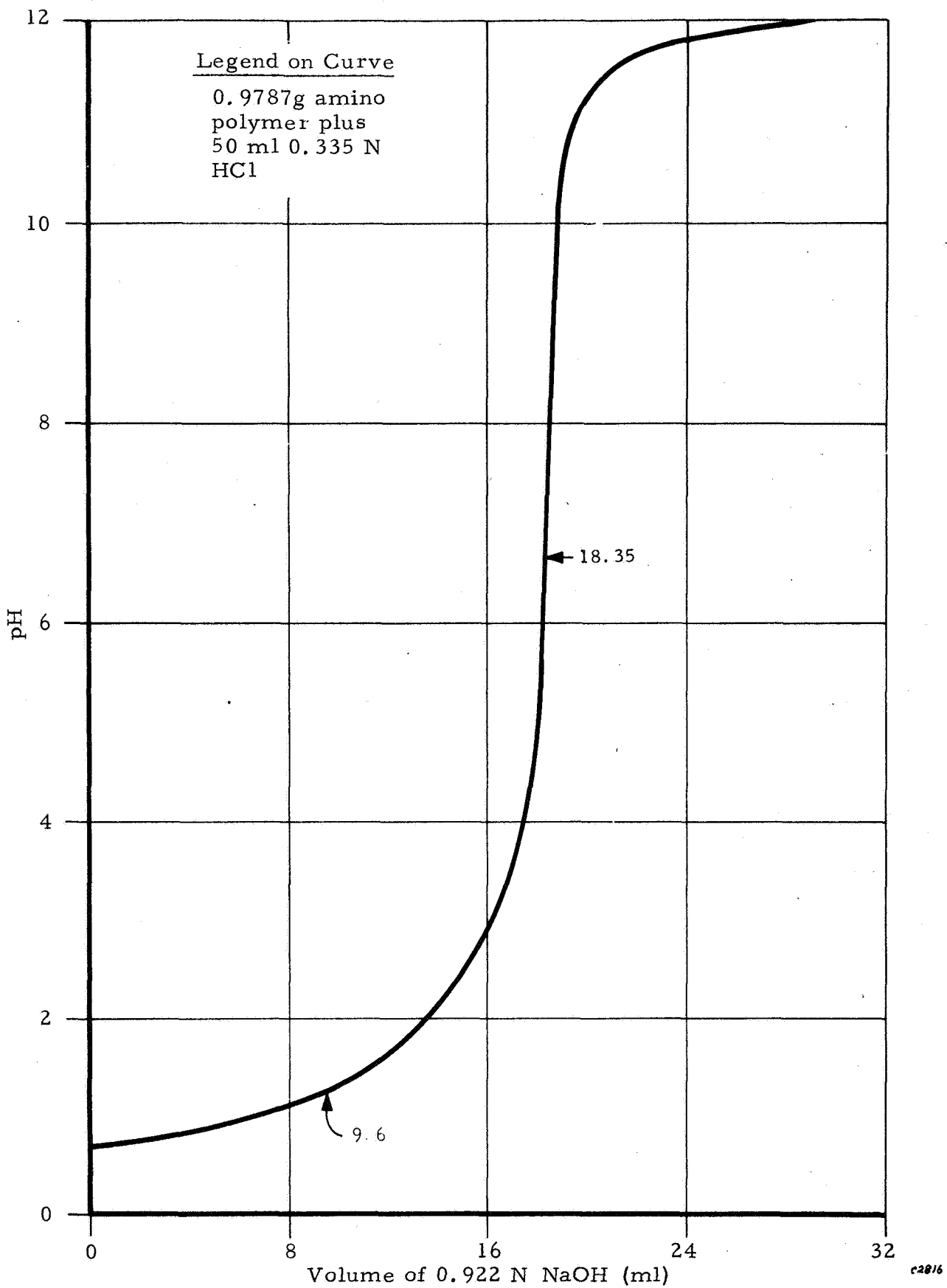


Figure 8. pH Titration Curve of Poly(p-aminophenylacetylene) From Polymerization of Phenylacetylene Followed by Nitration and Reduction

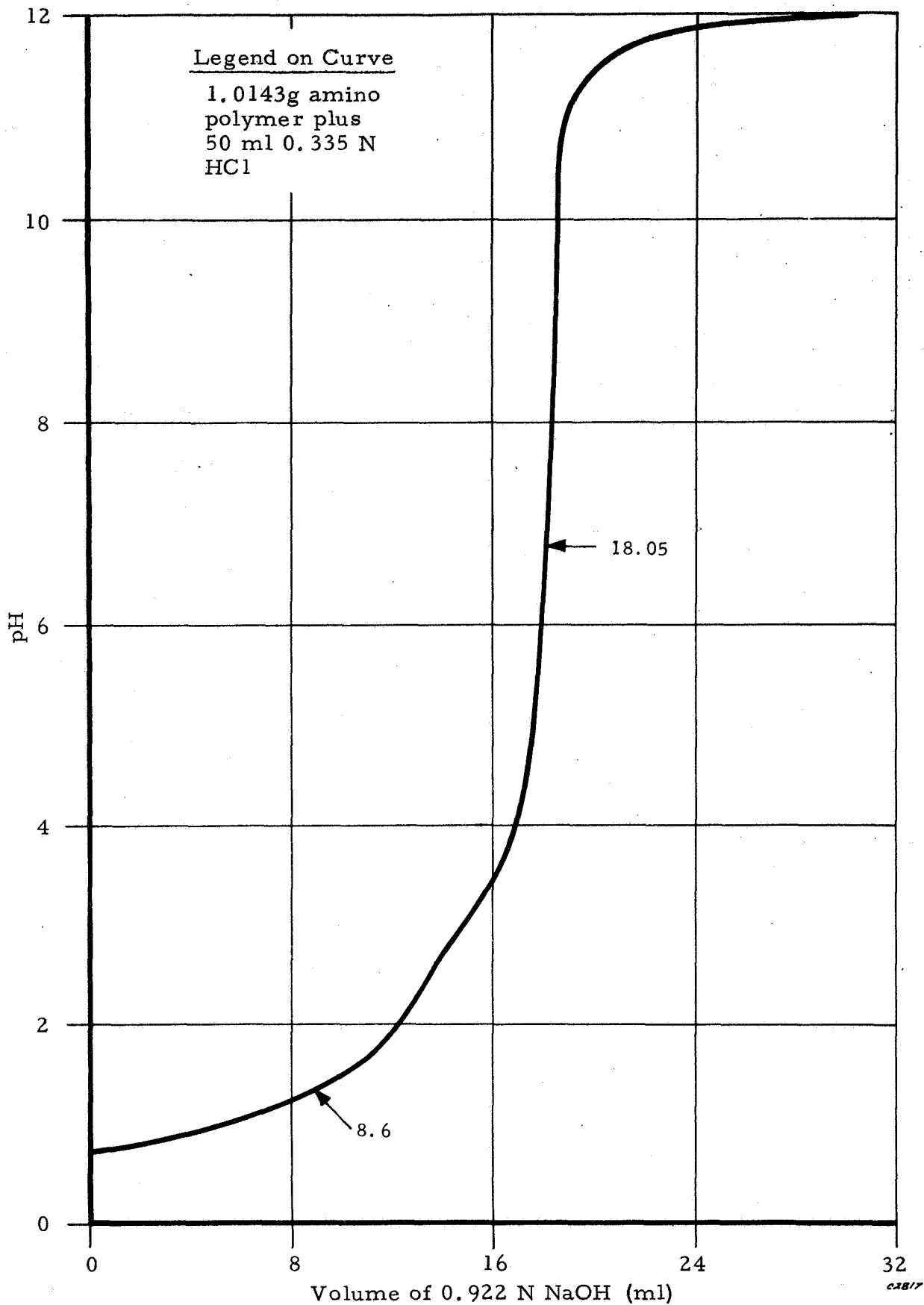


Figure 9. pH Titration Curve of Poly(p-aminophenylacetylene) Prepared by $ZnCl_2$ Dehydrohalogenation of Poly(alpha chlorostyrene) Followed by Nitration and Reduction

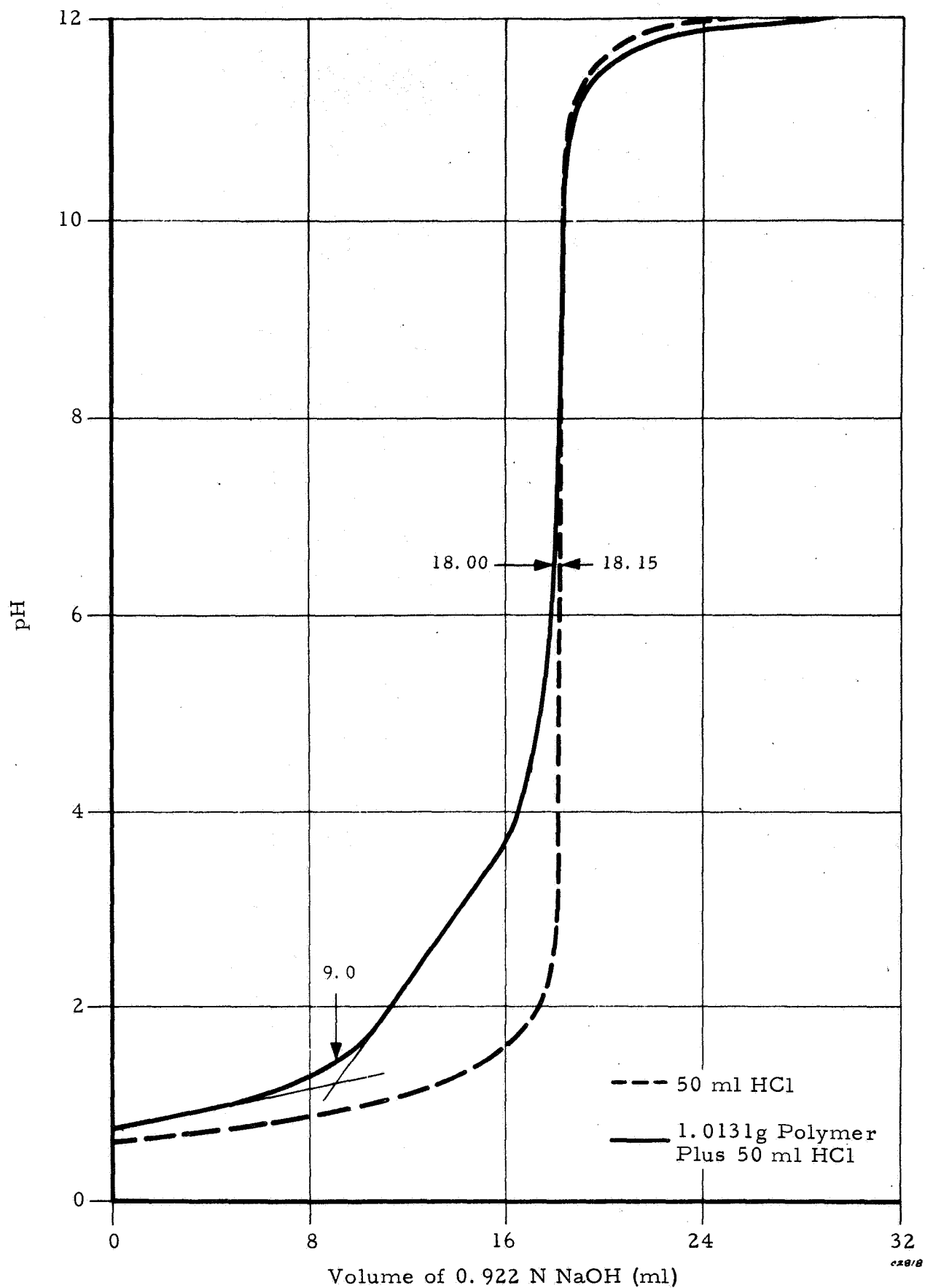


Figure 10. pH Titration Curve of Poly(p-aminophenylacetylene) Prepared Six Months Previously by Lithium Chloride Dehydrohalogenation Technique

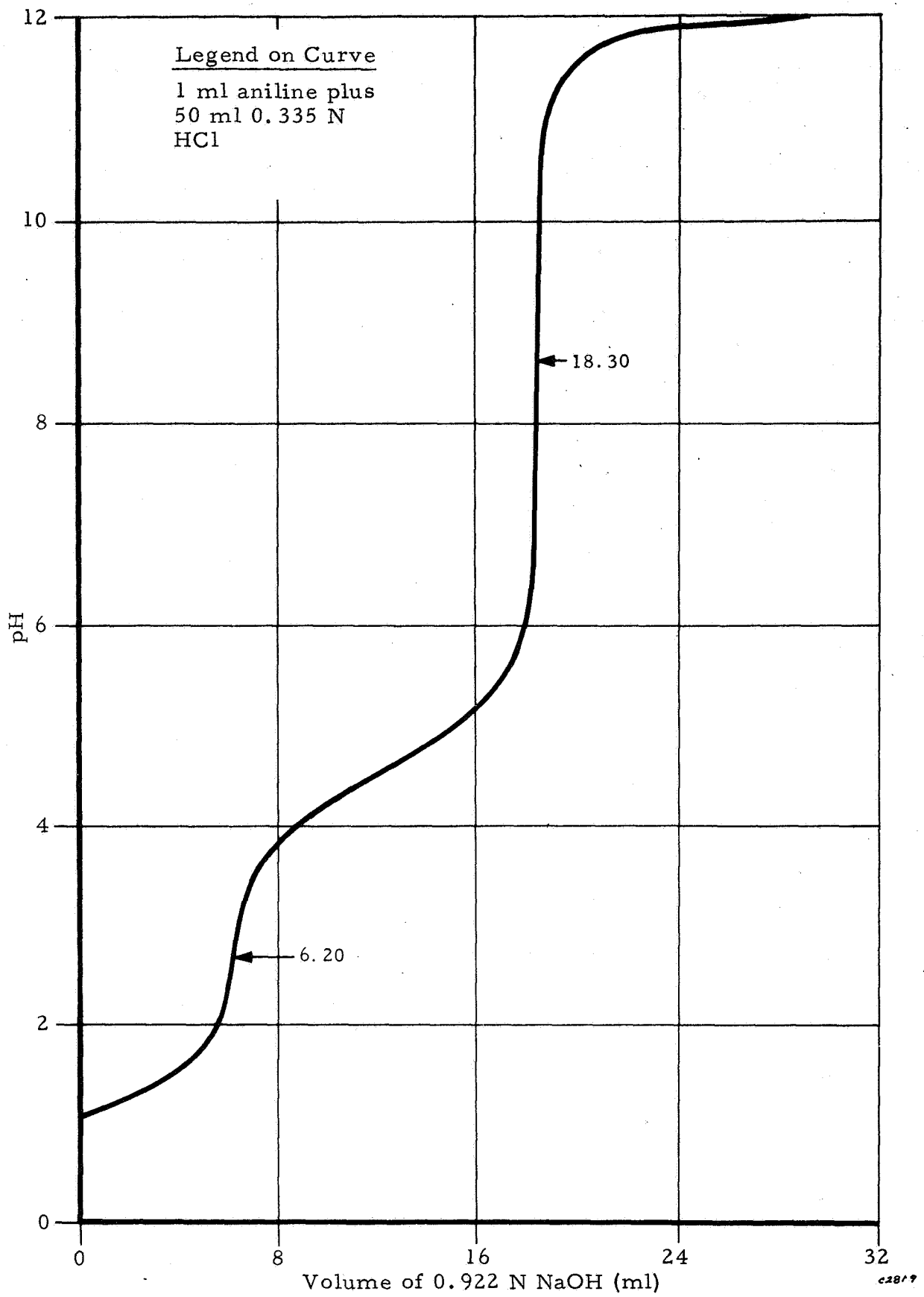


Figure 11. pH Titration Curve for Aniline

Figure 10 shows the titration of the HCl solution (without the polymer), and is given as a reference curve. When the polymer is titrated, the first end point is a weak one. It is found by extrapolating the two straight lines formed by the lower (horizontal) leg and the upper (vertical) leg of the curve to a point of intersection. (Although difficult to observe, there is actually a slight change in slope depicting the end-point.) Taking the difference between the first end-point and the final end-point, one calculates one amino group per phenyl moiety in the polymer. It was further observed that the amino polymer, in solid form, is more stable to air oxidation than anticipated. This was evidenced by the fact that the titration of the amino polymer shown in Figure 10, which had been standing for six months, gave the same analysis as for the most recent samples (Figures 7 through 9). Thus, although the elemental analysis is not too good (possibly due to the residual chlorine), its reasonable agreement with theory (particularly for the hydrogen and nitrogen), and the fact that the titration data indicate one amino moiety per monomer unit, are strongly indicative that the reaction proceeds quite readily from poly(phenylacetylene) to poly(p-aminophenylacetylene).

2.2.2 Electrical Properties of Polymers

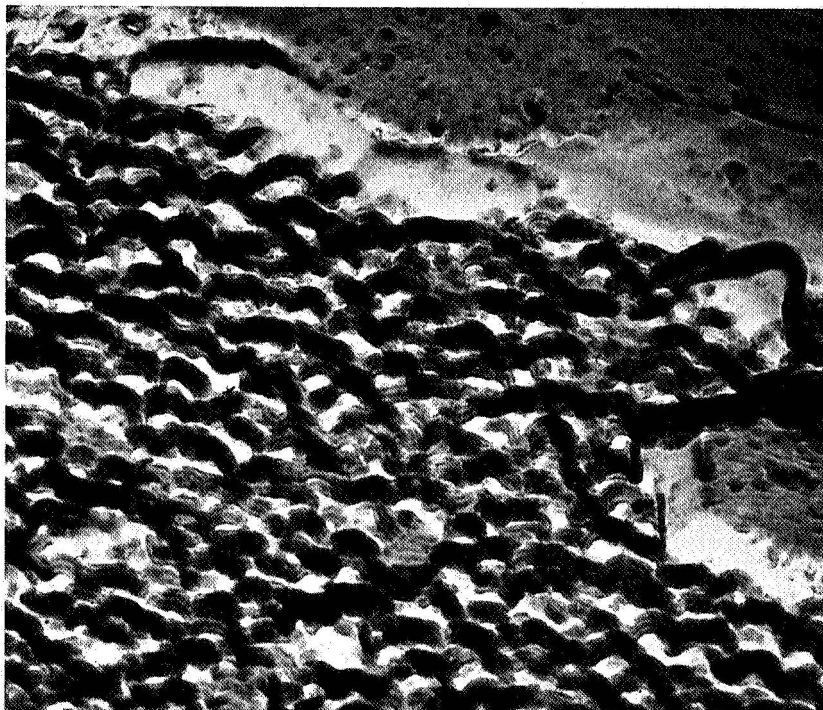
2.2.2.1 Effect of Structure and Morphology on Electrical Characteristics of Polymers

Before we discuss the gas response behavior of the various sensors and polymers, let us consider the relationship between polymer structure and morphology and the electrical characteristics of these polymers.

The degree of crystallinity, crystal orientation and the mode of crystallization are known to affect significantly the conductivity and the effect of surface adsorbants as well as trapped charge carriers in polymeric materials. A difference of two orders of magnitude was observed by Labes⁽³⁸⁾ in 1,6-diaminopyrene-chloranil between single crystal material and discs of compacted powder; a difference of two orders of magnitude in 1,5-diaminonaphthalene-chloranil along two crystallographic directions. The hydrocarbon-halogen and quinone complexes are believed to form chain-like structures.

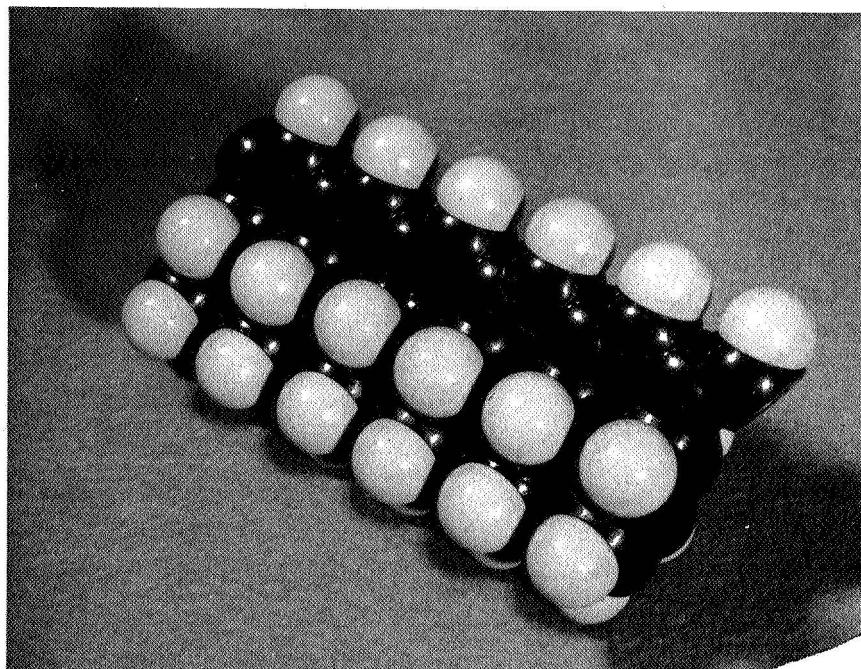
Paths of greater overlapping of π -electron orbitals are created between parallel molecules and intermolecular overlap with ligands affecting the conductivity.

To obtain a relationship between mode and degree of crystallization and conductivity, poly(phenylacetylene) was examined by electron microscopy. The polymer sample was treated at 195-210°C for 20 minutes and annealed at 160°C for two hours under atmospheric conditions. A portion of the polymer was thus crystallized, as was observed in polarized light. Electron microscopic studies of replicas of the material showed a distinct aggregation indicating a preferred molecular orientation, and lamination was observed in certain regions (see Figure 12). By examining the structure of poly(phenylacetylene), as depicted with atomic models (Figures 13-16), it can be observed that this polymer in its lowest energy state in the trans configuration (the thermodynamically-stable form) can only have a linear, close-packed crystalline arrangement. However, in this low energy state, the molecule cannot show any interaction between the phenyl groups and the backbone due to lack of coplanarity. In fact, the aromatic moieties are all aligned parallel to each other, and the plane of the benzene ring is at right angles to the plane of the backbone (Figure 13). Therefore, unless energy is put into the system or repulsion forces operate, the interaction between appendage and backbone will be nil. On the other hand, even if rotation did occur around the alternating single bonds (assuming bond localization along the backbone), the phenyl groups would still not be coplanar. Instead, at the maximum rotation point (120° from the closely-aligned position), the phenyl groups could now twist about 45° from the vertical (Figure 14). Thus, a possibility exists in this configuration for some degree of electron overlap between the backbone and the ring. It is this hypothesis that helps to explain some of the observations of the conduction behavior of the poly(p-nitrophenylacetylene) and the poly(p-formamidophenylacetylene). Figures 15 and 16 depict the structural arrangement of the cis-configuration. In this position the phenyl groups can exhibit coplanarity, either in the aligned form (Figure 15), or in the unaligned form (Figure 16). However, this type of tacticity is difficult to obtain.



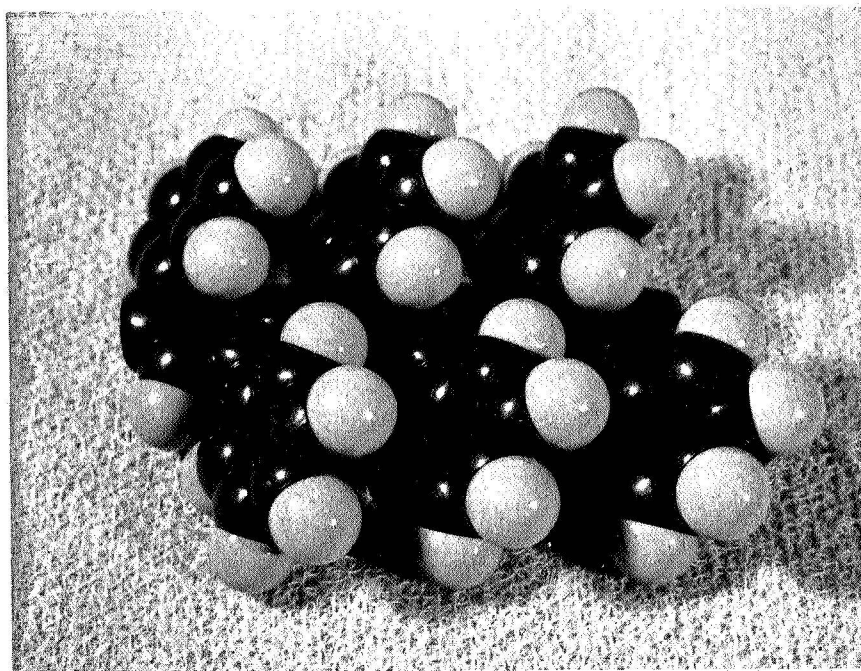
C/990

Figure 12. Electron Photomicrograph of Poly(phenylacetylene)
Illustrating a Distinct Preferred Molecular Lamination.
Magnification - 60,000X



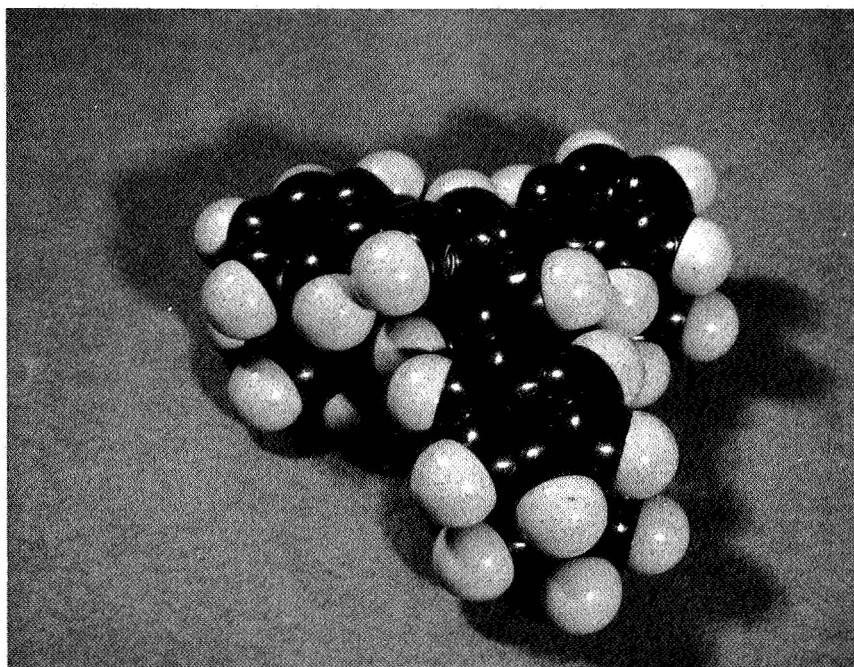
C1882

Figure 13. Poly(phenylacetylene) Low Energy State Trans Configuration (Highest Alignment)



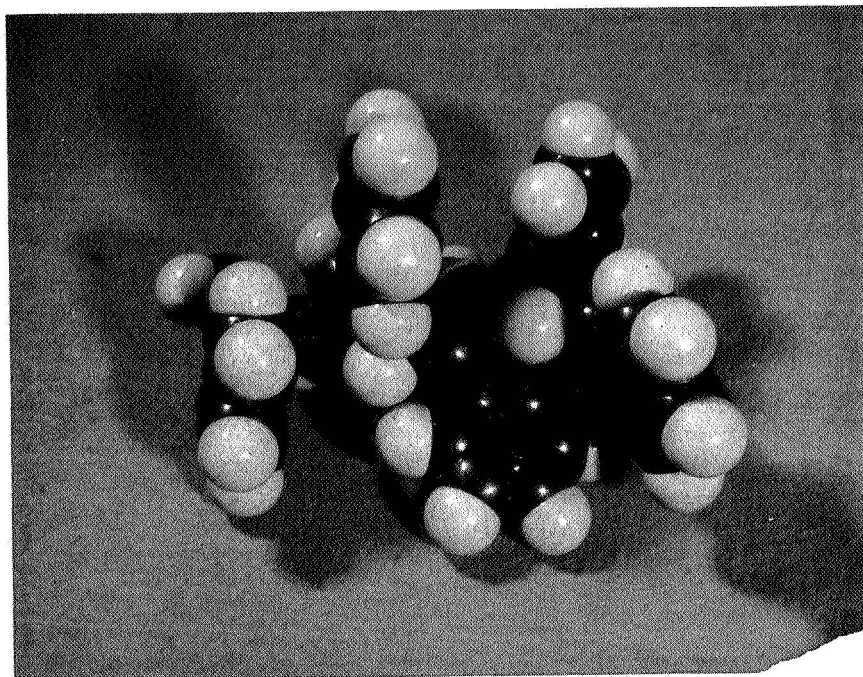
c/883

Figure 14. Poly(phenylacetylene) Trans Configuration
Unaligned Form



c/884

Figure 15. Poly(phenylacetylene) Low Energy State Cis Configuration (Highest Alignment)



C1895

Figure 16. Poly(phenylacetylene) Cis Configuration
Unaligned Form

2.2.2.2 Electrical Response of Organic Semiconductors

Prior to utilizing any polymer as a gas detection sensor, information was needed relative to the intrinsic electrical behavior of the polymer. The E for poly(phenylacetylene) prepared either by dehydrohalogenation or polymerization was found to be 0.54eV. It was obtained from Equation (1),

$$\sigma = \sigma_0 e^{-E/2kT} \quad (1)$$

wherein k = Boltzmann's constant, σ = conductivity and σ_0 and E are constants for the particular material, their values being obtained from a plot of $\log \sigma$ versus $1/T$, with σ_0 being the intercept and E being the slope. Furthermore, the resistivity of these two samples of poly(phenylacetylene) was essentially the same, viz. about 10^{17} ohm-cm. This compares favorably with the literature value for the thermally-polymerized phenylacetylene, i. e., $\rho = 10^{16}$ ohm-cm at room temperature. (30)

In view of the fact that the dehydrohalogenated product was only about 90% conjugated, it would probably have a few high impedance areas to affect the charge carrier mobility. On the other hand, the poly(phenylacetylene) from the thermal polymerization of phenylacetylene is presumably more conjugated, but it has a lower molecular weight. (30) Thus, in the latter polymer, when a conducting species reaches the end of a chain, it has to "hop" to another chain to continue its motion. This requires energy, just as was required in the transfer of the conduction species around the high impedance area of the dehydrohalogenated polymer. However, by some coincidence, the balance between the molecular weights of the polymers and the 10-13% break in the conjugated path are about equivalent in the energy requirements for the conducting charge carrier; thereby resulting in equivalent conductivities.

It should be pointed out that this concern with conjugation and molecular weight is quite important. (26) Aside from electrode effects, in other words, ohmic or non-ohmic contact and carrier injection, the major charge carrier is in the polymer. Once it has formed a complex, the current has to be carried through the system. If there is a contiguous conjugation and the molecular weight is high enough to allow for the electrodes to touch the polymer

but maintain the desired spacing from each other, then there will be little to affect the transfer of charge from one electrode to the other. If, on the other hand, there are many short, but conjugated, polymer chains, the ability for the charge to proceed from one electrode to the other is hindered, and a hopping mechanism has to be invoked to transfer the charge. This creates high resistance areas, and the conductivity will be decreased proportionately to the number of such high resistance spots. By the same token, if one had a high molecular weight polymer to get electrode contacts with a chain and maintain electrode separation but there was not total conjugation to the system, the same high energy sites would have to be traversed either within a chain or from chain-to-chain to get around these sites. Furthermore, the situation could be more aggravated if the polymer chains were small (low molecular weight) in addition to having breaks in the continuities of conjugation. In this case, hopping would have to occur many times from chain-to-chain, as well as within a particular chain. It is for these reasons, therefore, that a need exists for a high molecular weight, totally (or as highly) conjugated a polymer as possible.

By themselves, these results would be of little consequence; but in the development of a sensor, they are critical. Although the exact requirements of molecular weight are not, as yet, known, it can be safely assumed that it should be large enough so that the end-to-end distance of the polymer be close to the spacing between the electrodes in the sensor. In other words, if the spacing is about 10^3 - 10^4 Å, the molecular weight should be close to 100,000. However, this may be impractical for other reasons (viz., highly crystalline, therefore poor mechanical properties). Therefore, as an alternative, a lower molecular weight polymer, but one which is totally conjugated may be just as adequate; for it may be possible, after a film is cast, to crosslink the polymer to an infinite molecular weight. Thus, the problem of degree of conjugation is of more paramount importance than molecular weight, as long as the molecular weight is not as low as the aforementioned poly(phenylacetylene).

Subsequently, the electrical properties of poly(p-aminophenylacetylene), poly(p-nitrophenylacetylene) and the poly(p-formamidophenylacetylene) as

well as the poly(phenylacetylene) were measured under various conditions for comparative purposes. One-inch pellets were pressed at 13,000 psi, aluminum electrodes were vacuum deposited and the volume resistivity was measured following the procedure outlined in ASTM D257-61, using a guard ring to prevent leakage caused by surface conductivity. With poly(p-formamidophenylacetylene) as a representative polymer, its I-V plot, shown in Figure 17, measured in the dark under vacuum at ambient temperatures, shows an ohmic relationship. This was found to be the case for the other polymers, as well, when measured with pressed discs.

Figure 18 shows a plot of conductivity versus reciprocal temperature for the above-mentioned four polymers. Poly(phenylacetylene) showed a linear relationship for conductivity versus temperature; for all the other polymers, with nitrogen in the para position, a definite break in the slope was observed. This might be attributable to an entropy effect since each of these polymers has a reasonably large group in the para position while the poly(phenylacetylene) has only a hydrogen atom. It could well be that its break in the slope would occur at a higher temperature. No appreciable differences in conductivities were noted between measurements made during the heating and the cooling cycles. Poly(p-formamidophenylacetylene) showed the highest conductivity with the poly(p-nitrophenylacetylene) showing the next best. Next came the poly(p-aminophenylacetylene), while least conductive was the poly(phenylacetylene). The activation energies from the higher temperature region of the curves, tabulated in Table II, are obtained from Equation 1.

TABLE II
ACTIVATION ENERGIES FOR D. C. ELECTRICAL CONDUCTIVITIES

<u>Polymer</u>	<u>Activation Energy (e. v.)</u>
Poly(phenylacetylene)	1.08
Poly(p-aminophenylacetylene)	1.14
Poly(p-nitrophenylacetylene)	1.96
Poly(p-formamidophenylacetylene)	1.56

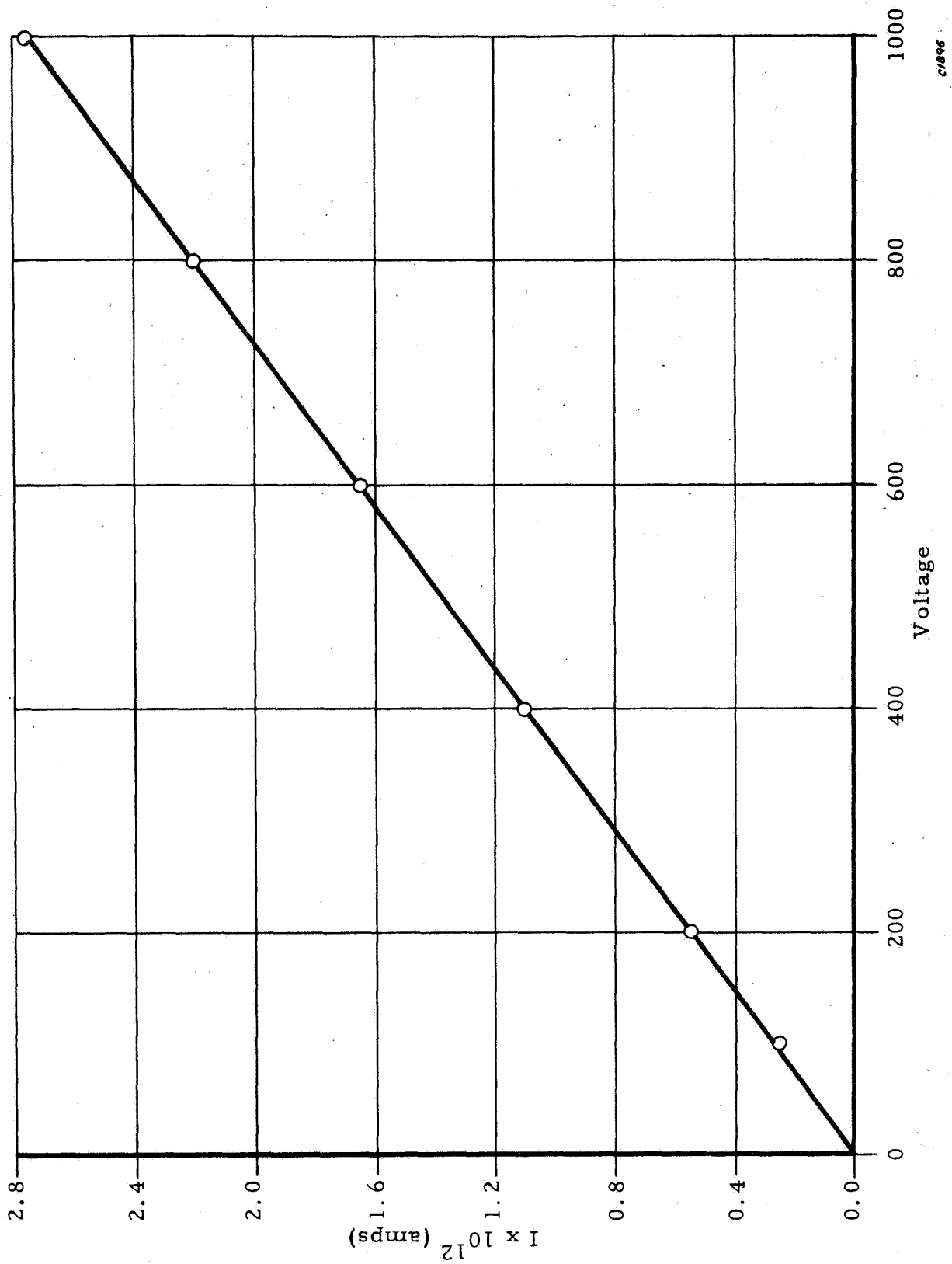


Figure 17. Current-Voltage Plot on Pressed Pellet of Poly(p-formamidophenylacetylene)

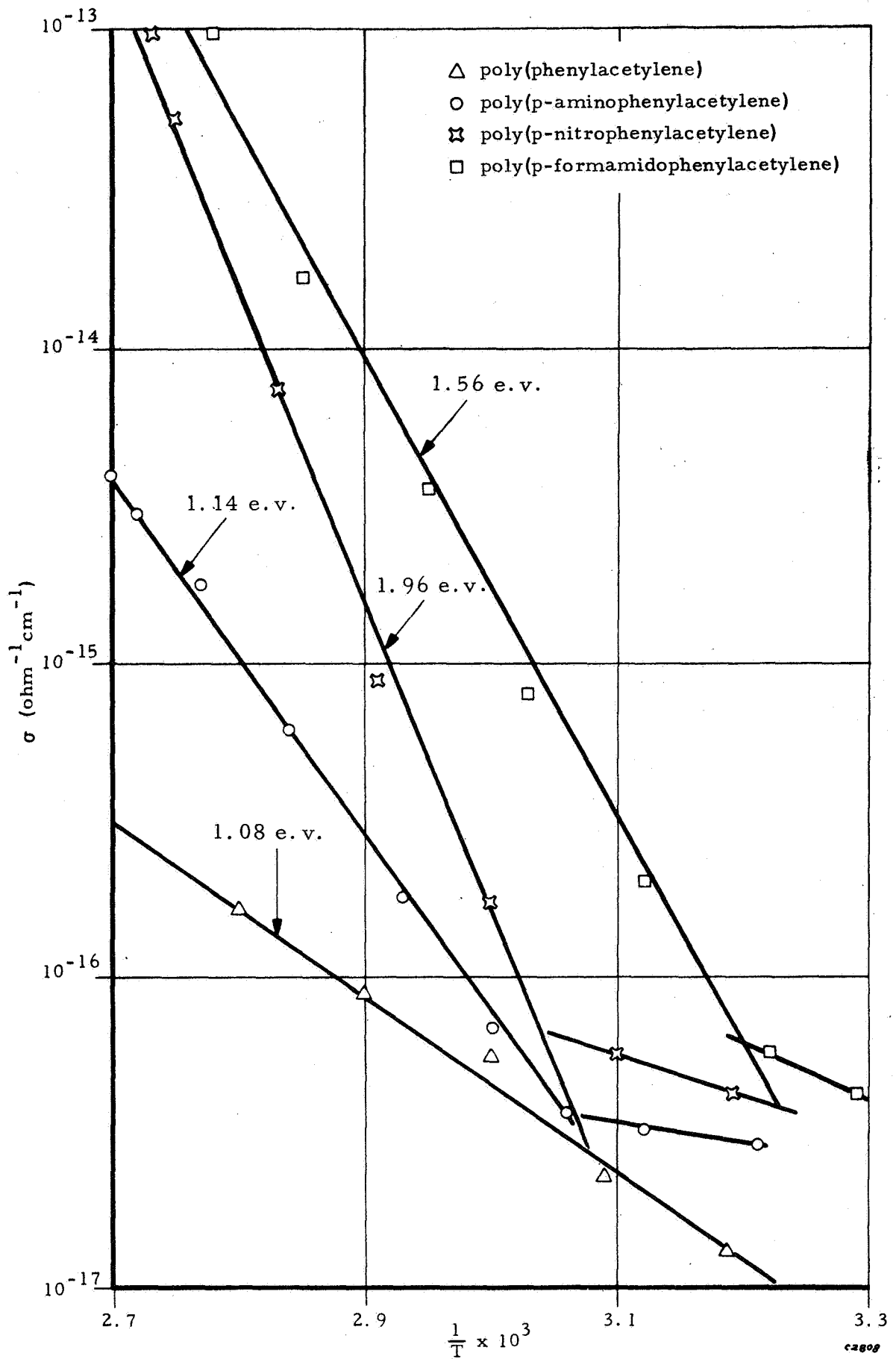
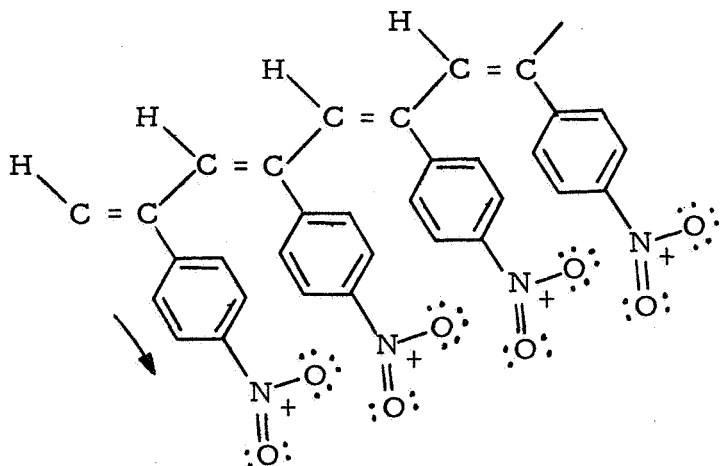


Figure 18. Conductivity— Temperature Plots on Pressed Pellets

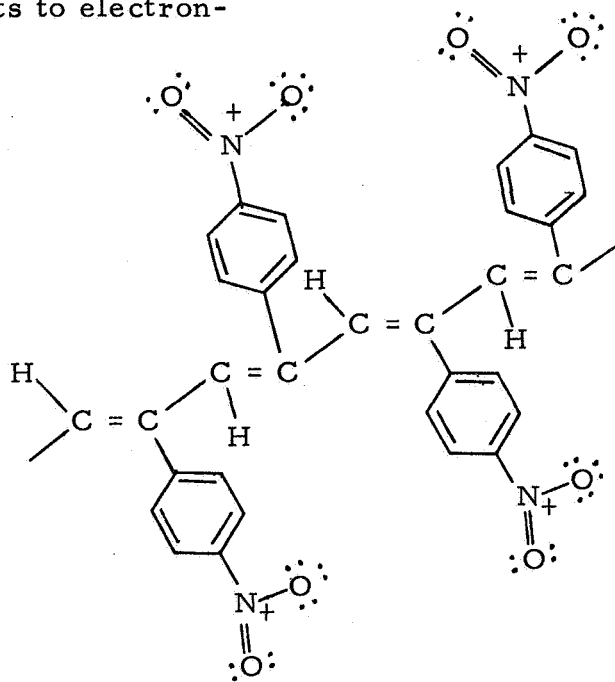
The structure of poly(phenylacetylene) is believed to have its lowest energy state with the phenyl groups parallel to each other and perpendicular to the backbone of the conjugated polymer (Figure 13). In this configuration the phenyl groups are in a close-packed arrangement, and the possibility for interaction of pi electrons between the rings is greatest. In addition, the pi electrons of the phenyl group, in their nodal distribution, are at right angles to the pi electrons in the backbone of the polymer. Thus, the phenyl group makes little, if any, contribution to the conduction mechanism, according to the molecular orbital theory. However, if some energy were put into the system, viz., thermal or photon, the polymer could flip into the configuration shown in Figure 14. Here, the phenyl group could rotate slightly to where it is only about 45° out of coplanarity with the backbone. In this state, some $\pi - \pi$ overlap can occur between the ring and the backbone, although not as freely as in a completely coplanar structure. Ideally, that structure which showed complete coplanarity between the backbone and the appendage would be in the lowest energy state.

Poly(p-aminophenylacetylene) has a similar structure to the poly(phenylacetylene) except for the amino group in the para position. In actuality, the amino group is not bulky enough to involve itself with steric interactions from one ring to another. When the phenyl groups are closely aligned, the hydrogens can lie in the plane of the ring and not interfere with each other. Therefore, although the NH_2 group is an electron-donating species, it is a very weak base, as shown by our titrations (Figures 7-10), and it makes only a small, but noticeable, contribution to the electron density on the backbone. From the shape of the curve in Figure 18, it can be seen that the amino polymer conducts better than the poly(phenylacetylene), both before it experiences a break in the curve and after. It may be, then, as mentioned earlier, that the poly(phenylacetylene) also has a break in its curve, but it occurs at a higher temperature. Thus, increasing the bulk of the group in the para position would increase the entropy effect.

In order to understand the unexpected enhanced conductivity of the poly(p-formamidophenylacetylene) and the poly(p-nitrophenylacetylene), we may consider the fact that the nitro group and the formamido group have two



(a) Trans-aligned poly(p-nitrophenylacetylene)
 (See Figure 13) Arrow points to electron-withdrawing tendency.

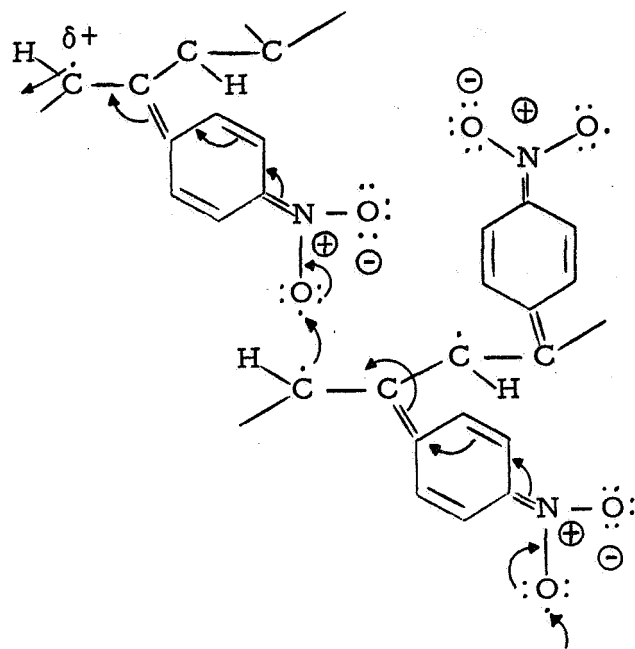


(b) Trans-unaligned poly(p-nitrophenylacetylene)
 (See Figure 14)

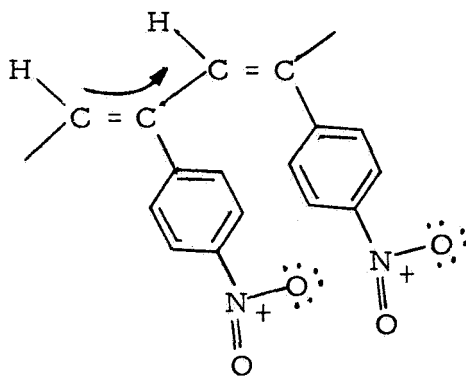
C2200

(Continued Next Page)

Figure 19. Poly(p-nitrophenylacetylene), Aligned and Unaligned, and the Conduction Path for Each



- (c) Conduction path through ring and backbone in unaligned form
 Arrow points path of electron flow in a field, holes (charge carrier) migrate in opposite direction – both along a chain and from chain-to-chain.



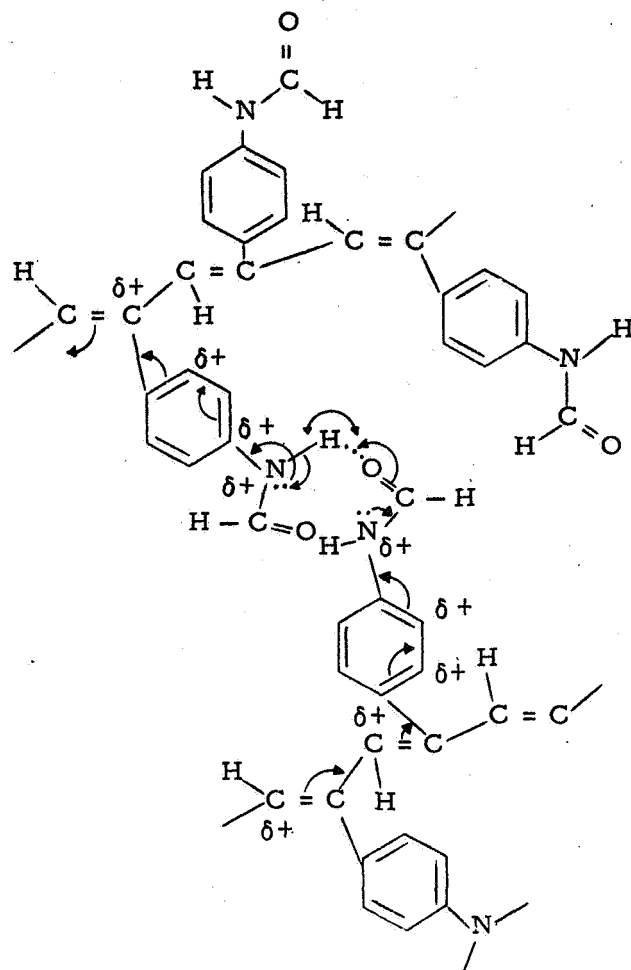
- (d) Conduction path along backbone in aligned form
 Arrow points out conduction path.

c2220

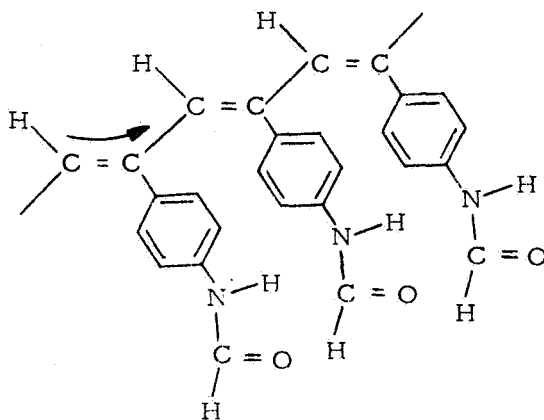
Figure 19. Concluded

factors operating. First, they are electron-withdrawing groups, i. e., the electron density is at its highest around the oxygens in the former case, and on the carbonyl in the latter. This causes repulsive forces to operate and force the polymer to rotate to the trans unaligned form of Figure 14. In addition, they are somewhat more bulky than the hydrogens in the amino group, and this causes steric factors to come into play; again rotation around the carbon-carbon single bonds results in the trans unaligned form. When in this form, a greater probability exists for electronic interaction between the rings and the backbone. However, another factor makes a contribution in the case of the nitro and formamido polymer, namely, either intermolecular charge-transfer or intermolecular hydrogen-bonding.

If we consider that the electron distribution in the nitro polymer is towards the oxygen atoms of the nitro group, then, if an electron separation occurs to form a diradical, one of the electrons could ultimately rest on one of the oxygen atoms (by resonance stabilization). In addition, if ring-backbone interactions can occur (especially in the trans-unaligned case — Figure 14), then in the presence of an applied potential, the free electron on the backbone could move to the electrode, leaving behind a "hole"; and this "hole" is the charge-carrier. In the formamido polymer, a similar mechanism could apply, but now the carbonyl is the electron-withdrawing species; and again, "hole" conduction can occur. Figure 19 depicts the possibilities for the interaction in the nitro polymer, and Figure 20 is that for the formamido polymer. A further possibility for the formamido polymer is that conduction might take place via some hydrogen bonding mechanism, analogous to that reported for proteins (see Figure 21 for the conduction path in a protein or other polyamide). Thus, in the case of the nitro and the formamido polymers, charge-carriers can go in any direction, either along the backbone or through the rings from chain-to-chain. This situation cannot prevail as readily in poly(phenylacetylene) or in the amino polymer. They presumably conduct primarily along the backbone. If, therefore, they are not oriented correctly with respect to the electrodes, they cannot have an efficient carrier-injection process, nor can they have an efficient conduction path; there is too much chain-hopping. While for the nitro and formamido polymers chain-hopping is minimized by the fact that carriers can be readily injected and easily



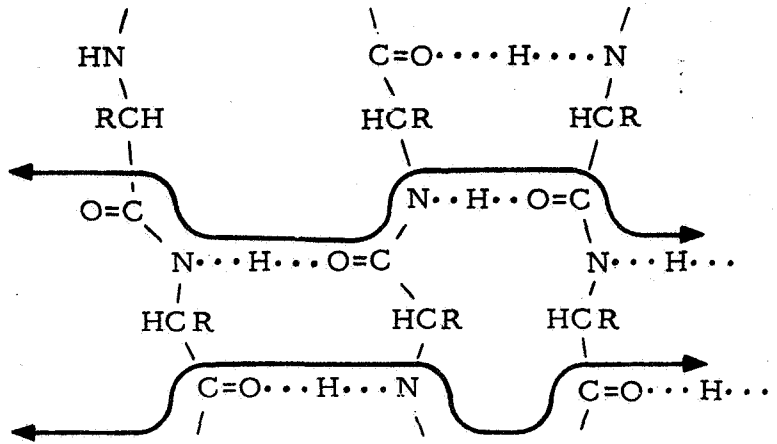
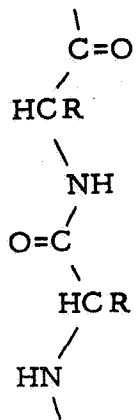
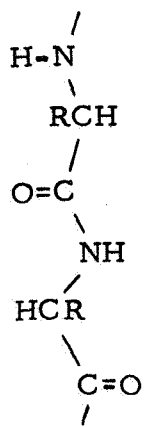
(a) Conduction path for unaligned structure
 Arrow points path of electron flow in a field, holes (charge carrier) migrate in opposite direction - both along a chain and from chain-to-chain.



(b) Conduction path for aligned structure
 Arrow points path along backbone.

c4827

Figure 20. Poly(p-formamidophenylacetylene), Aligned and Unaligned, and the Conduction Path for Each



(a) Separate Protein Chains

(b) Hydrogen-bonded Chains

C0350

Figure 21. Conduction Path Through Hydrogen-Bonded Proteins

transferred — whether by the backbone or by the interchain interaction. Thus, these latter two polymers can almost exhibit isotropic conduction behavior.

In order to establish the best measurement parameter so that a fast real time responsive gas sensor could be developed, a comparison had to be made between d. c. and a. c. conductivity methods. For an a. c. field, the time required for polarization shows up as a phase retardation of the charging current. The phase shift corresponding to a time lag between an applied voltage and induced current causes loss currents and energy dissipation in a. c. circuits which do not require charge carrier migration. For a sinusoidal applied voltage, the charging current is given by

$$I_c = I\omega\epsilon' E \quad (2)$$

where ϵ' is the dielectric permittivity and E is the electric field strength. The loss current is given by

$$I_e = \omega\epsilon'' E = \sigma E \quad (3)$$

where ϵ'' is the dielectric loss factor and $\sigma = \omega\epsilon''$ is the dielectric conductivity. The loss tangent, or dissipation factor, is then

$$\tan \delta = \frac{\epsilon''}{\epsilon'} \quad (4)$$

and it can be written in terms of the electrical conductivity as

$$\tan \delta = \frac{\sigma}{\omega\epsilon'} \quad (5)$$

The electrical resistivity is then expressed as

$$\rho = \frac{1}{\sigma} = \frac{1}{\omega\epsilon'\tan\delta} + \frac{1}{\omega K\epsilon_0\tan\delta} = \frac{1}{(2\pi f)K\tan\delta(8.85 \times 10^{-14})} \quad (6)$$

where the resistivity is in ohm-cm, K is the dielectric constant, $\omega = 2\pi f$ where f is the frequency and ϵ_0 is the dielectric permittivity of a vacuum.

The dielectric properties of poly(phenylacetylene) were determined using one-inch diameter pressed discs, and with metal electrodes applied by vacuum deposition. An electrode area of one cm^2 and a guard ring were

applied on one side of the disc while the entire surface of the opposite face was metallized to form the other electrode. Measurements were made with a General Radio type 1608-A Capacitance Bridge. Table III shows the measured capacitances and dissipation factors as a function of frequency for a 0.071 cm thick disc having aluminum electrodes. It can be concluded from these measurements that the dielectric constant is independent of frequency (500 to 10^5 cycles/sec.). The electrical resistivity of poly(phenylacetylene), as calculated from Equation 6, therefore, is approximately 6.0×10^{11} ohm-cm, or six orders of magnitude lower than the d. c. resistivity measurement.

It is established that the power dissipation in an insulator or capacitor is directly proportional to the dielectric loss factor, $\epsilon' \tan \delta$. Energy losses in dielectrics below about 10^{11} cycles/sec result from two primary ion migration processes: (1) d. c. conductivity losses and (2) ion jump or dipole relaxation losses. In the frequency range 10^4 to 10^5 cycles/sec, the loss factor was constant. Thus, the increase in loss tangent at lower frequencies may be due to ion jump processes. However, this measurement is not considered to be highly reliable, at present, due to a high noise level in the amplifier, and the loss factor may well be independent of frequency.

Dielectric measurements were made with gold electrodes applied by high vacuum deposition on pressed poly(phenylacetylene) discs. The dielectric constant and the loss factor agreed very closely with the measurements made with aluminum electrodes. This indicates that good electrical contacts were obtained between the metal electrodes and the polymer.

The dielectric properties of the other polymers were also measured using the same type of pressed pellets as had been used for the d. c. dark electrical conductivity. The dielectric data were obtained on the pressed pellets since they were easier to handle. Continued work with a. c. measurements was difficult due to the excessive lossiness of the polymers.

Another matter of vital concern was the question of ohmic versus non-ohmic behavior of the various polymers. Earlier, it had been stated that all four polymers showed ohmic behavior when the I-V plot was made on pressed pellets. It was subsequently found that a current-voltage plot for the

TABLE III

DIELECTRIC PROPERTIES OF POLY(PHENYLACETYLENE)

<u>Frequency</u> <u>(cycles/sec)</u>	<u>Capacitance</u> <u>(picofarads)</u>	<u>Loss</u> <u>Tangent</u>	<u>Dielectric</u> <u>Constant</u>
500	3.9	<0.04	3.1
10^3	3.9	<0.04	3.1
5×10^3	3.9	<0.005	3.1
10^4	3.9	<0.001	3.1
5×10^4	3.9	<0.001	3.1
10^5	3.9	<0.001	3.1

poly(p-nitrophenylacetylene), using a thin film in the finger electrode geometry (to be described later), resulted in ohmic behavior (Figure 22). On the other hand, the I-V plot for the amino polymer, under the same conditions, was non-ohmic, as was previously observed for the poly(phenylacetylene).⁽⁴²⁾ This points up some peculiarity of behavior, and apparently an anomaly exists in the thin film case.

2.2.2.3 Charge-Transfer Complexes

In order to determine whether chemisorption or physical adsorption takes place between a gas and the polymer, it would be of interest to examine the polymer/gas interaction by spectrophotometry. In chemisorption, a charge-transfer complex develops which would change the spectral peaks of the original components. Physical adsorption would show little change in the spectra over that of the separate components. Since gas/polymer complexes are difficult to prepare and study by UV spectral analysis, a model compound analysis was made using a solid electron acceptor, e.g., iodine (representative of electron receptor gases), and a polymeric electron donor, e.g., poly(phenylacetylene). Furthermore, the stoichiometry involved in generating an optimum complex would also be of concern. In other words, the mole ratio of iodine to poly(phenylacetylene) that would form a complex and that shows optimum electrical effects or maximum spectral change would be determined. With this information, it would be possible to understand the behavior of the polymer when gases would be used as the complexing agents in place of the iodine.

In addition to the spectral responses, a study would be made of the electrical response of the iodine/poly(phenylacetylene) mixtures. In this way, a relationship could be established between optimum electrical response and maximum spectral response; and these data correlated with the mole function of the complex.

A solution of 0.0025% poly(phenylacetylene) in CHCl_3 was prepared and various amounts of I_2 were added to this. Figure 23 shows the UV-visible spectrum for the pure poly(phenylacetylene), and it is to be noted that there appears to be no maximum above 250 $\text{m}\mu$. By varying the mole ratio of the

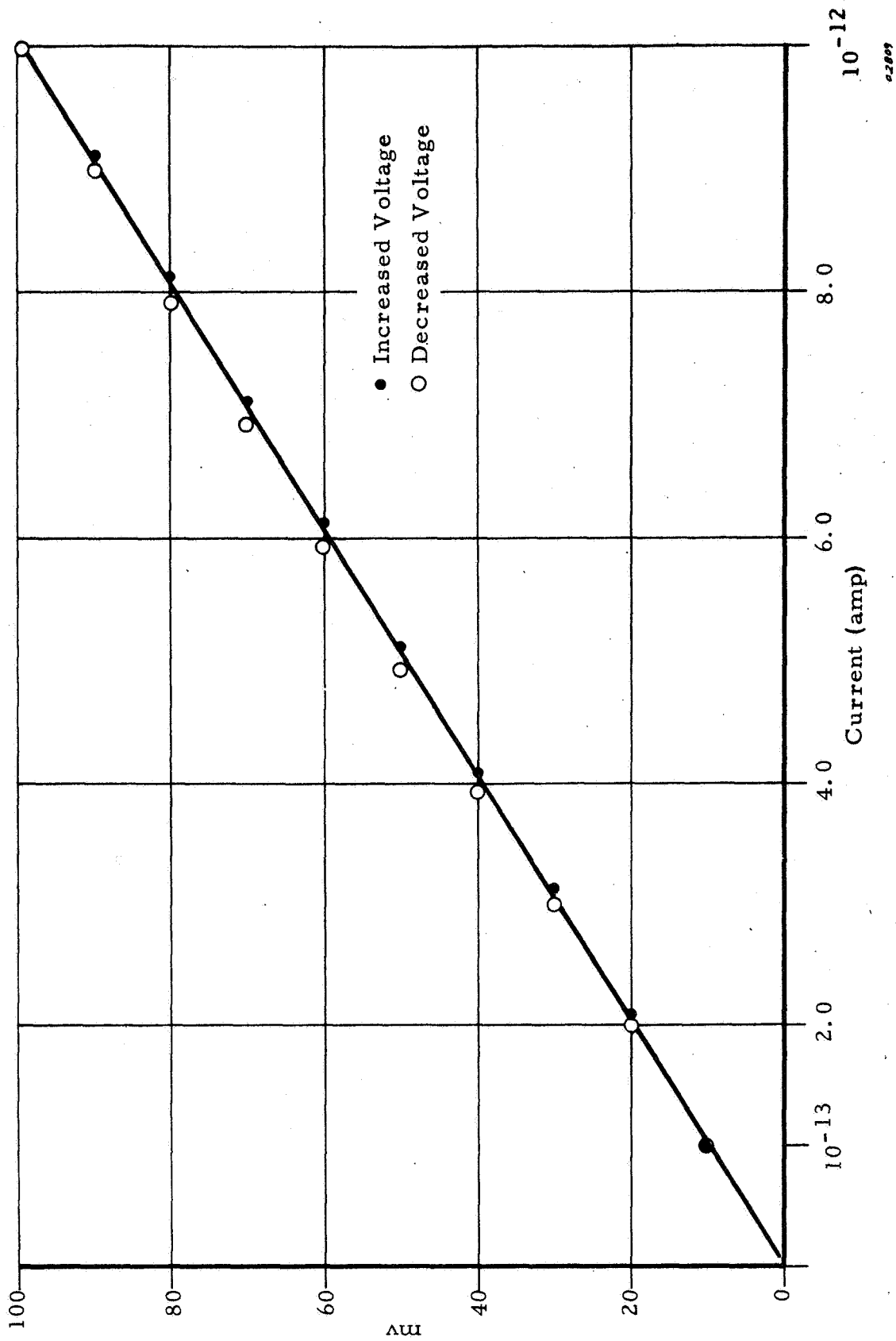


Figure 22. Current-Voltage Plot of Poly(p-nitrophenylacetylene) Film

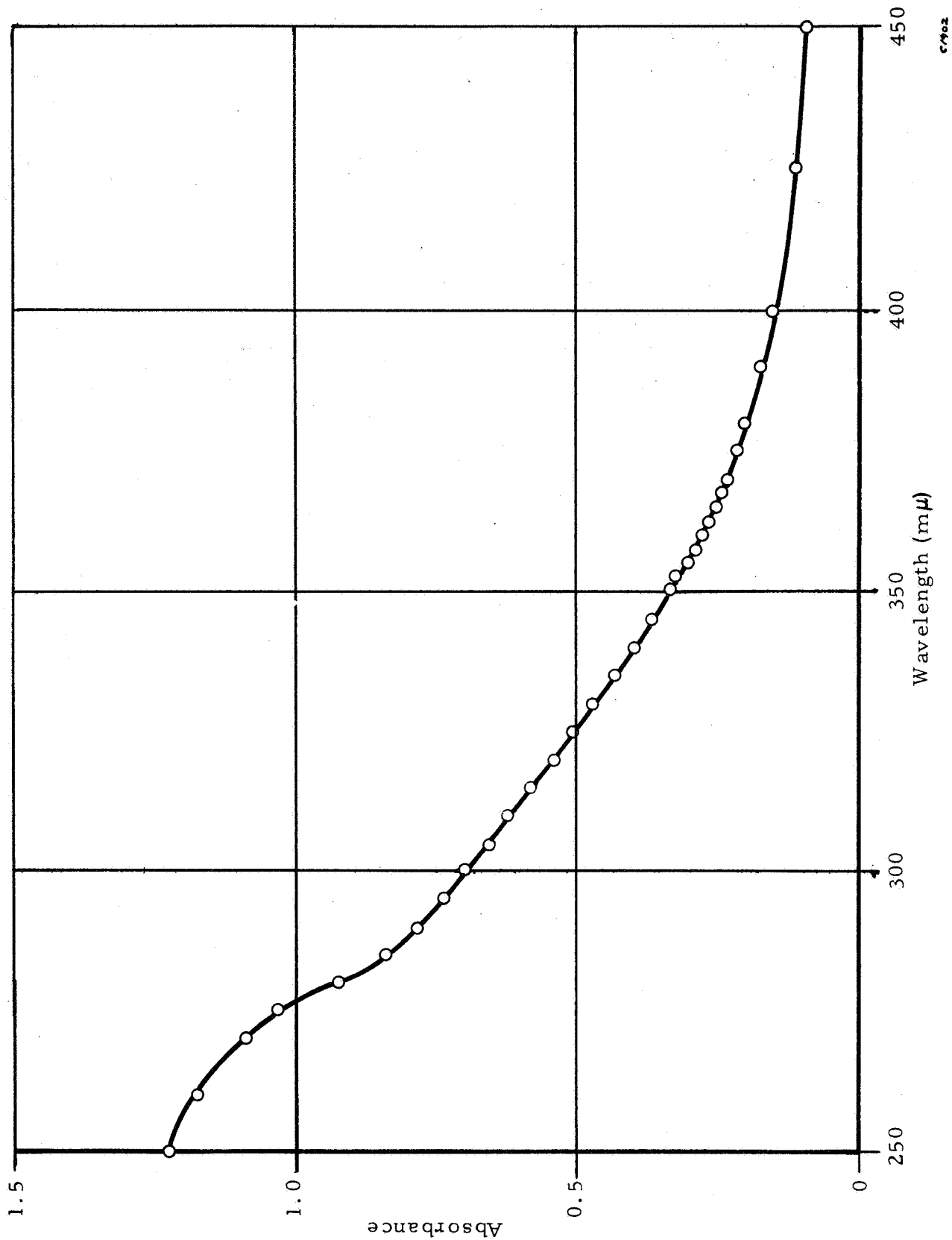


Figure 23. UV - Visible Spectrum of Poly(phenylacetylene) (0.0025% in CHCl₃)

iodine in the mixture, changes developed in the spectra, shown in Figure 24, such that two new peaks appeared – at 295 m μ and 365 m μ – which were I₂-concentration dependent. In addition, it was observed that a ratio of 2:1 (I₂ to poly(phenylacetylene)) gave the greatest absorbance. This is observable from Figure 25 which is a plot of I₂/poly(phenylacetylene) in the mixture versus maximum absorbance. To obtain these absorbances of the mixture, the absorbance of the poly(phenylacetylene) solution (A_{PPA}) and the absorbance of the iodine solution (A_{I₂}) were obtained. The absorbance of the complex (Δ), was then obtained from

$$\Delta = A_{(I_2 + PPA)} - (A_{I_2} + A_{PPA}) \quad (7)$$

where A_(I₂ + PPA) is the absorbance of the mixtures. When a chloroform solution of the iodine complex was subjected to infrared analysis, no visible changes over the pure poly(phenylacetylene) could be detected.

Resistivity data of the various mixtures of I₂/poly(phenylacetylene) were obtained by separately dissolving the I₂ and the polymer in chloroform, in known mole concentrations, mixing these solutions and evaporating to dryness. The residual powder complexes now had mole ratios of varying amounts of iodine/polymer.

The resistivity was determined on pressed pellets of the I₂/poly(phenylacetylene) complex at varying I₂ concentrations in the mixture, and using aquadag electrodes. It was difficult to obtain these data since the iodine tended to sublime out of the system. Table IV shows the results of the resistivity measurements, and they are graphically depicted in Figure 26.

TABLE IV

EFFECT OF I₂ ON RESISTIVITY OF
POLY(PHENYLACETYLENE)

<u>Fraction I₂ in Polymer</u>	<u>Resistivity</u>
0	5 x 10 ¹⁴ ohm-cm
0.08	1 x 10 ¹⁰
0.72	1 x 10 ⁶
1.3	4 x 10 ⁵

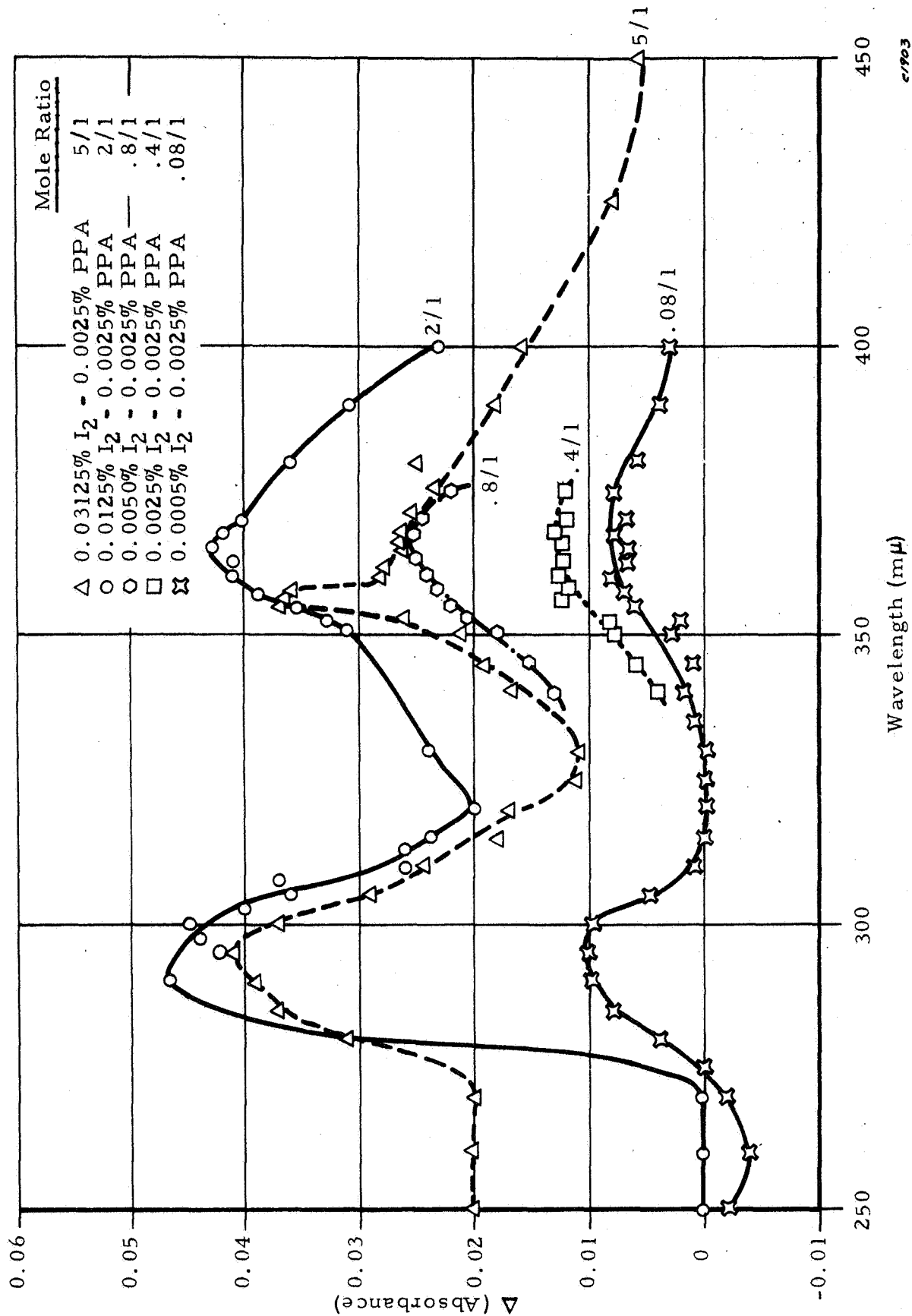
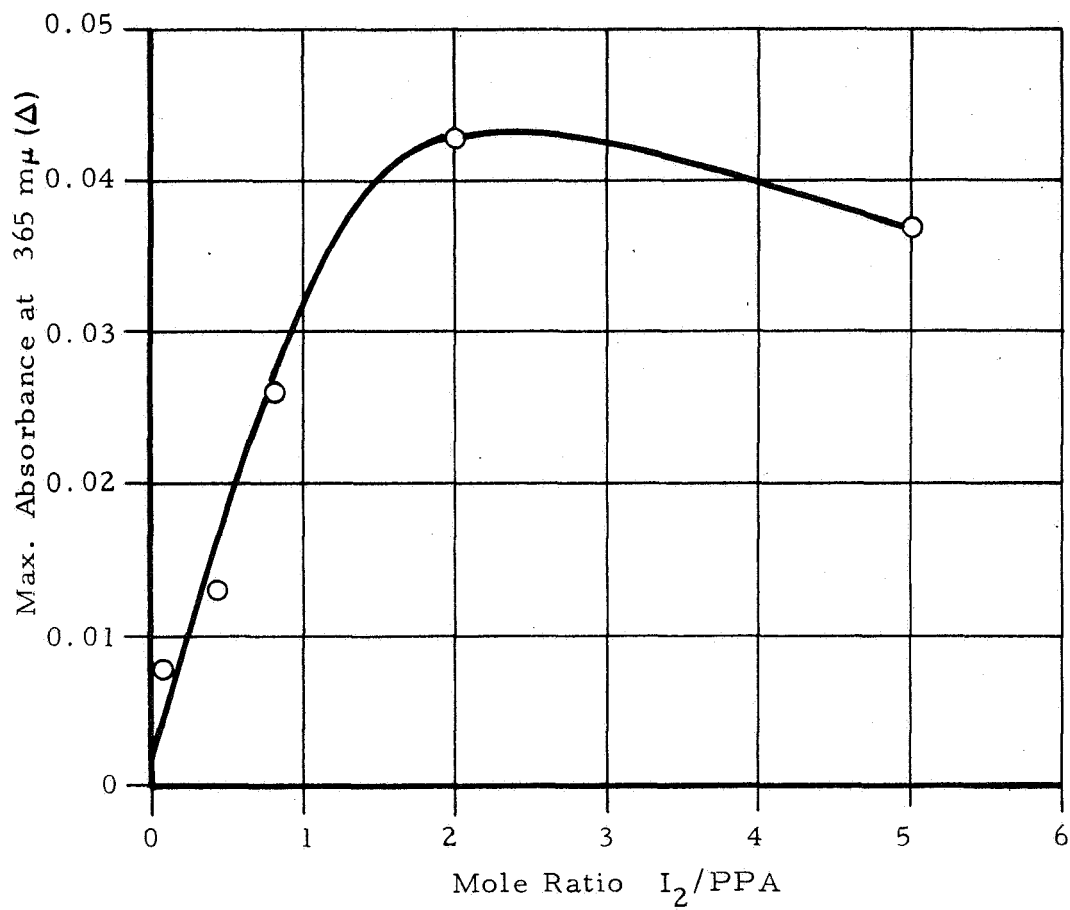
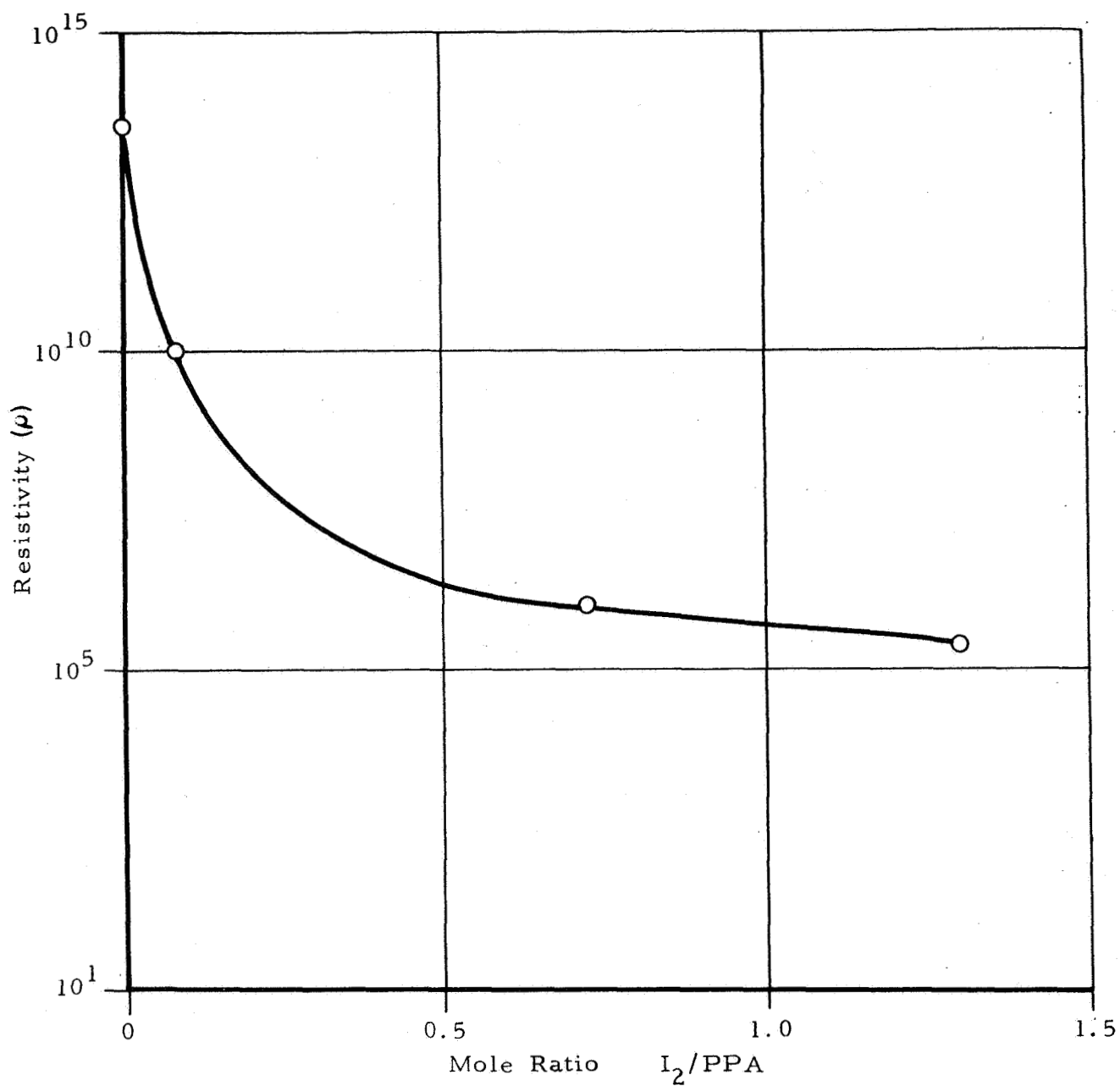


Figure 24. UV - Visible Spectra of Charge-Transfer Complexes (I₂ Plus Poly(phenylacetylene))



C/904

Figure 25. Maximum Absorbance (Δ) Versus Mole Ratio of I₂/Poly(phenylacetylene)



C/905

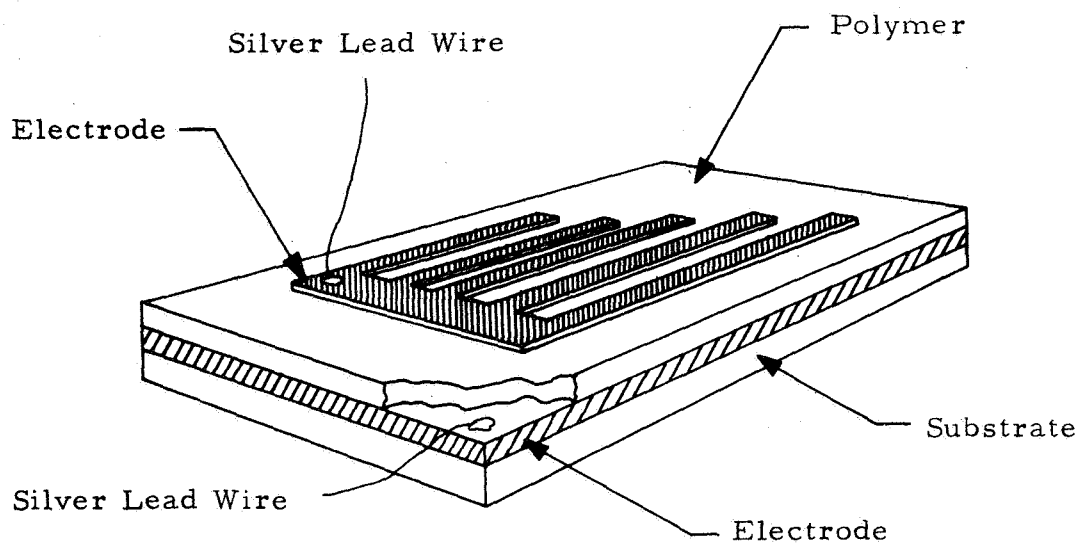
Figure 26. Resistivity Versus Composition of I_2 /Poly(phenylacetylene)

2.2.3 Sensor Preparation

One of the most critical problems of this program had been the preparation of the sensor. This involved the combination of the polymer with the proper electrode geometry and electrical circuitry such that a maximum response, in the shortest possible time and with the greatest sensitivity could be accomplished. A number of possibilities were considered, e. g., pressed pellets, films sandwiched between upper and lower electrodes (finger electrode geometry⁽²⁾) and one-surface polymer-electrode systems (lock-and-key geometry^(36, 40)), among others. The pressed pellets were quickly discounted as they would probably be least sensitive in a bulk-interaction system, plus the fact that grain boundaries and discontinuities would affect the electrical conductivity.

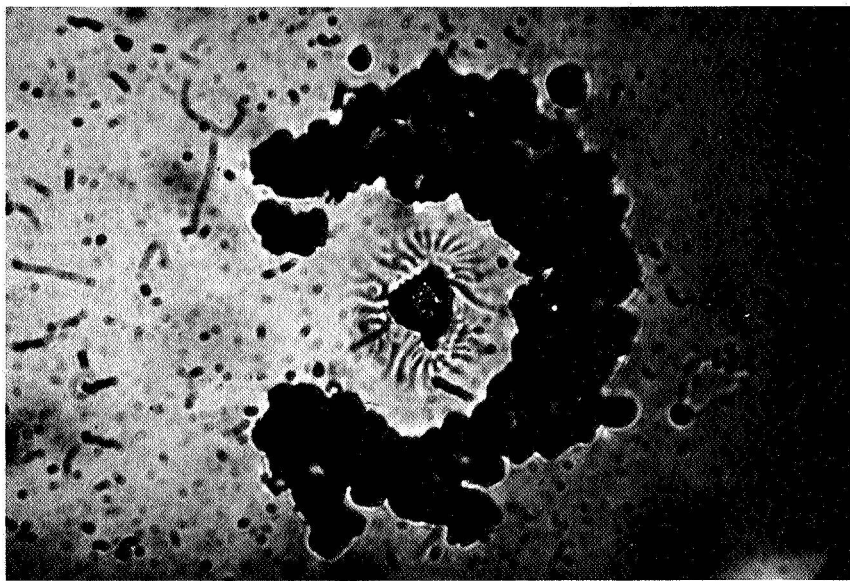
The finger electrode (Figure 27) had one desirable feature in that dissimilar metals could be used for the electrodes, thereby taking advantage of a possible rectification effect due to the couple. Another advantage was the fact that the film thickness between the electrodes could be controlled to the point of having an extremely short distance between electrodes. This is useful in the case of high-resistivity material where the resistivity is possibly due to a number of hopping processes involved in the conduction mechanism which is related to the low molecular weight of the polymer. However, the disadvantages outweighed the advantages. It required the most stringent conditions for its preparation, and the presence of a trace of dust could result in a shorting out of the sensor.^(40, 41) Figures 28 and 29 point up the effect of dust on this sensor. In addition, there appeared to be a limitation to the type of metal feasible for use as an electrode. Gold was preferred, but it resulted in punch-through upon deposition on the polymer. Thus, only aluminum could be used.

Additionally, the force field between the upper and lower electrodes was the greatest beneath the upper electrode finger — not the region between the fingers and the lower electrode. However, it was in this latter region where the gas coming onto the surface would first sit. It would then have to migrate to the region of greatest field (beneath the upper electrode) before a major interaction could occur. The region beneath the upper electrode is polarized



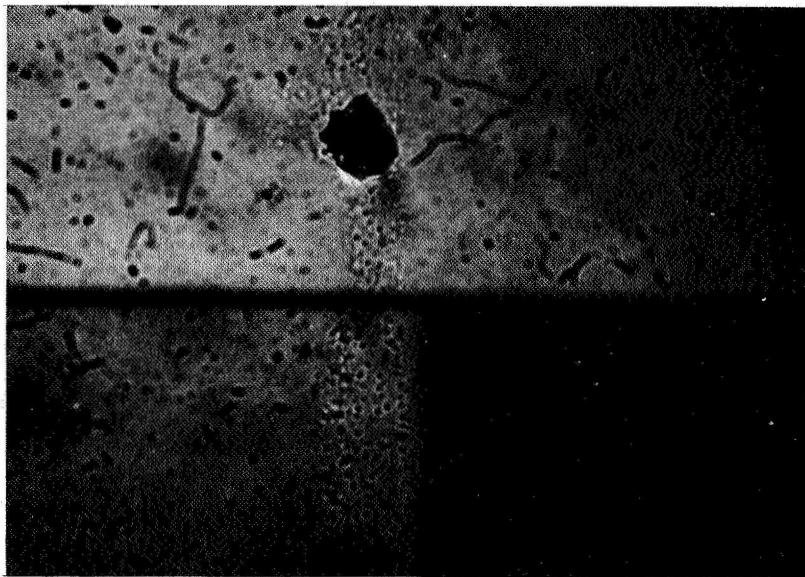
6110

Figure 27. Finger Electrode Gas Detector



C/609

Figure 28. Major Breakdown Point of Sensor



c1608

Figure 29. Minor Breakdown Point of Sensor

with a space-charge distribution at each electrode. Due to this polarization in the space-charge-limited region, the first effect of an incoming gas is to upset the space-charge distribution. If the gas is "inert" to the sensor, it only causes a temporally-dependent effect. The time factor is probably related to the diffusion rate and the pressure of the gas; the charge-redistribution is probably related to the electron-distribution on the gas molecule as well as its molecular size plus the nature of the polymer in the sensor.⁽³⁹⁾ All-in-all, therefore, the finger electrode posed many problems.

In the early phase of the program, a lock-and-key geometry sensor had been given first consideration.^(36, 40) A number of substrates were considered, but there always appeared to be some evidence for contribution by the substrate surface to the electrical response. In addition, it was not possible, at first, to get a narrow line width between the electrodes (a very necessary consideration). The most ideal electrode spacing, related to the polymer molecular weight, would be about 0.1 to 0.3 microns (approximately 0.01 mils). However, this is not readily available by most of the present techniques for photoetching. Therefore, we would have settled for 0.3 to 0.6 mils. Considering the fact, though, that a 45-inch line length would have been the line formed in a 0.3 mil space sensor, and considering the fact that this length with this spacing could not be obtained defect-free, a first approximation to this electrode geometry was a 5 mil width. Advantages of this sensor are that the polymer being on top of the electrode would be more completely exposed to the gas, which should decrease its response time. In addition, increased sensitivity could be achieved from orientation of the polymer in a favorable direction with respect to the electrodes. A further advantage is the fact that the incoming gas can readily get directly to the region of maximum force field without having to migrate, rather than primarily to the equipotential point and then migrate, as in the case of the finger electrode.

A lock-and-key geometry sensor was fabricated by means of the following technique. A thin coat of chromium was vacuum deposited on a good grade of optical glass (Corning 7059), and gold was vacuum deposited on top of this chromium. An electrode configuration was made by means of a photoresist

and mask technique and then removing the gold and chromium by etching. The electrode configuration which was used in the electrical and gas response studies is the 5 mil spacing, 43-line electrode with each line being 2.1 cm long, as shown in Figure 30.

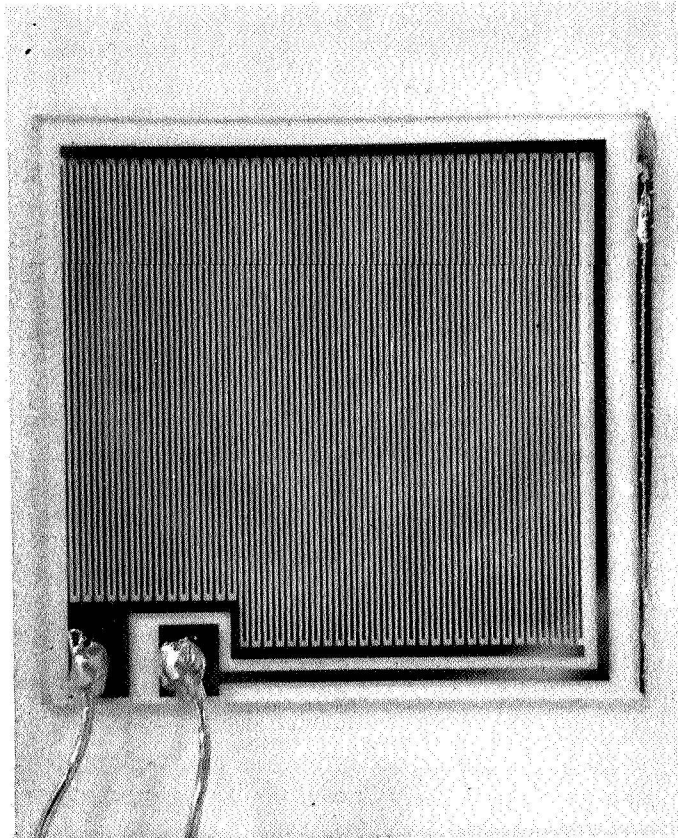
2.2.4 Gas-Polymer Interactions

2.2.4.1 Finger Electrode Geometry

In the early stages of the program, only the finger electrode geometry (Figure 29) with a guard ring was available. In addition, poly(phenylacetylene) was the only polymer available; thus, this polymer on the finger electrode was the most extensively studied system.

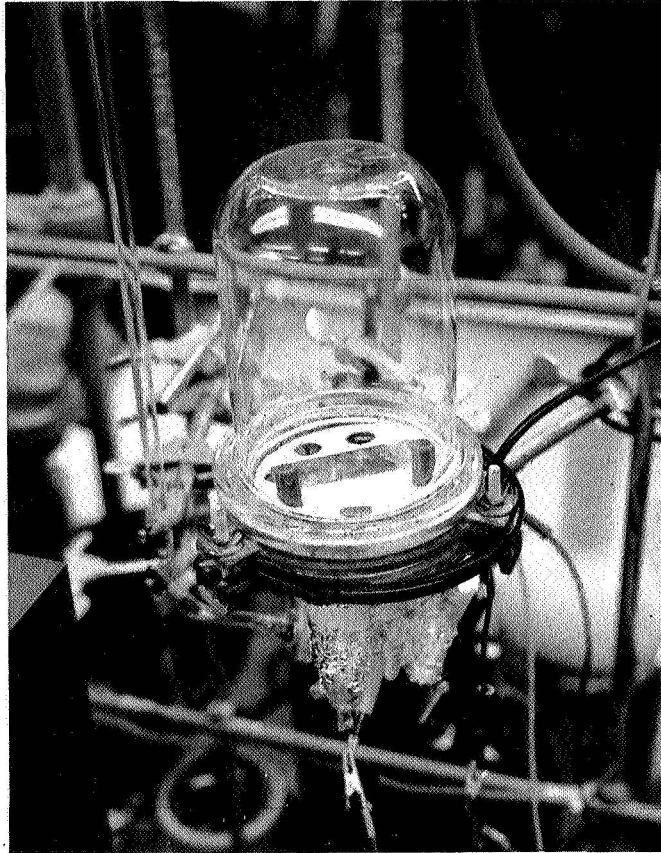
In the first phase of the program, the technique involved was placing the sensor in a chamber of the sort shown in Figure 31, which is connected to the vacuum rack, as seen in Figure 32, and using the measurement circuitry shown in Figure 33. After evacuating to about 10^{-5} torr, the steady-state vacuum reading of the sensor was obtained, i. e., the current at 0.5 volts. A gas was then introduced at a particular partial pressure. An initial change in the current was observed; the magnitude and direction of this change being related to the polarity of the upper electrode, the type of gas, the length of time of evacuation between sample introductions, and the partial pressure involved. Then, after a few minutes, or longer, depending upon the gas, a new steady-state value was obtained. This behavior was exactly the same as that observed by Reucroft, Rudyj and Labes⁽¹⁸⁾ in that they had response times varying from seven minutes (for 0.4 mm pressure NH_3) to about 0.25 minutes (for 84.5 mm pressure NH_3) in order to reach a maximum value. After reaching this maximum value (from the initial steady-state value), there was a slow change to a new equilibrium value slightly lower than the maximum value. They chose the steady-state value as their response time.

Figures 34 through 36 depict some of our earlier responses to ammonia using poly(phenylacetylene) in the finger electrode. It will be observed that varying the pressure from 16 mm to 760 mm caused a pronounced change in the magnitude of the response and a slight decrease in time to reach a new



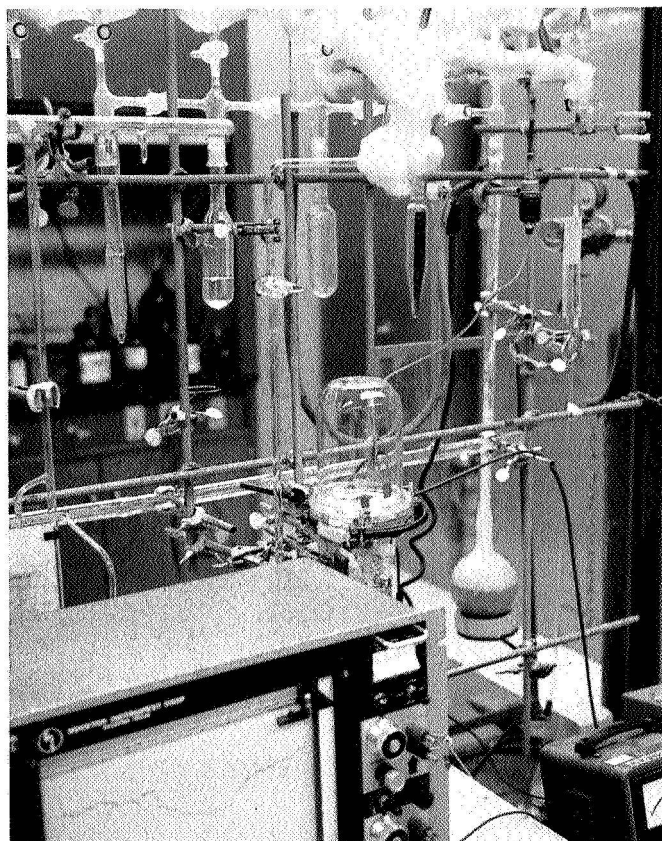
C/894

Figure 30. Five Mil Spacing, 43-Line Lock-and-Key Electrode on a Glass Surface



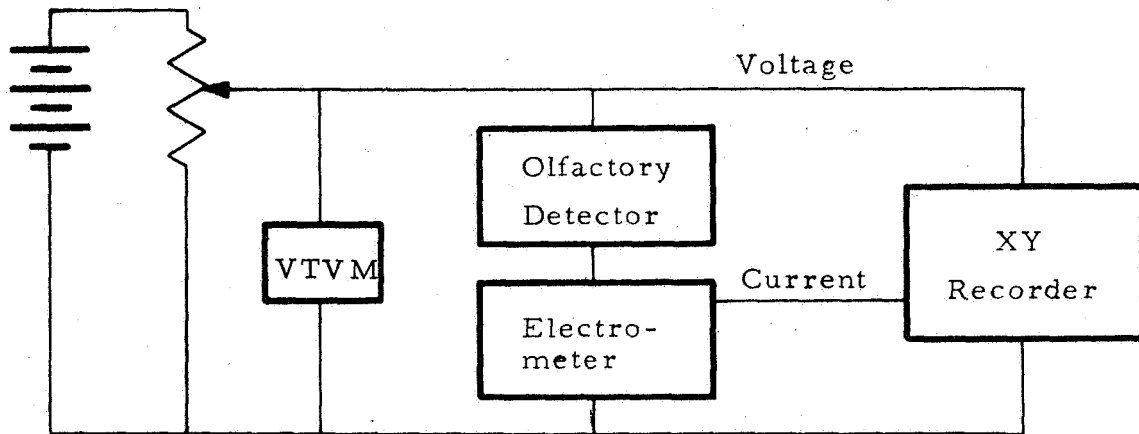
C102

Figure 31. Bell-jar for Maintaining Constant Atmosphere on Sensor



c/103

Figure 32. Constant Atmosphere Chamber
Connected to Vacuum Rack



C1108

Figure 33. Measurement Circuitry

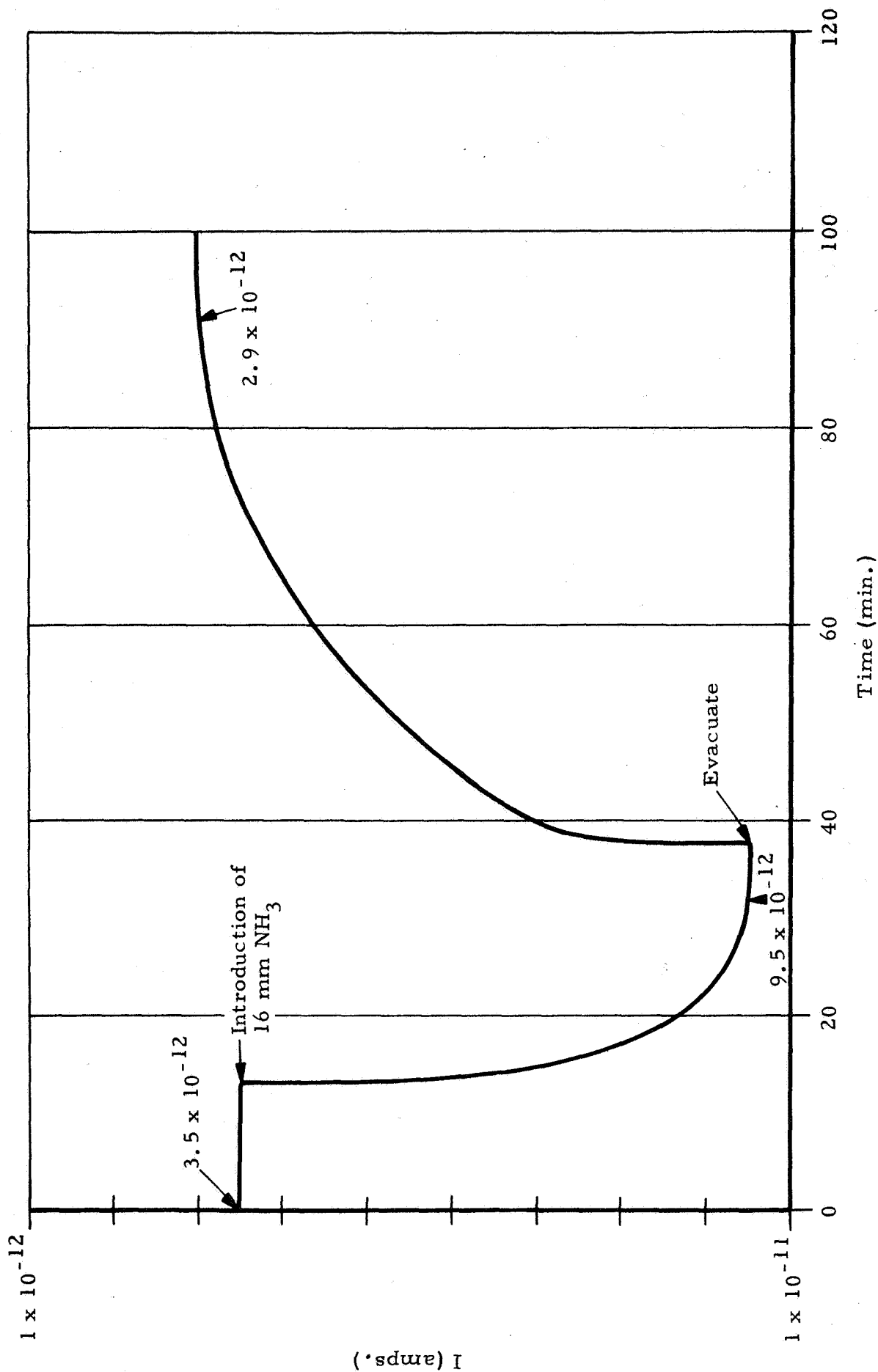


Figure 34. Response of Poly(phenylacetylene) to 16 mm Ammonia (in Dark); Top Electrode (-0.5 Volt)

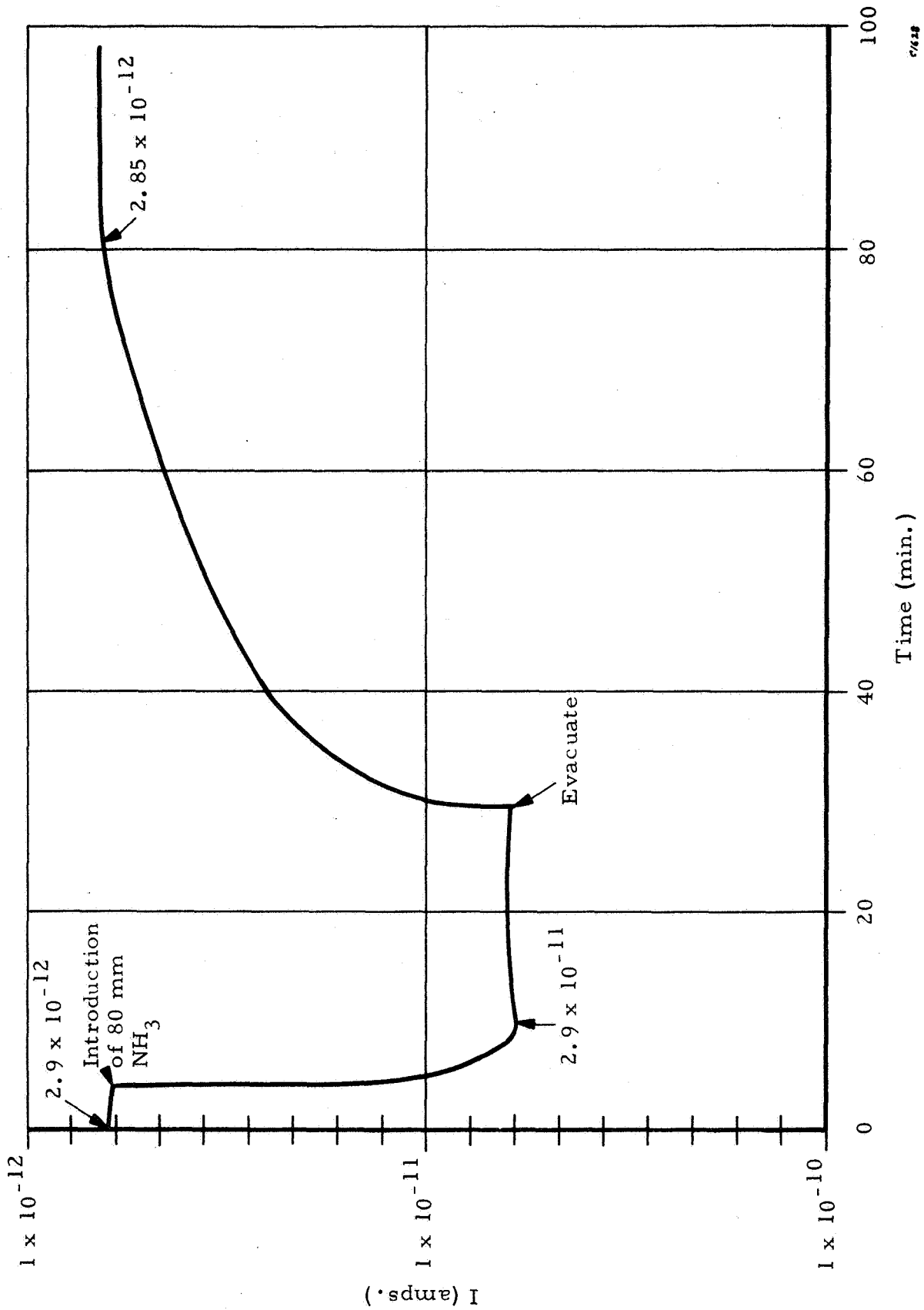


Figure 35. Response of Poly(phenylacetylene) to 80 mm Ammonia (in Dark); Top Electrode (-0.5 Volt)

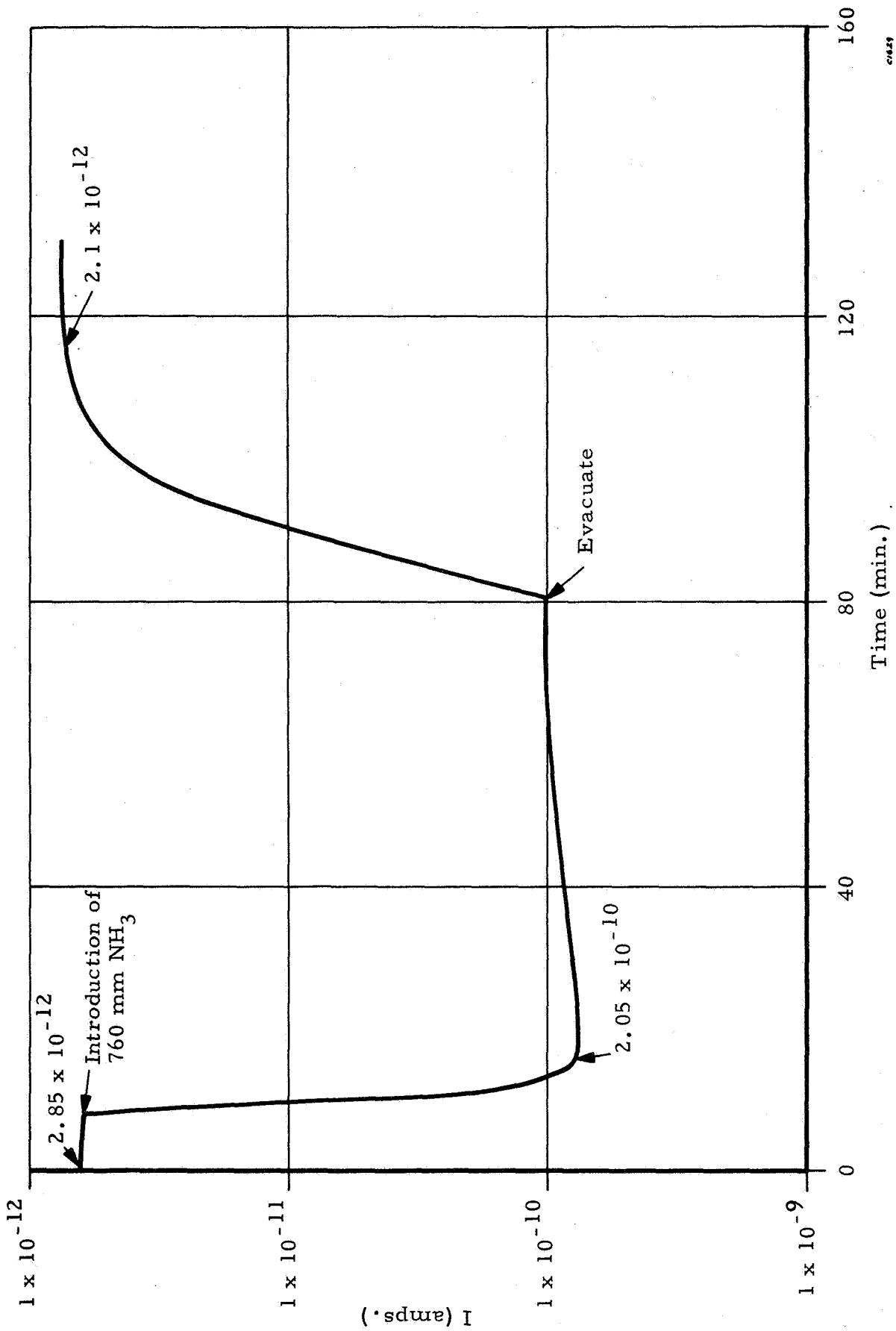


Figure 36. Response of Polyphenylacetylene to 760 mm Ammonia (in Dark); Top Electrode (-0.5 Volt)

steady-state value. This latter effect can probably be related to the space-charge region and the distribution of carriers. In the finger electrode geometry, the incoming gas does not "see" the maximum force field immediately. In fact, it usually hits the polymer surface at the equipotential point. From here, it has to migrate into the bulk film and combine with carriers present. The polymer, however, in this electrode geometry, exists in a polarized form between the upper and lower electrode. Thus, the incoming gas, if it has an electron-donating or an electron-withdrawing tendency, causes a gradual redistribution of the charges in the space-charge region, and it is this gradual redistribution of charges which shows up as the slow response from the initial steady-state value to the final steady-state value.

With the upper electrode negative, the uppermost layer in the space-charge region will consist of holes (p-conductors). Then, as the gas diffuses into the bulk of the material, and the rate of adsorption equals the rate of desorption, a new steady-state develops. This, apparently, is the true steady-state related to the formation of a charge-transfer complex within the bulk of the material, and it is this charge-transfer complex that is responsible for the current-carrying capability of the system. Thus, addition of electron-donating substances will form a strong charge-transfer complex with a corresponding increase in current, which means injection of carriers into the space-charge region. Therefore, the stronger the complex, the larger the current. This current, however, is not related to the surface effect caused by the initial adsorption of the gas on the surface which, in turn, causes the charge redistribution to occur in the uppermost layers. It was earlier shown how a charge-transfer complex, i. e., poly(phenylacetylene) with I_2 , could have a pronounced effect on the conductivity. This same phenomenon is presumed to occur whenever a gas/polymer interaction shows a strong response. Appendix A presents a theoretical discussion of charge-transfer complexes, and how they may affect the polymer.

In some respects, this is analogous to the double layer conductance on silicon and germanium semiconductors on which exist an oxide layer. ⁽⁴²⁾ In creating a double layer, the surface develops a net charge, and the only surface states readily influenced are those due to adsorbed surface

atoms. Some substances that give surface charges upon adsorption are ammonia, acetone vapor, water vapor, dioxane vapor, pyridine vapor and some other electron-donating substances. These give positive charges. Such substances as ozone, oxygen, chlorine, and boron trifluoride give negative charges.

The molecules giving positive charges must introduce energy levels in the vicinity of the normal position of the Fermi level (Figure 37a) which are filled in the neutral atom. In Figure 37b is seen that condition corresponding to an atom adsorbed on the normal position of the Fermi level at the surface. This level is slightly above the Fermi level and is empty in the neutral molecule.⁽⁴²⁾ It is quite likely that a similar phenomenon occurs in the polymeric semiconductors. In other words, just as a double layer was presumed to exist on germanium due to adsorbed gas on the surface, so, too, adsorption of a gas on the organic polymer could create a double layer.

Although a gas may show a quick response when in contact with a sensor if it does not attain a steady-state value different from the start, the effect is not related to complexing characteristics or double layer changes. Rather, it is simply a physical adsorption effect and only related to temporary upsetting of the charge distribution in the space-charge region due either to a pressure effect or a change in the dielectric strength. In other words, the original polarization phenomenon is equivalent to the charging of the plates in a capacitor. When a gas enters and does not complex with the polymer, it acts as a dielectric causing a discharging of the capacitor. However, since it is not an "active" gas, the capacitor can rebuild the charge and the original steady-state returns. Within a short time, the original equilibrium is re-established, and that particular sensor has no capability for detecting a gas of this nature. This effect was observed early with oxygen, CO₂ and argon.⁽³⁹⁾ They gave initial responses, but did not make any major changes from the initial equilibrium condition. Representative of this situation is Figure 38 showing the response of poly(phenylacetylene) to 19 mm oxygen in a finger electrode geometry. After the initial sudden change in current, there was a return to the original equilibrium position. In light of this, it is readily seen

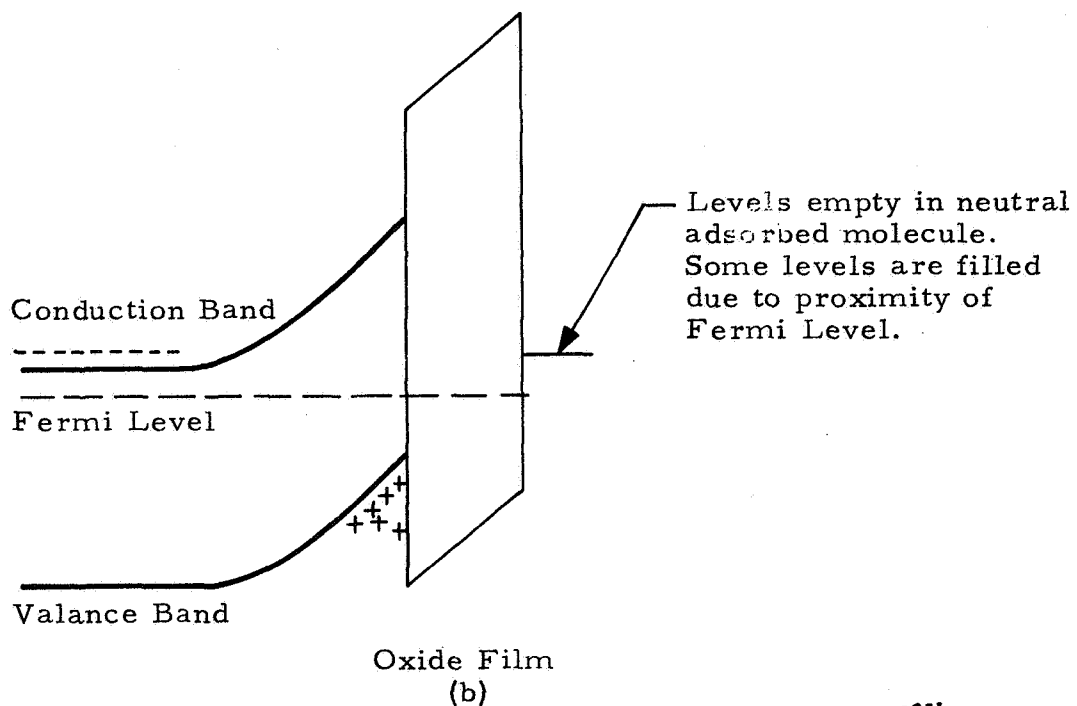
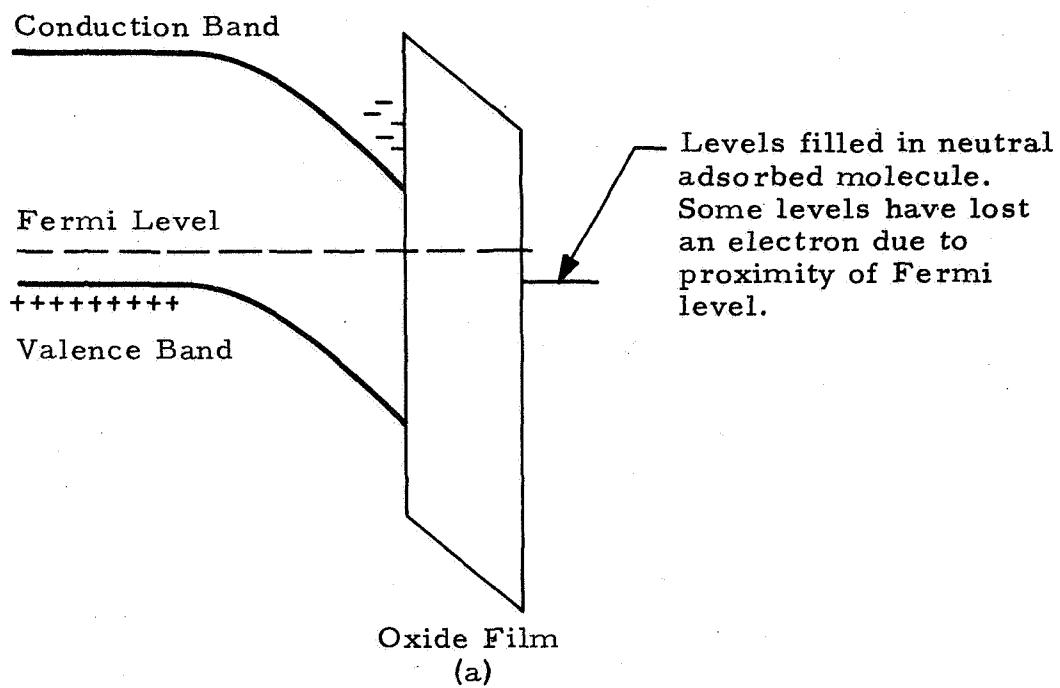


Figure 37. Energy Bands at Surface with Adsorbed Molecules Giving (a) Donor Type Surface States, and (b) Acceptor Type Surface States⁽⁴²⁾ - Q6

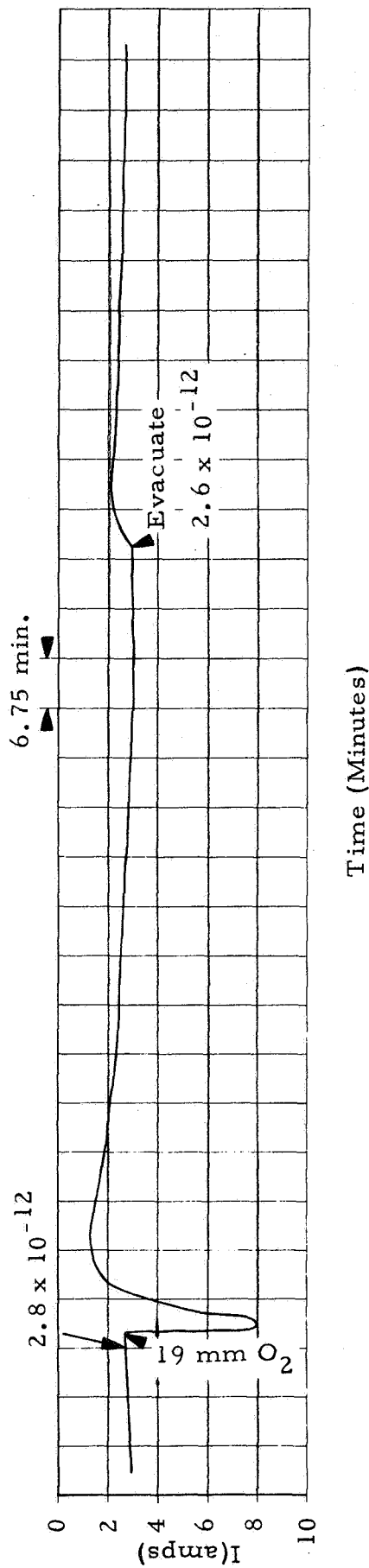


Figure 38. Response of Poly(phenylacetylene) Finger Electrode Sensor to 19 mm Oxygen (in Dark); Top Electrode (-0.5 Volt)

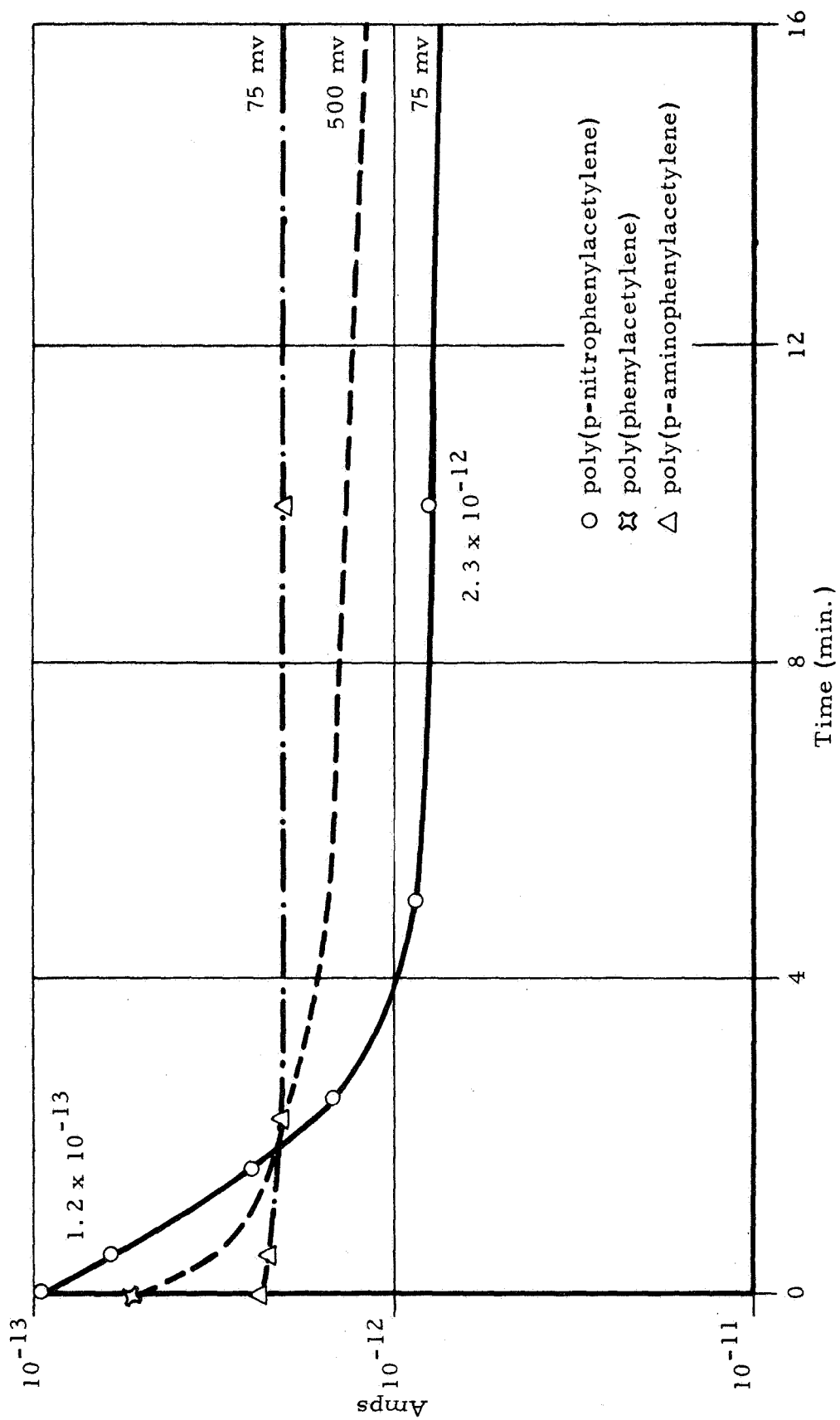
42870

that a gas such as NH_3 could be detected in a mixture with argon or O_2 using the poly(phenylacetylene) as a sensor material.

As the poly(p-nitrophenylacetylene) and the poly(p-aminophenylacetylene) became available, their response behavior to gases was also examined. Using the finger electrode sensor geometry, the dc dark conductivity response of poly(phenylacetylene), poly(p-nitrophenylacetylene) and poly(p-aminophenylacetylene) to 13 mm of ammonia was measured at ambient temperature, as shown in Figure 39. The greatest response was shown by poly(p-nitrophenylacetylene), going from 1.2×10^{-13} amps to 2.3×10^{-12} amps (one order of magnitude) in five minutes. Poly(p-aminophenylacetylene) showed practically no response, and poly(phenylacetylene) showed an intermediate response. If the poly(phenylacetylene) had been run at 75 mv instead of 500 mv, it would most likely have shown a smaller, but definite, response.

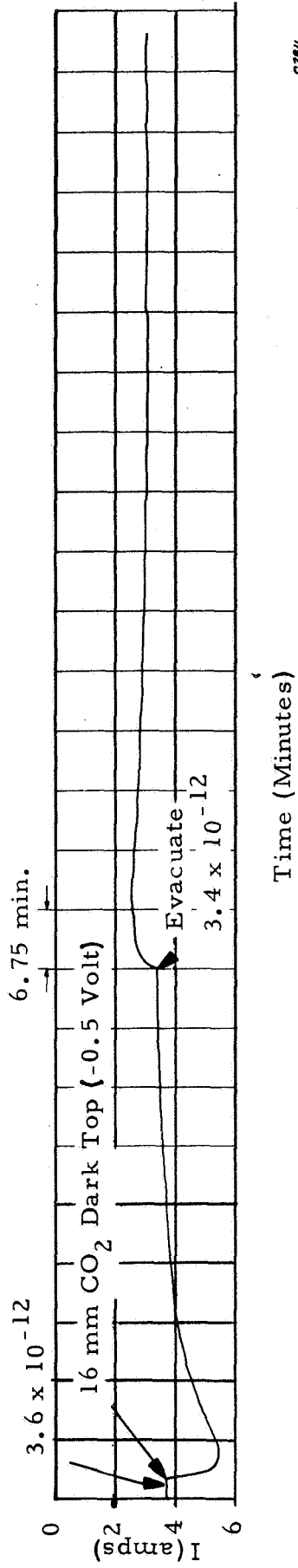
Keeping in mind the electrode geometry, and the types of polymers used, it is relatively simple to explain the response characteristics. With the upper electrode negative, the charged layer at the polymer-metal interface becomes positive, i. e., electron-seeking. In addition, with an electron-withdrawing polymer, such as poly(p-nitrophenylacetylene), this positively-charged region is further enhanced as an electron-deficient region. Thus, any electron-donating gas can more strongly interact at this site. The poly(phenylacetylene) is also electron-withdrawing, but less so than the nitro polymer. However, the amino polymer is electron-donating, thereby orienting more towards the bottom electrode and leaving predominantly neutral sites at the surface, thus, there is no tendency to interact with an electron-donating species. Furthermore, although a resonance form of the amino polymer depicts a positively-charged site on the nitrogen atom, the polarization to a positive interface near the upper electrode would lower the tendency for the amino polymer to assume this resonance structure when used in the finger electrode geometry.

When electron-withdrawing gases were evaluated, their response characteristics were not as striking as for the ammonia system. The effect of SO_2 on the electrical properties of films of the amino and nitro polymer was examined with the finger electrode. When an electric field was applied, the interaction of SO_2 with the nitro polymer caused a small decrease in the d. c. conductivity



62195

Figure 39. Response of Sensors to 13 mm Ammonia (in Dark)



CSB//

Figure 40. Response of Sensor to 16 mm CO₂ (in Dark); Top Electrode (-0.5 Volt)

while for the amino polymer, no change occurred. Tables V and VI show a d. c. electrical response of the nitro and amino polymer after exposure to 13 mm SO₂.

There is some evidence that the SO₂ is very strongly adsorbed on the nitro polymer and required heating to a high temperature (100°C in vacuum) in order to restore the properties of the polymer. This is understandable when one considers that the nitroaromatics are radical traps and that SO₂ is a diradical. Thus, they can combine quite readily. However, just as in the case of polysulfones, made from SO₂ and a vinyl monomer, heating regenerates the SO₂ and the monomer.

The response of CO₂ on the nitro and amino polymer was very similar to that found previously for poly(phenylacetylene),⁽³⁹⁾ and Figure 40 depicts the CO₂/poly(phenylacetylene) interaction response curve. A small initial response was observed on the d. c. conductivity, but the final steady state value was approximately the same as the initial value.

Figure 41 is the response curve for trimethylamine, and Figure 42 is that for triethylamine. In these two instances there was an initial change to a decrease in current followed by a change towards an increase in current. With trimethylamine, at 16 mm, the changes were quite small. However, with triethylamine, they were quite pronounced. In fact, the sign of the current changed at the initial maximum, and then it went back to another maximum before leveling off to a new steady-state. Obviously, it is important to know what the mechanism of action is before one can decide which datum point to use as being indicative of the response characteristics of the system. Reucroft, et al,⁽¹⁸⁾ used the final steady-state value (after it had passed through its maximum value).

It is interesting that inorganic semiconductors have shown similar responses, and could possibly be related to our systems. For example, the effect of oxygen adsorption on the electrical properties of a semiconductor solid, such as zinc oxide, has been amply demonstrated.⁽⁴³⁾ In addition, it has been shown that a p-type semiconductor, such as chromia-alumina, had changes in conductivity over several orders of magnitude, as well as change in

TABLE V

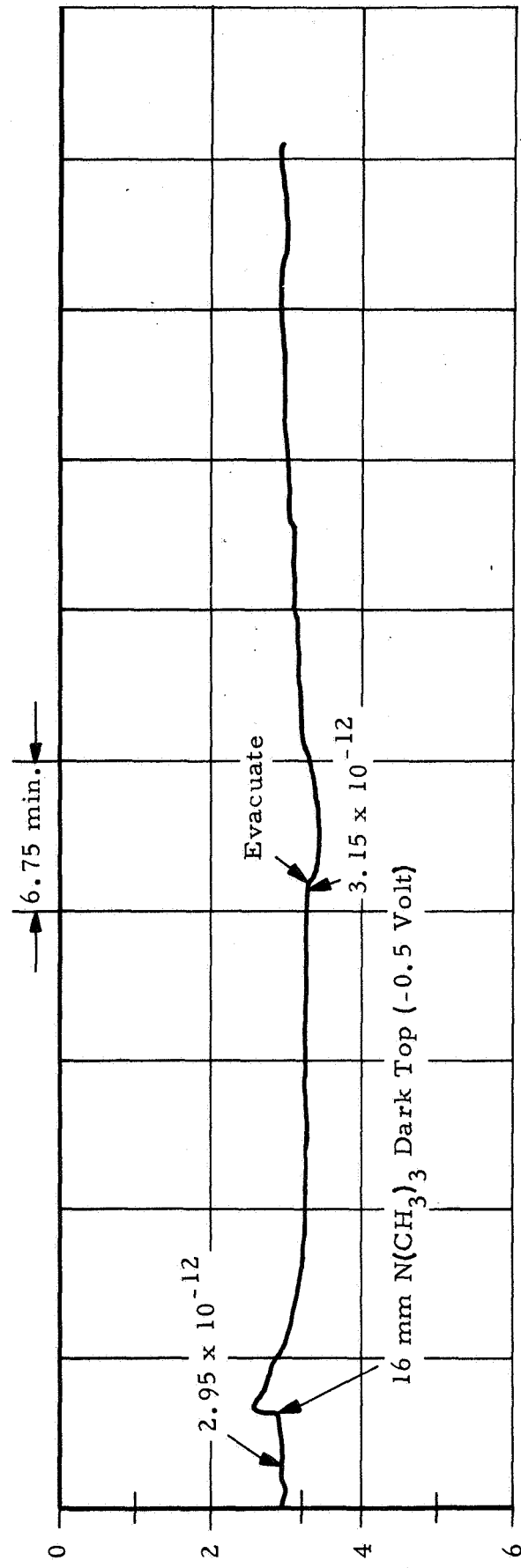
RESPONSE OF POLY(P-NITROPHENYLACETYLENE) TO
13 MM OF SO₂ WITH 75 MV APPLIED POTENTIAL

<u>Time (sec)</u>	<u>I (amp)</u>
0	8×10^{-14}
20	$< 10^{-15}$
100	$< 10^{-15}$
450	$< 10^{-15}$
600	$< 10^{-15}$
900	$< 10^{-15}$
Evacuate	
0	$< 10^{-15}$
30	1.5×10^{-14}
100	2.8×10^{-14}
300	5.7×10^{-14}
900	8.0×10^{-14}

TABLE VI

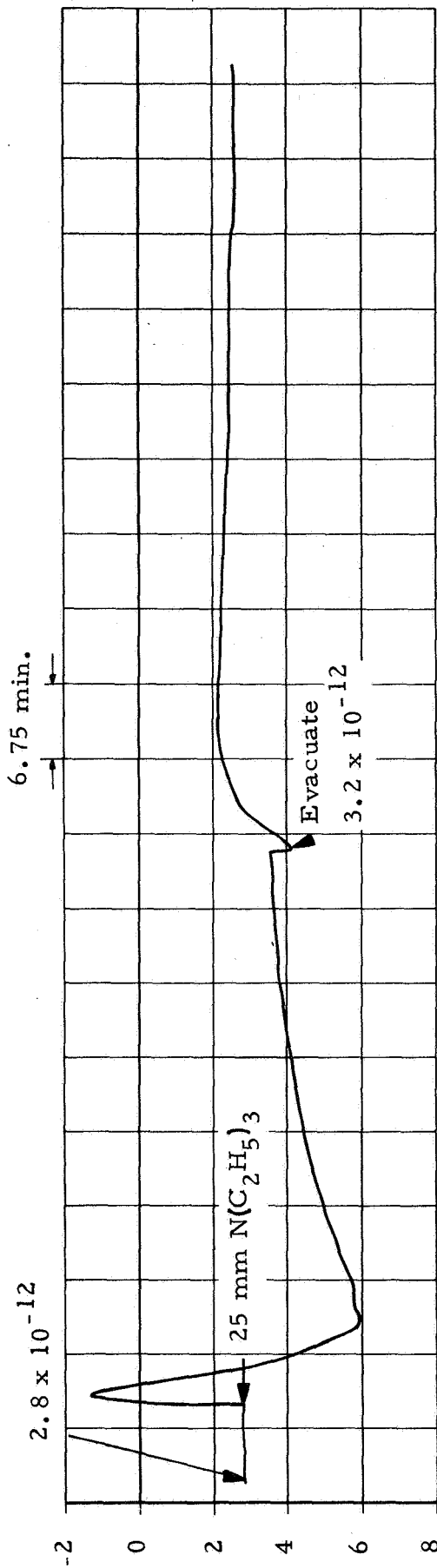
RESPONSE OF POLY(P-AMINOPHENYLACETYLENE) TO
13 MM OF SO₂ WITH 75 MV APPLIED POTENTIAL

<u>Time (sec)</u>	<u>I (amp)</u>
0	2.4×10^{-13}
20	2.2×10^{-13}
40	2.2×10^{-13}
120	2.2×10^{-13}
300	2.1×10^{-13}
600	1.8×10^{-13}
900	1.8×10^{-13}
Evacuate	
0	1.7×10^{-13}
120	1.9×10^{-13}
300	2.1×10^{-13}
600	2.1×10^{-13}
900	2.1×10^{-13}



c/430

Figure 41. Response of Poly(phenylacetylene) Sensor to 16 mm Trimethylamine (In Dark); Top Electrode (-0.5 Volt)



2/63/

Figure 42. Response of Poly(phenylacetylene) Sensor to 25 mm Triethylamine (In Dark); Top Electrode (-0.5 Volt)

semiconductor type (p to n) within seconds of a change in the gaseous environment.⁽⁴³⁾ Weisz⁽⁴⁴⁾ has claimed that it is logical to consider the possibility of compound formation between the adsorbate and the solid, accompanied by donation or acceptance of electrons, depending on the relative position of the chemical potential in the adsorbate and in the solid (i. e., the Fermi level). Such a contact between an adsorbate and a semiconductor would then lead to charge redistribution. Then, as chemisorption proceeds, the potential of the electrical barrier layer grows and a progressive change takes place in the Fermi level of the solid relative to the adsorbate. Thus, the energy release for successive electron transfers changes.

If the upper electrode is negative, the uppermost layer will consist of holes (p-conductors). Addition of electron-donating substances will cause a strong charge-transfer complex to form with a corresponding increase in current. Then, as the gas diffuses into the bulk of the material, and the rate of adsorption equals the rate of desorption, a new steady-state can develop. This apparently is the true steady-state related to the formation of a charge-transfer complex within the bulk of the material, and it is this charge-transfer complex that is responsible for the current-carrying capability of the system. Thus, the stronger the complex, the larger the current.

Another consideration to keep in mind regarding response capability is the steric factor. Although ammonia is a weaker base than trimethylamine or triethylamine, it is less sterically hindered, and being a smaller molecule it can diffuse more readily. Furthermore, when the first layer of ammonia molecules are adsorbed on the surface and form a complex with the active species in the space charge region adjacent to the electrode, they present a surface of hydrogen atoms to the gas molecules which have not yet had a chance to become adsorbed. On the other hand, adsorption of trimethylamine on the surface (and its subsequent complexing in the space charge region) presents a mass of methyl groups to the oncoming gas molecules. Bewig and Zisman⁽⁴⁵⁾ have reported that a surface whose outermost aspect comprises methyl groups in closest packing has the lowest surface energy (and the least adsorptivity) of all hydrocarbon surfaces. Thus, the hydrogen atoms in ammonia will neither interfere sterically nor, with respect to

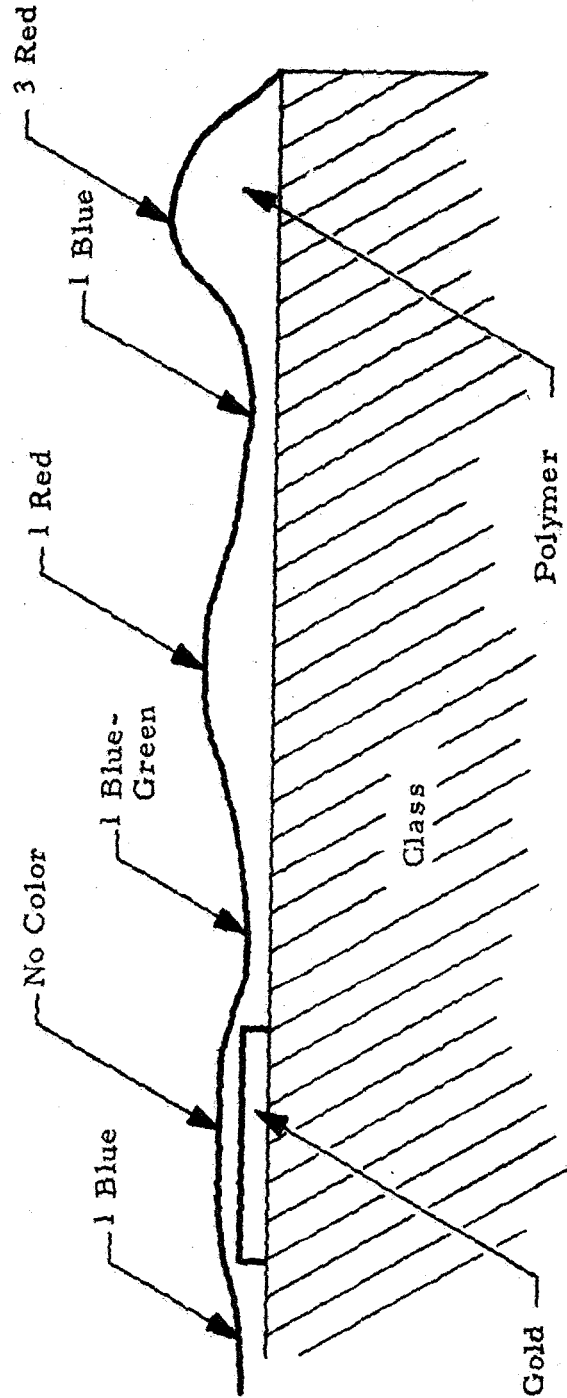
surface energy, with further adsorption and migration into the polymer; the trimethylamine will act both sterically, and with respect to surface energy, to minimize adsorption. In view of this, the ammonia can complex with more sites per unit concentration of gas than the other amines, thereby showing the greatest conductivity.

2.2.4.2 Lock-and-Key Electrode Geometry

As has been indicated, considerable difficulty was encountered with the sandwich (finger electrode) system. There was not only the problem of obtaining sensors that were not shorted through the polymer, but the response speed was poor. Apparently, there was a diffusion controlling step between the time the gas became adsorbed on the polymer and the time it took to reach a maximum response. To overcome this, the surface (lock-and-key) electrode geometry was developed. A number of electrode spacings were made (one mil, two and a half mil and five mil, among others), but the system most extensively used was the five mil spacing electrode (Figure 30).

After a number of sensor coating methods were tried, an approach was finally settled upon that appeared to give good, reproducible films. The sensor was held on one edge with tweezers, keeping the electrodes in the vertical position. It was dipped into the polymer solution and then slowly withdrawn as gradually and as steadily as possible, allowing the surface tension of the solution to pull excess liquid off the surface. The sensor was then stood on edge on a piece of Kimwipe and allowed to dry. While in this position, the Kimwipe pulls off any bead which tends to form at the bottom edge of the sensor.

Film thickness measurements were attempted by using a microscope and counting interference fringes due to internal reflection between the glass substrate and the surface of the polymer,⁽⁴⁶⁾ or, as it is commonly known, the multiple internal reflection technique. Figure 43 is a profile of the coating of a 4% polymer solution on a sensor. It depicts the last line of the electrode before the edge of the sensor is reached, and it extends to the right to the edge of the glass. The colors shown refer to the fringe color at the high or low point in that area. The thickness of the polymer is a multiple of $1/2$ the wavelength of the color shown. Extending to the left, the color was found to



43288

Figure 43. Profile of 5 Mil Sensor Coated with 4% Solution of Poly(p-nitrophenylacetylene) Colors Refer to Interference Fringes.

be the same between all the electrode lines, and the film thickness of the polymer between the electrodes was found to be approximately 2400 Å (~0.24 microns). Using the 4% solution as a standard, it was also found that the polymer film on top of the electrode surface showed no interference fringes, and it was assumed to be about 2000Å, or less, thick. Since the gold electrodes are about 3000Å thick, it was believed that the polymer was very close to the gold electrode surface and then dipped down somewhat between the electrodes, depending on the solution concentration from which it was cast. This technique was used for casting films from a 4%, 1%, 0.1%, 0.01% and a 0.001% solution. The resultant films were evaluated for the effect of film thickness versus gas response.

One last film was prepared on a sensor, namely, a monomolecular film. The technique used was essentially that described by Daniels, et al.⁽⁴⁷⁾ A six inch petri dish was fitted with glass baffles to minimize turbulence, and filled with deionized water. A piece of filter paper was placed on the surface and allowed to sink, carrying with it any dust particles, etc., which might have settled on the surface. A glass stirring rod was used to pick up a drop of the 4% polymer solution [poly(p-nitrophenylacetylene) dissolved in nitrobenzene], and the drop touched to the surface of the water where it spread into a film. A large enough dish was used so that the film did not touch the edges. The nitrobenzene was allowed to evaporate off, and there was left, on the surface, a thin, unbroken film of polymer. It is stated⁽⁴⁷⁾ that if the film spreads uniformly over the surface of the water and does not touch the edge of the dish, it exists as a monomolecular film.

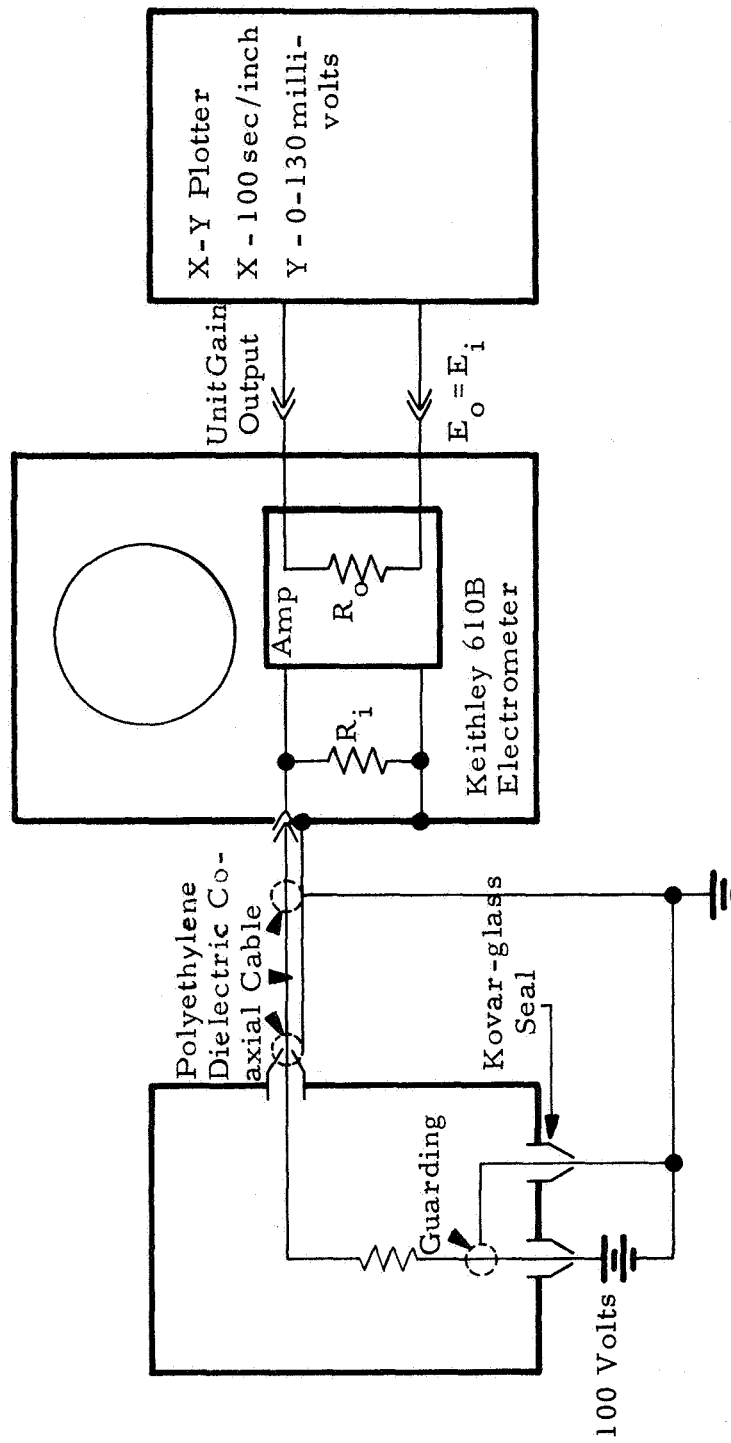
The sensor to be coated was thoroughly cleaned, dried and inserted into the water beneath the film while holding it with a pair of spring-closed tweezers. The sensor was then raised slowly through the film at an angle such that the film adhered to the top of the sensor first, and the water could flow off the sensor between the film and the sensor surface. Some water remained trapped between the two, however, and the behavior of the trapped water was taken as evidence for the existence of a film on the sensor. The coated sensor was allowed to dry until no water was visible.

After considerable experimentation with voltages, power supplies, electrometer configurations, surface leakage paths and guarding techniques, the circuitry described schematically in Figure 44 finally evolved for use in the conductance measurements. The guarding method, which consists of a copper braid surrounding the high voltage electrode, prevents current from the +100 volt input electrode from leaking across the glass of the bell jar to the electrometer input side. It does not prevent possible shunting by leakage paths of the electrometer input back to the high voltage electrode. However, this is exceedingly small compared to the former possibility.

The electrometer provides an impedance-matching amplifier to permit the voltage read across its input resistor to be recorded on a low impedance input recorder. The recorder is calibrated at 20 mv/inch (100 mv full scale). This arrangement insures that the sensor will always have no less than 99.9 volts across it, so that the current read on the recorder is inversely proportional to the resistance of the sensor. Furthermore, the input lead to the electrometer will never have much more than 100 millivolts across it, and shunt current leakage will be minimized.

The electrometer-recorder combination is capable of recording voltage rise-times at a rate no greater than approximately 50 mv/sec, or full scale deflection on the recorder of no faster than 2.6 seconds. The recorder mechanism will move faster than that with an excessive voltage applied, but in order to reduce the errors due to inertial effects, it is believed that little credence can be given to results obtained that fast. In fact, due to the time scale used in these measurements, times of less than 5 seconds cannot be measured accurately.

It should be noted, for clarification in reading the strip chart recorder data, that there is noted, on some of the charts, the value of the input resistance, viz., $10^9\Omega$, $10^{10}\Omega$, $10^{11}\Omega$, etc. The vertical scale is calibrated in millivolts, and it represents the voltage drop across the input resistance caused by the current generated in the sensor under an applied potential of 100 volts. Thus, the current is found from $I = E/R = mv \times 10^{-3}/R$. Once all these manipulations and standardizations were made on the system, all the data obtained became more meaningful.



c3289

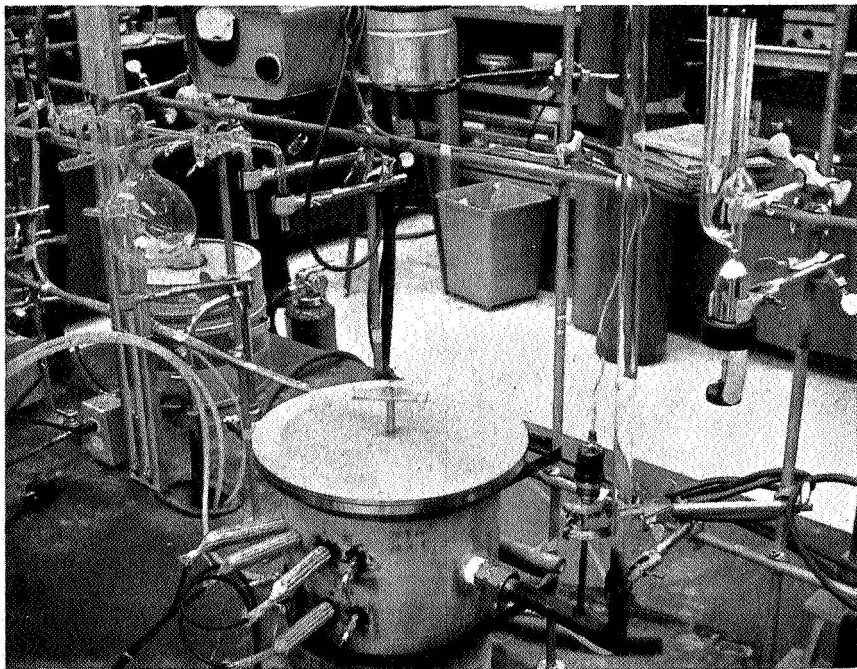
Figure 44. Schematic Drawing of Measurement Circuitry

Subsequent to the earlier method of using a glass bell-jar for maintaining a constant atmosphere on the sensor (Figures 31 and 32), a modified system was adopted (Figure 45) that used a stainless steel vacuum chamber. This eliminated the need for a metal can over the bell-jar (used to minimize RF effects). The leads were soldered to terminals brought out through aluminum oxide insulators, and utilized the same circuitry shown in Figure 44. All high impedance leads were carefully shielded and a 100 volt battery-powered potential source was applied across the sensor.

In the finger electrode geometry, surface effects could be eliminated by using a guard ring. This was not possible with the lock-and-key electrode. Thus, to resolve whether a surface or bulk effect was the operating factor, a number of 5 mil spacing sensors were prepared by the dipping technique mentioned earlier, and from various solution concentrations. Using the 4% solution as a standard (the film thickness from this concentration was described above), poly(p-nitrophenylacetylene) solutions of 1%, 0.1%, 0.01%, and 0.001% concentrations were prepared. In addition, the monomolecular film, described earlier, was also prepared. It was assumed that the films would decrease in thickness proportionately and coat the sensor in a manner somewhat like that shown in Figure 46. It should be noted that the sizes shown are not proportional to actual dimensions. The space between the electrodes and the electrode widths are equal (5 mil), but the electrode height is only 0.3 microns, and it could not be shown in proper perspective. However, the major intent is to give some relative idea of the change in film thickness as one decreases the bulk. The limit, therefore, is that of a true "surface" with no bulk, viz., the monomolecular film.

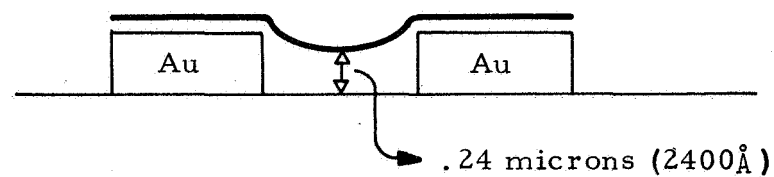
The coated sensor was placed in the vacuum chamber, and the system evacuated overnight at a pressure of about 1×10^{-4} torr. A "base" current was then read at 100 volts and recorded on the strip chart.

It is well-established that the conductivity of any material (insulator or semiconductor) increases with decreasing thickness, and that an insulator at about 100\AA thickness can behave like a semiconductor.⁽⁴⁸⁾ Figure 47 appears to further document this. It is seen that the maximum conductance was found



68727

Figure 45. Modified Vacuum Chamber for Gas Measurements



(a) - 4% solution



(b) - 1% solution

Thickness not determined



(c) - 0.1% solution

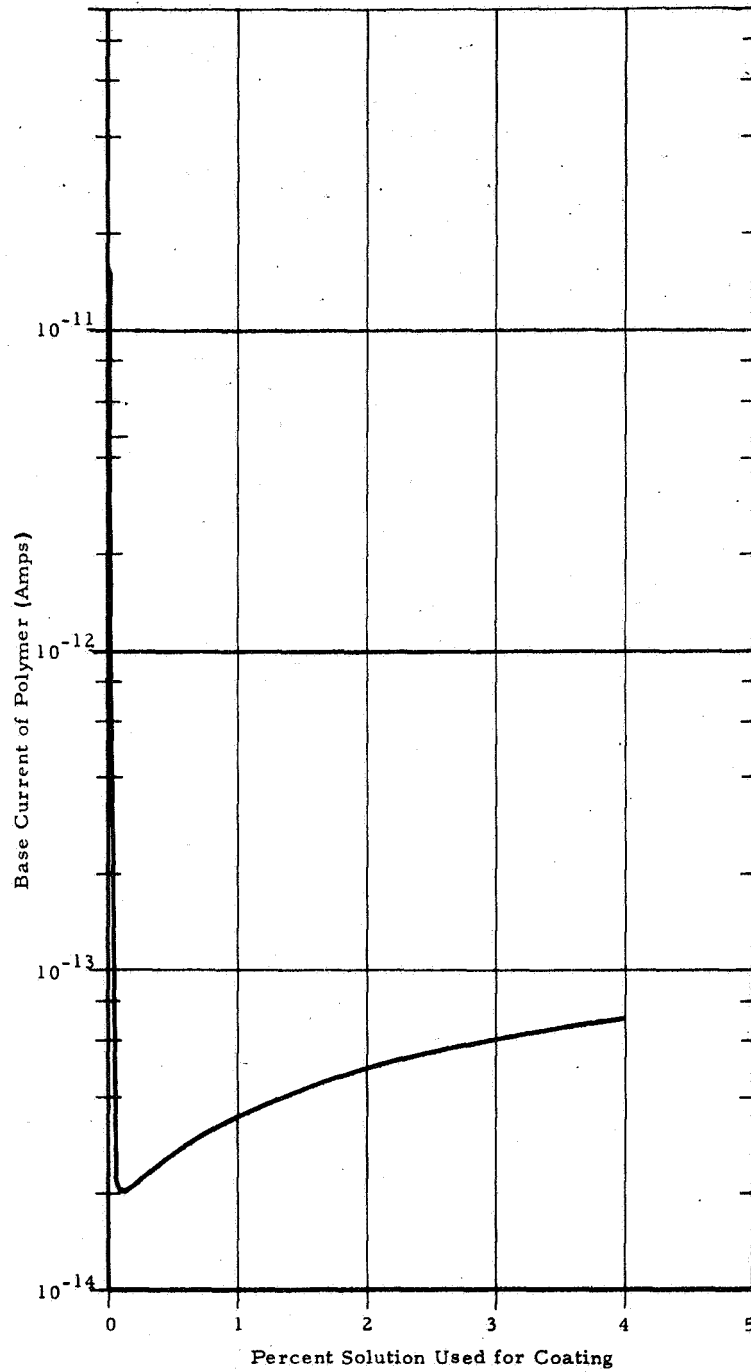
Thickness not determined



(d) - Monomolecular Film

03290

Figure 46. Variation in Polymer Film Thickness with Decreasing Solution Concentration



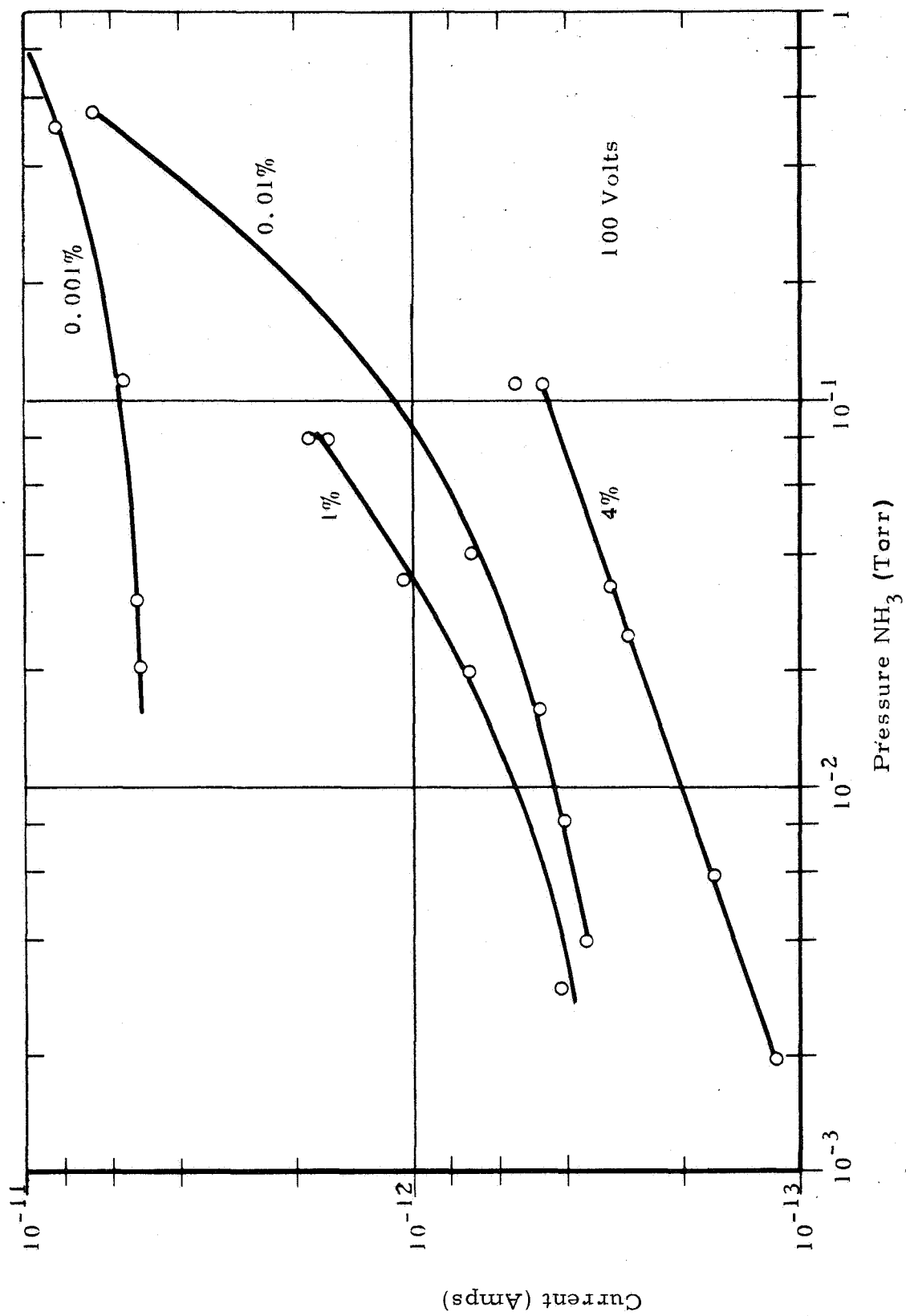
65291

Figure 47. Current/Thickness Correlation for Poly(p-nitrophenylacetylene) on the 5 Mil Sensor.

for the monomolecular film. It went through a minimum for the 0.1% and went up to a constant figure for the 4% film (which was considerably below that of the monomolecular film). These values are the so-called I_{p0} values for use in determining the ratio I_p/I_{p0} for current changes in the presence of a gas.

Next, came the experiments with ammonia on the various thicknesses of the poly(p-nitrophenylacetylene) polymer. Figure 48 is a direct comparison of all the absolute conductance data obtained on the five mil spacing sensor with respect to polymer thickness at low pressures of NH_3 . However, if a plot is made of the ratio of the current obtained for each pressure of gas to the current of the conditioned sensor without the gas, i. e., the I_p/I_{p0} ratio, then a clear picture emerges with respect to bulk versus surface effects. Figure 49 is a direct comparison I_p/I_{p0} plot of all the thicknesses versus pressure of NH_3 . Included on this plot are also the data for the 1% thickness on the 2-1/2 mil and 1 mil spacing sensor. The other data are all for the 5 mil spacing. Not shown on the plot, however, is the I_p/I_{p0} for the monomolecular film. In the pressure range that the data of Figure 49 described, the ratio for the monomolecular film was essentially unity (conductance without NH_3 was 1.31×10^{-11} amps; at 9 torr NH_3 , it was 1.74×10^{-11} amps). The plot on Figure 49 immediately points up the fact that the bulk effect is most pronounced; the thicker the film, the larger the I_p/I_{p0} ratio and the greater the ultimate sensitivity. The data for the film from the 0.1% concentration solution were not included due to excessive scatter indicating a faulty sensor. However, the remaining data from the 4% to the 0.001% are consistent.

Since the final to initial current ratios are quite indicative of the response capability it is of interest to compare our data to that of Reucroft, Rudyj and Labes⁽¹⁸⁾ for the case of ammonia. In their data, they showed no response capability below 4×10^{-1} torr (no ratio given). However, they show a ratio of unity (their limiting value) for one torr of NH_3 and a ratio of about 20-30 for 760 torr. By examining Figure 50, it is found that the 4% film gave a ratio of I_p/I_{p0} of close to 10^3 for about 28 torr NH_3 and a ratio of 7.5 for one torr. Thus, our system is considerably more sensitive than that of Reucroft, et al.



63101

Figure 48. Relative Plot of Effect of NH₃ on Varying Film Thicknesses on the 5 Mil Sensor.

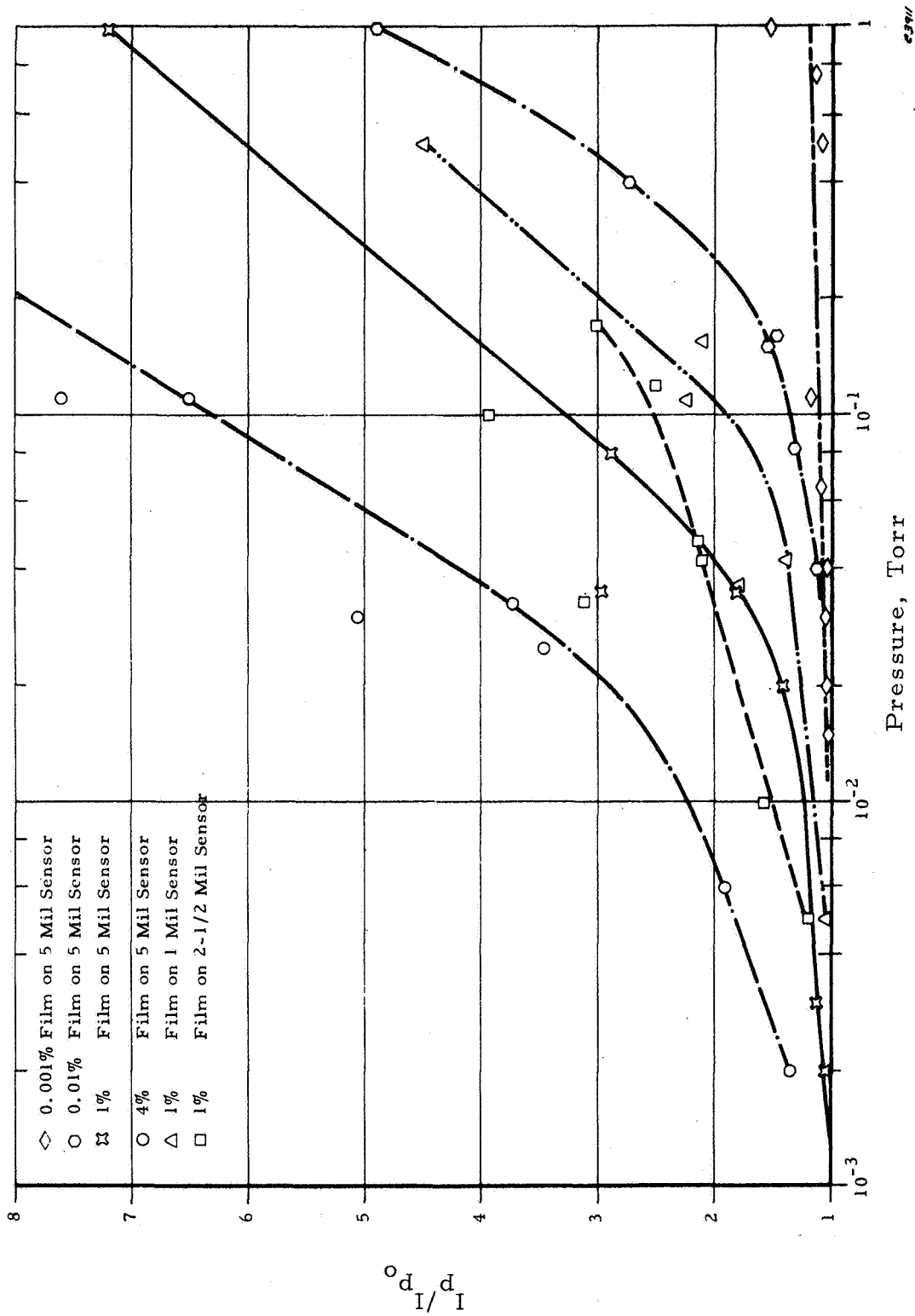
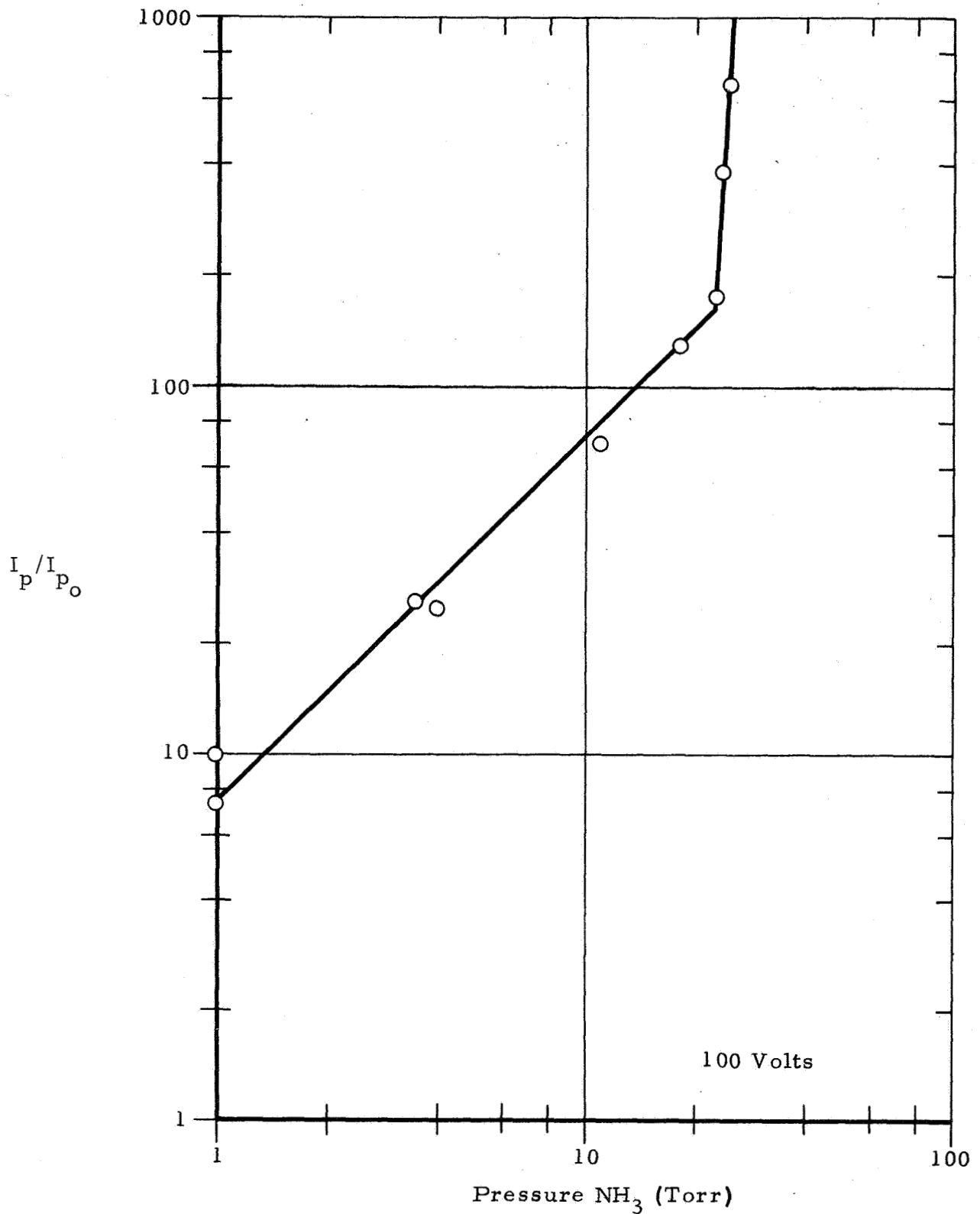


Figure 49. Ratio of I_p/I_0 at Varying Pressures of NH_3 for Different Film Thicknesses



c3903

Figure 50. I_p/I_{p_0} Ratio for 4% Film on 5 Mil Sensor at High Pressure Level

A matter of some concern is the so-called rise time and reversal time. That is, the time it takes the sensor to show a 90% change in current either by introducing the gas or evacuating the system. Considerable scatter was obtained in attempting to plot these data. However, Figure 51 is representative of some of the plots and is that for the rise time of the 4% film in the 5 mil sensor. As is to be expected, the rise times increase with decreasing pressure. On the other hand, it is expected that the recovery time, upon evacuation, should be fastest for the lowest pressure. Figure 52, however, which shows the reversal time for the 4% film, indicates that the converse is true. Similar results were obtained for other thicknesses.

In view of the fact that gas/solid interactions involve the phenomena of adsorption, sorption and desorption, the answer to this apparent anomaly lies in the question of what happens to the gas when it encounters the polymer. The first step, of course, is adsorption. This can be physical or chemisorption. If physical, no further interaction would occur. If chemisorption, then sorption into the bulk of the polymer would be next. At this point, some involved interactions could ensue, notable among them being complex formation between the gas and the polymer. Then, under static conditions, an equilibrium could develop such that there would be a rate of formation (of the complex) and a rate of decomposition. Tied in with this would be the rate of desorption. One other factor is the concentrations involved. Thus, the more polymer present (the thicker the film), the more gas that can be accommodated by the polymer. However, for any thickness, only a certain percentage of the gas can complex, the rest will be held as a dissolved gas in a solid. This "excess" gas will be easily removed upon evacuation, and then the equilibrium will shift; the gas/polymer complex will break only at the rate at which the gas can come out of the system. Therefore, high pressures of gas (for any given thickness) will have a fair amount of non-complexed gas. At low pressures, the amount complexed will be proportionately greater. Thus, it will take longer to remove this gas from the low pressure gas input.

This fact is hinted at in the shape of the curve of Figure 53. In Figure 53, for example, 130 microns of NH_3 were added at the start, but at equilibrium, the pressure read 110 microns in the system, and the electrical response

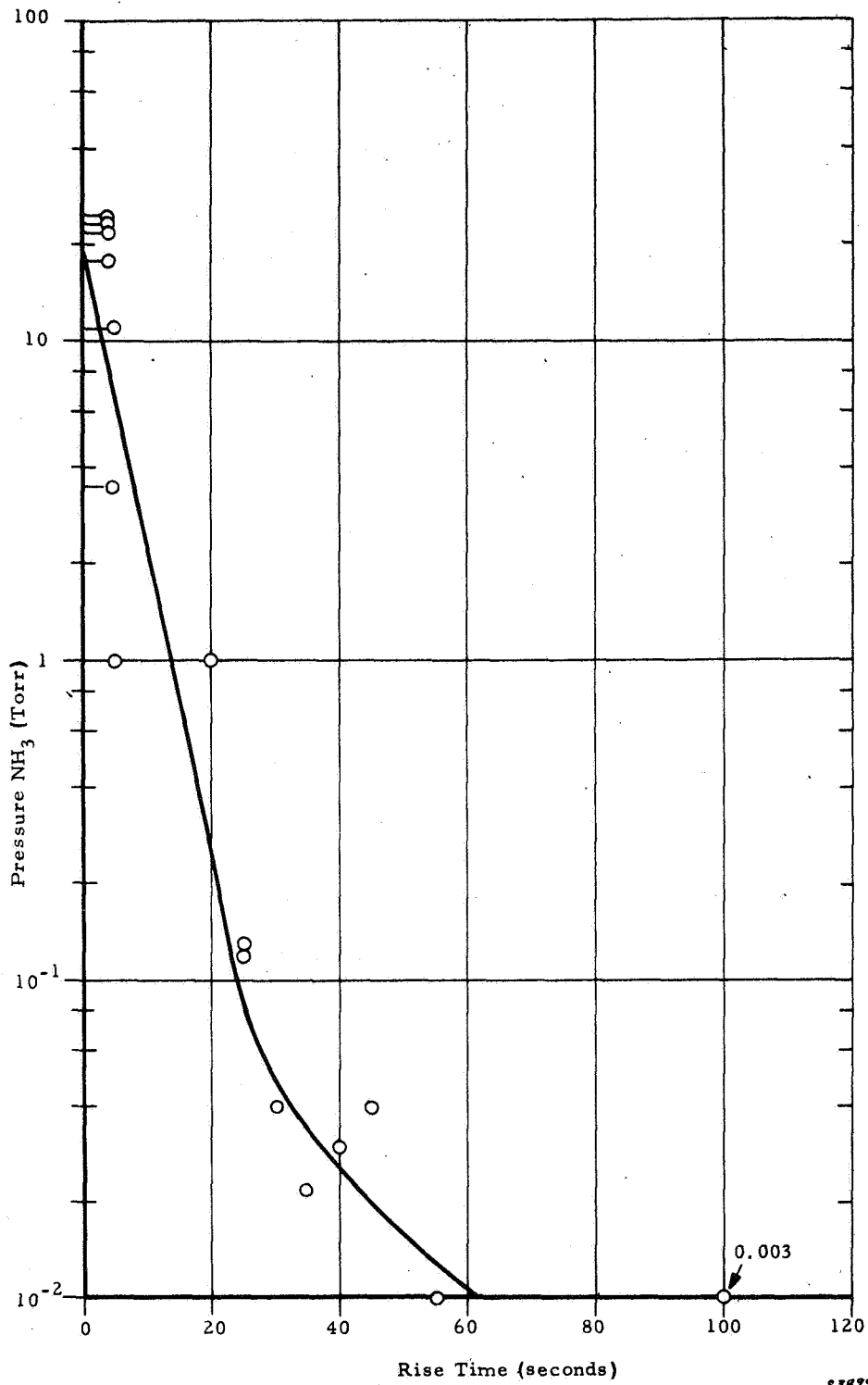
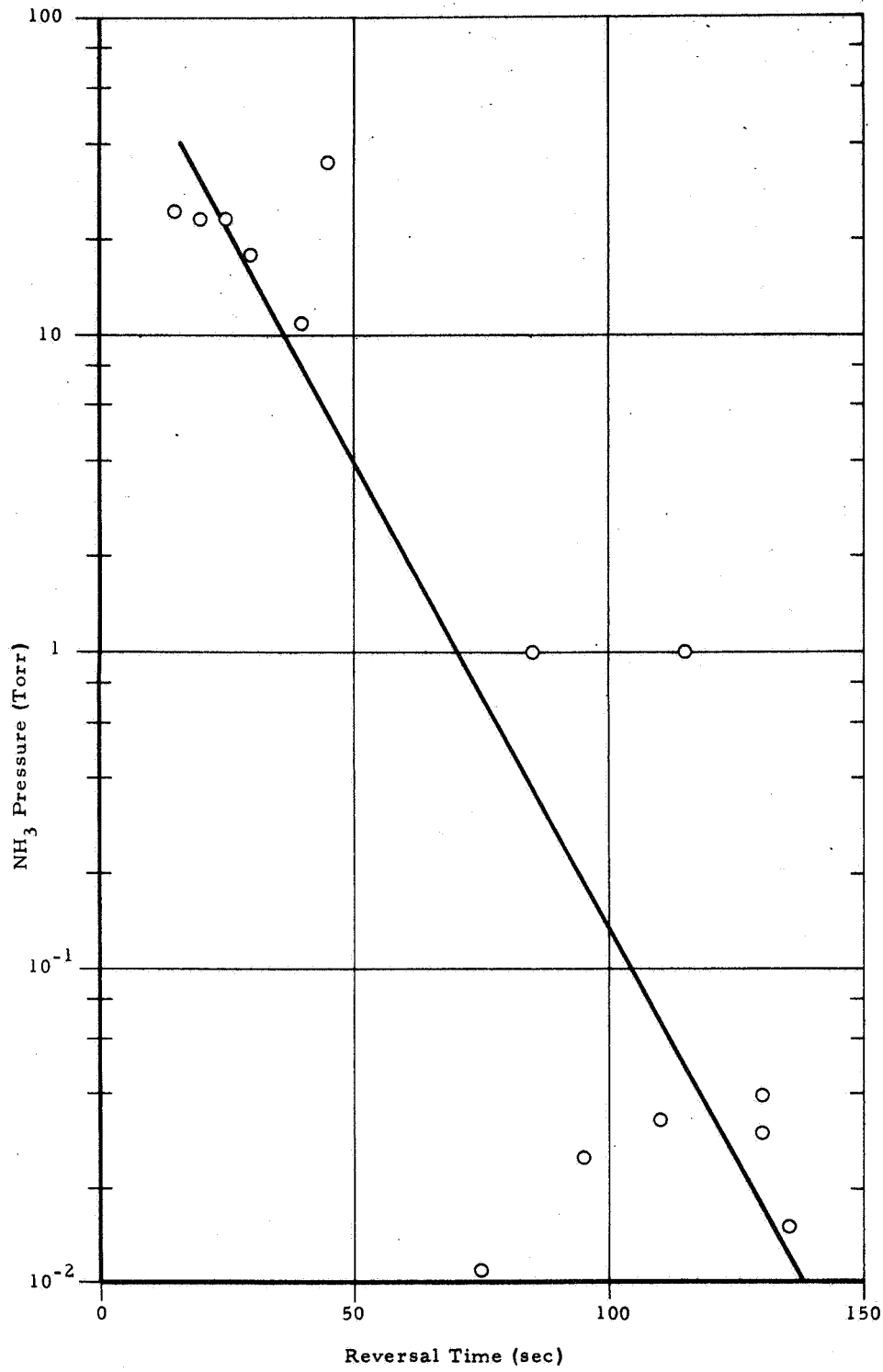


Figure 51. Rise Time Versus Pressure for 4% Poly(p-nitrophenylacetylene) Film on 5 Mil Sensor



c 3307

Figure 52. Reversal Time Upon Evacuation After Exposure to NH₃ for a 4% Film on 5 Mil Sensor

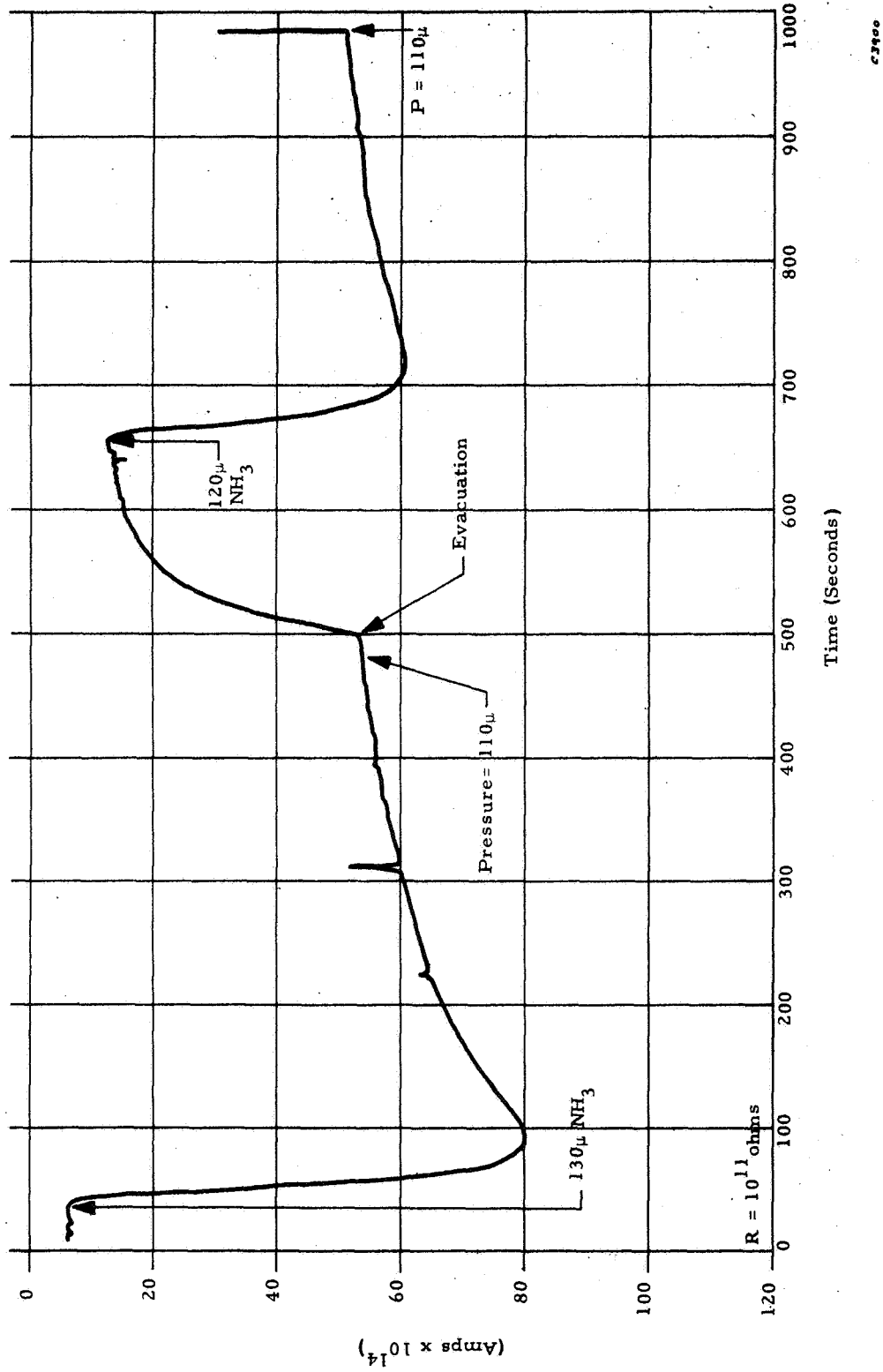


Figure 53. Strip Chart Recording of 4% Poly(p-nitrophenylacetylene) Film Exposed to Different pressures of NH₃

changed in a corresponding fashion. In other words, the vapor pressure above the sensor was reduced by 20 microns (the amount absorbed by the polymer). Figure 54 depicts the pathways for the gas/polymer interaction and it indicates that a rate constant should be available for each step.

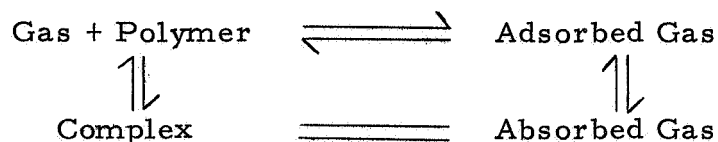


Figure 54. Various Pathways and Equilibria for a Gas/Polymer Interaction

Evidence of the response speed and sensitivity of a film from a 4% solution of poly(p-nitrophenylacetylene) on a 5 mil-spacing lock-and-key geometry sensor is found in the strip chart recording shown in Figure 53. It is seen that introduction of 130 microns of NH_3 results in a rapid increase in current followed by establishment of a new equilibrium value. Then, evacuation, followed shortly (within 3 minutes) by reintroduction of 120 microns of NH_3 returns the current level to a point proportional to the 130 micron value, and this subsequently reaches a new steady-state value again.

Finally, a further proof of the excellent response characteristics and reversibility of the system can be found in Figure 55. This is data obtained on a one mil sensor coated with a 1% solution. At $t = 0$, 45μ of NH_3 were injected into the evacuated system. At $t = 200$ seconds, the system was evacuated and the base current value reobtained. At $t = 340$ seconds, 500μ of NH_3 were injected, and the response was proportionate to the 45μ level (a scale change is shown which could be confusing with respect to this proportionality factor). At $t = 730$, it was evacuated again to return the current to the base value, and at $t = 1025$, 5μ of NH_3 were added giving an instantaneous response. Then at $t = 1120$, it was evacuated again to the original base current. These two experiments are excellent examples of the sensitivity of the system.

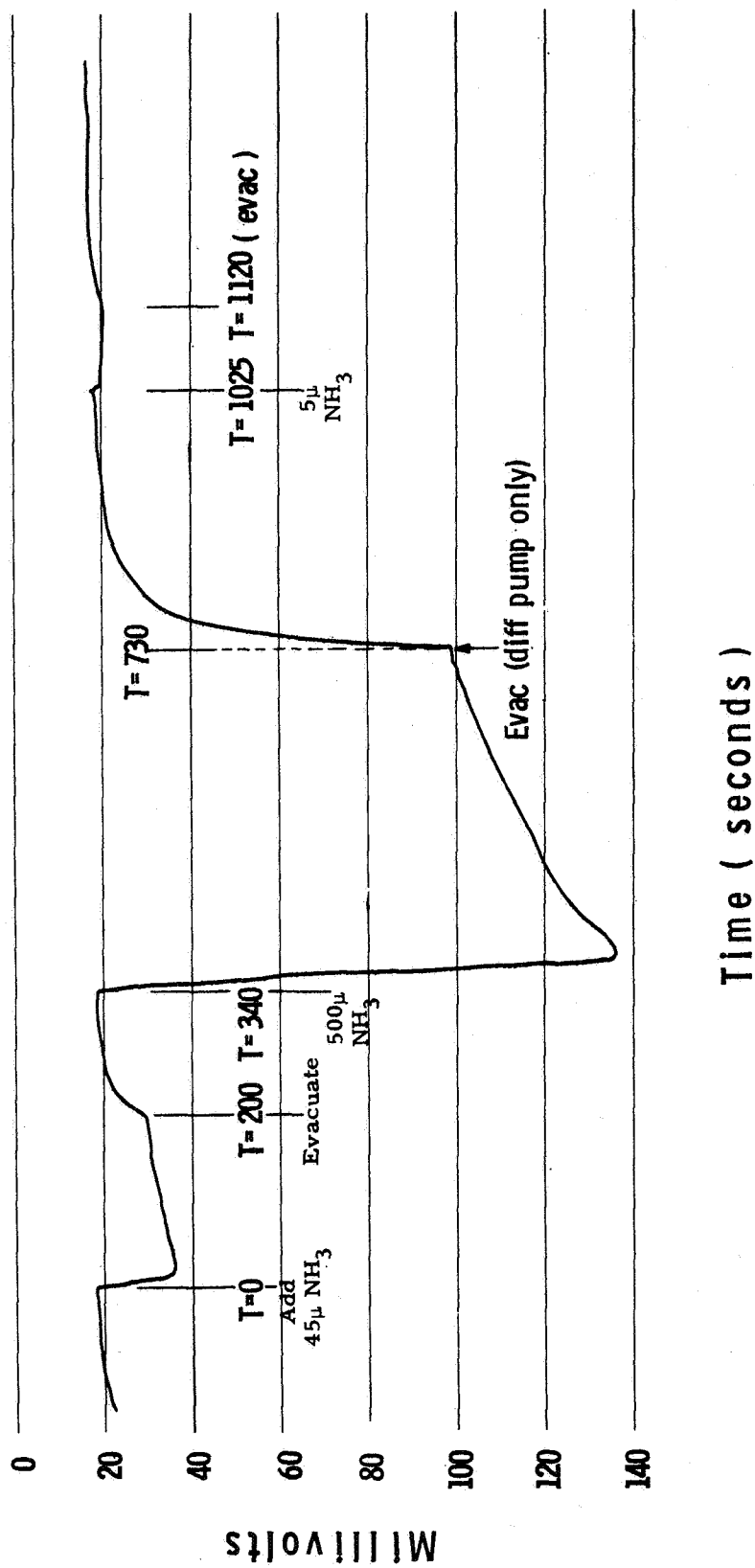


Figure 55. Reproduction of Strip Chart Recording of 1% Nitro Polymer Film on 1 Mil Sensor Exposed to Different Pressures of NH_3

Throughout this program, ammonia was used as a testing gas. Its choice was two-fold, (1) it is a very likely contaminant in a space cabin atmosphere,⁽⁴⁹⁾ and (2) it is a very reactive gas for interaction with various substrates.⁽¹⁸⁾

Earlier work centered largely on the use of ammonia with poly(p-nitrophenylacetylene) as a detecting polymer and it was used with this system mainly for standardization,⁽⁵⁾ viz., to optimize the electrical measurement technique. Thus, having developed an optimized method with the nitro polymer on the 5-mil spacing lock-and-key geometry, tests were subsequently conducted to determine the response of poly(phenylacetylene), poly(p-nitrophenylacetylene), poly(p-formamidophenylacetylene), and poly(p-aminophenylacetylene) to ammonia and various other gases using the same electrode sensor geometry.

Under actual conditions, the sensor will be located in the ambiance and connected to a bridge that is balanced under non-contaminated conditions. When a contamination develops, the sensor responds and unbalances the bridge by an amount made proportional to I_p/I_{p_0} . This ratio is related to a partial pressure of gas. After the contaminant is removed, the bridge is rebalanced. For rapid changes in atmospheric conditions, detection depends on I_p/I_{p_0} rather than I_p . However, normal random fluctuations in I_{p_0} may give an impression of instability of I_{p_0} . A slow contaminant buildup results in a continual change of I_{p_0} (non-random fluctuations). To differentiate this from long-term random fluctuations, automatic rebalancing of the bridge by means of a feedback loop and summing the corrections will result in a sum of zero for random fluctuations. A slow buildup of contaminant would give a constantly increasing sum.

The ideal way to test the response of the various sensors was to evacuate the chamber after a reading was taken at each pressure level, allow the sensor current to return to the level it had before any gas introduced, and then introduce a new pressure of gas for the next point. In order to expedite the testing process though, the following procedure was adopted.

For evaluation and experimental purposes, a different modus operandi prevailed. After the sensor was placed in the testing chamber and the system evacuated to 10^{-4} torr, the gas to be analyzed was introduced into the chamber and the pressure brought to about 20 torr. The current was then allowed to

stabilize for approximately five minutes. The gas was then pumped off in increments and the current allowed to stabilize for 300 seconds. If the current was found to be relatively stable at 100 seconds, the 300 second reading was bypassed. When the current no longer change with a change in pressure, all the gas was pumped off and a current reading taken at 10^{-4} torr. This is the I_{p_0} that was used to determine the I_p/I_{p_0} ratio. It should be noted that if the sensor was left in the vacuum, or under a particular partial pressure of gas, for a number of hours or days, the current reading gradually decreased. However, if the gas pressure was changed at any time, the current responded immediately and proportionately; the proportionality was indicated by the I_p/I_{p_0} plot.

Figure 56 is a plot of I_p versus P for ammonia on poly(phenylacetylene). It depicts what happens to the current as the gas is pumped off incrementally. In addition, when the pressure was left constant for two hours and a reading taken of the current, it was found to have dropped considerably. (The slight pressure increase is possibly due to outgassing from the walls of the chamber, the tubing and other surfaces.) However, when the next few incremental pressure changes were brought about by pumping off, the curve was found to continue with the same slope and shape as it had before, but displaced in parallel fashion from the original curve. Since the absolute current, I_p , through a sensor cannot be reliably reproduced, but the relative change, I_p/I_{p_0} , is reproducible, the response characteristics were plotted in terms of I_p/I_{p_0} .

Figure 57 is a plot of the response characteristics of poly(phenylacetylene) when exposed to various gases. With each of the polymers tried, water vapor gave a unique, pronounced and similar response. At around one torr, the curve went up quite steeply while below one torr it leveled off very rapidly to a ratio of about unity. It would appear from this that the ionizability of water is concentration dependent, i. e., as one approaches a monomolecular film, the water does not seem to ionize to conducting species. It is also of interest to note that poly(phenylacetylene) displays amphoteric character with respect to electron-donating or electron-withdrawing tendencies. Thus, it interacts quite strongly with BF_3 (an electron-seeking substance), reasonably

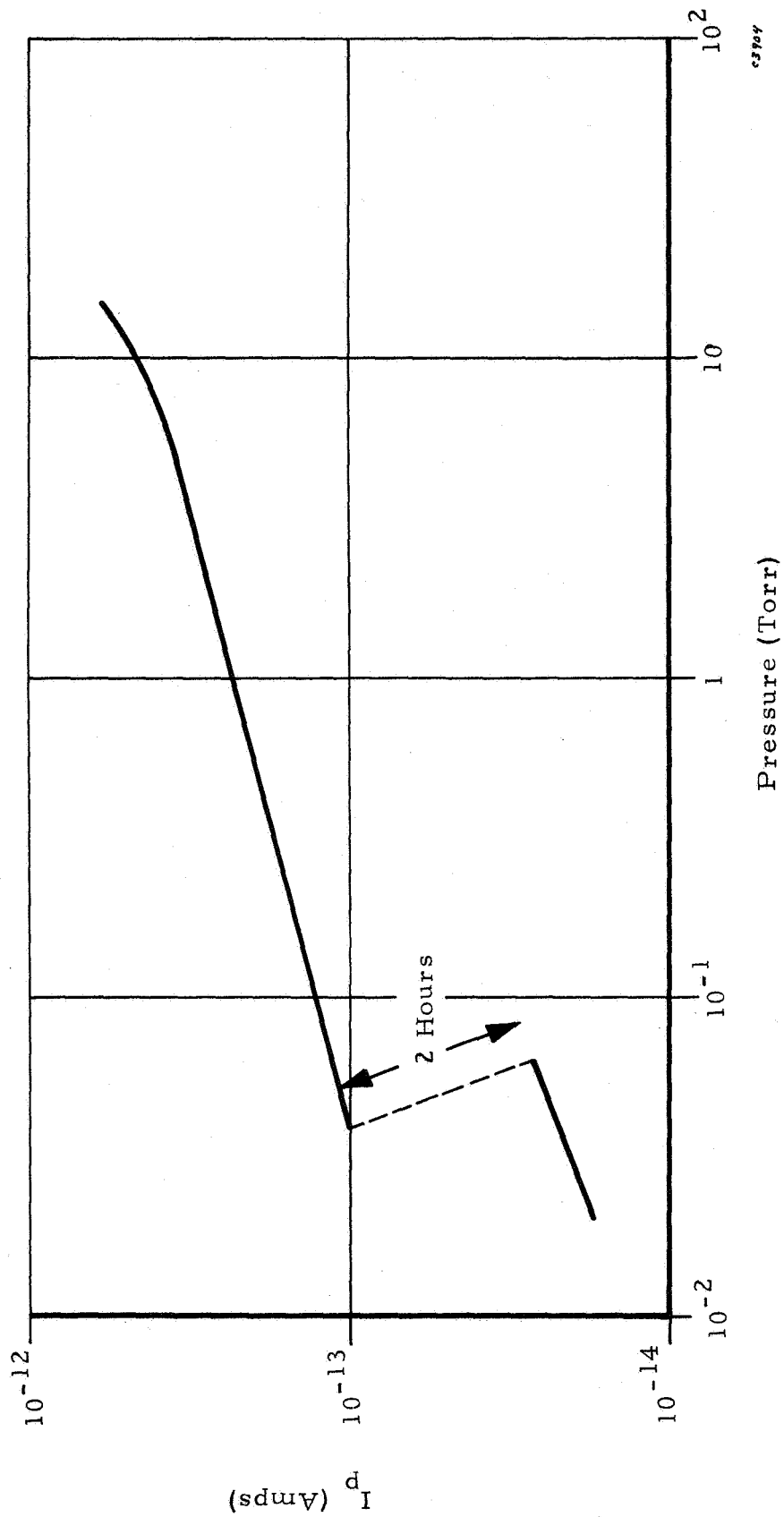
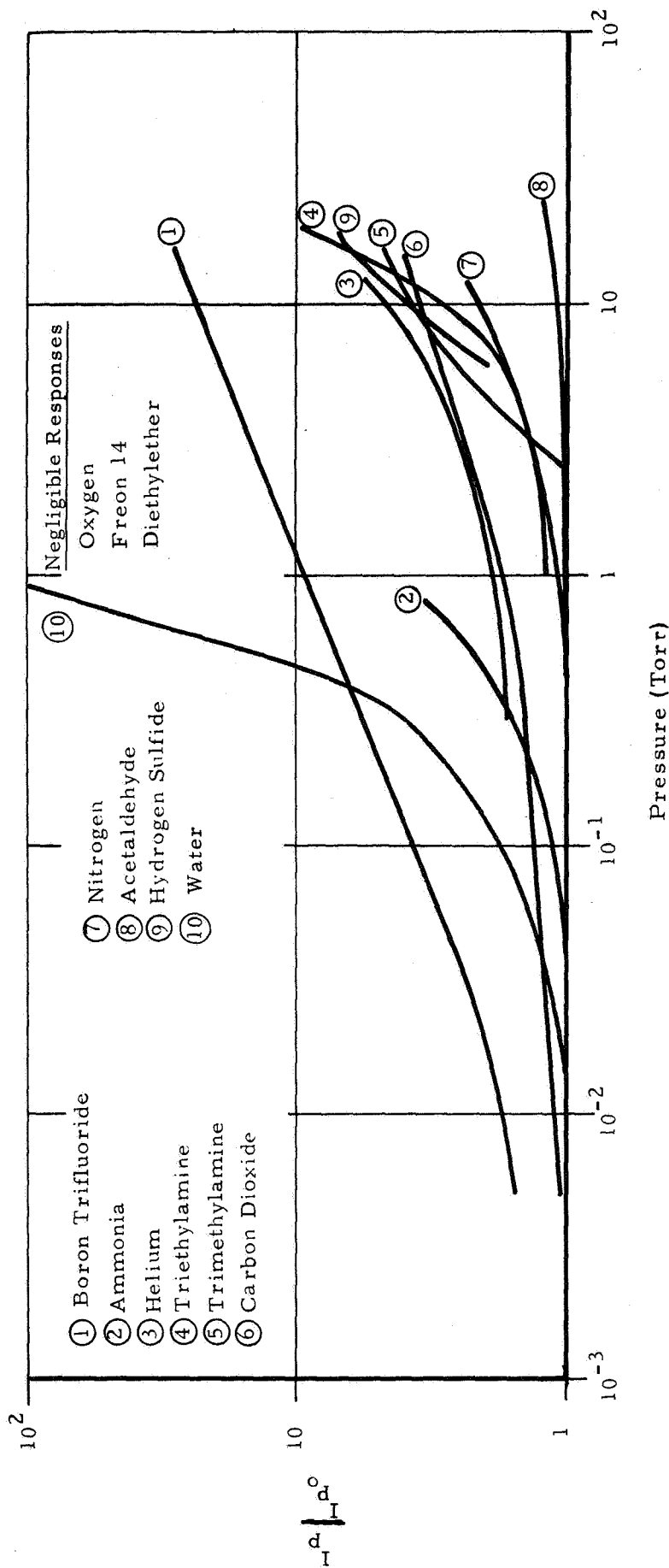


Figure 56. Poly(phenylacetylene) with Different Pressures of Ammonia



4538

Figure 57. Response of Poly(phenylacetylene) to Various Gases

well with CO_2 (another electrophilic agent) and fairly well with NH_3 (an electron-donating gas).

Figure 58 depicts the behavior of the nitro polymer with those gases that gave some response below one torr (as well as above), and Figure 59 shows the interaction of the nitro polymer with those gases that were most responsive above one torr. Aside from water vapor, the most responsive gas/polymer interaction was that due NH_3 . It is seen that its potential detectability is into the parts per billion range (from extrapolation of the curve). The ammonia data are highly reliable since they are based upon a large number of runs. It is also interesting to see that BF_3 interacted poorly; in keeping with the electronegativity of the nitro polymer. Although not readily observable from the curve, it was found that hydrogen reacted irreversibly with the nitro polymer. This could be due to a possible reduction of the nitro group by the hydrogen presumably involving free electrons on the nitro moiety. This is analogous to what has been observed with diphenylpicrylhydrazyl (DPPH) (a stable free radical). Thus, it has been shown by Eley and Inokuchi⁽⁵¹⁾ that DPPH caused dissociation of molecular hydrogen and formation of atomic hydrogen, which then entered into a covalent link with the surface molecules.

The response of the formamido polymer to various gases is shown in Figure 60. Again, aside from water vapor, the most pronounced response was obtained with NH_3 . However, this polymer is less electronegative than the nitro polymer, but more so than the poly(phenylacetylene). Thus, its response with NH_3 is intermediary.

From the data depicted in Figures 57 - 61 for the responses of the various polymers to ammonia, as well as other gases, it is readily seen that the electronegativity concept of gas/polymer interactions is amply borne out. Using NH_3 as an example of an electropositive species, it is seen that it interacted most with the nitro polymer (Figure 58). However, the amino polymer (Figure 61) showed the next greatest response behavior with the NH_3 . If one examines Figure 62, the resonance form for the amino polymer, it is seen

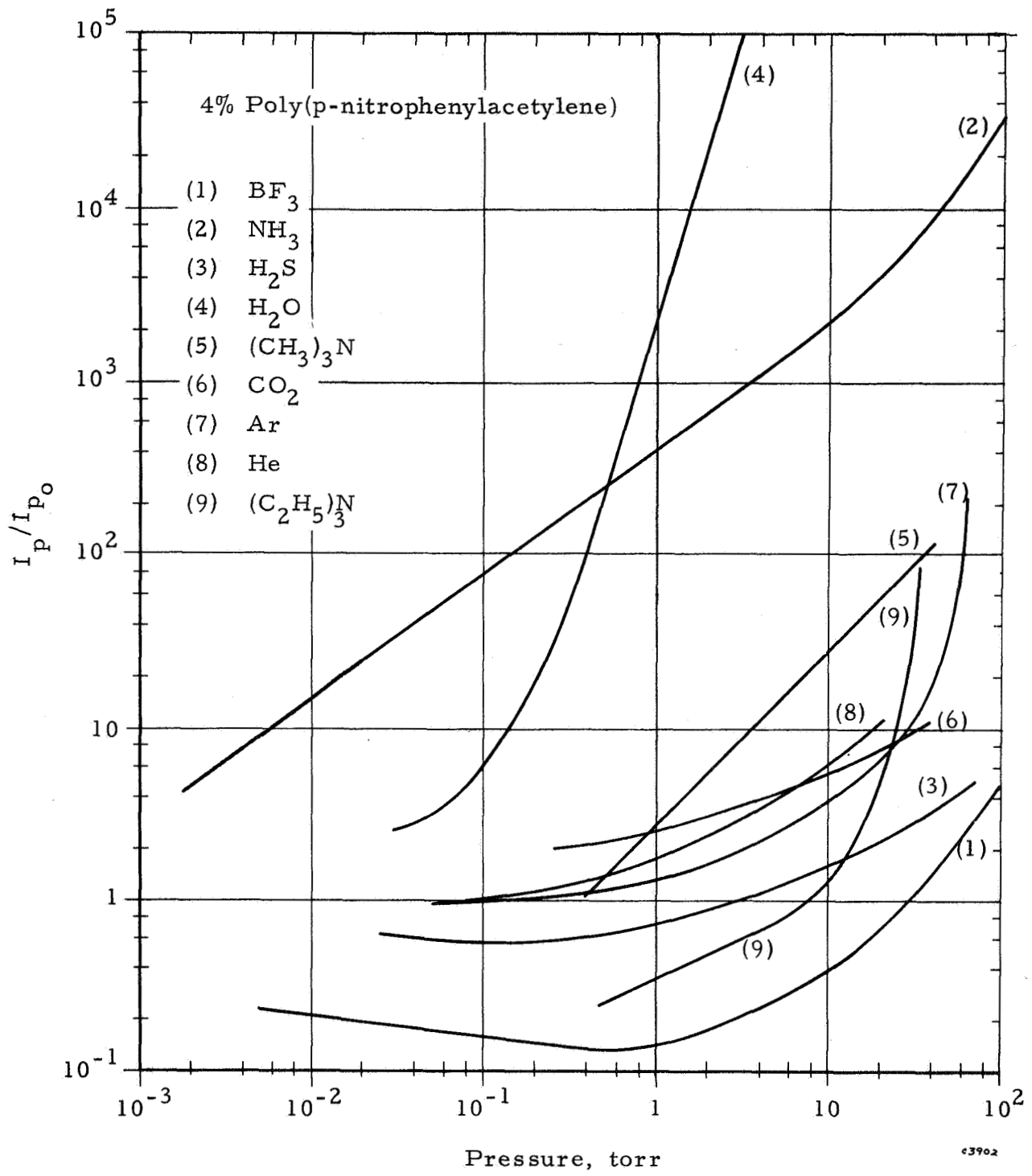


Figure 58. Response of Poly(p-nitrophenylacetylene) to Gases Below 100 Torr

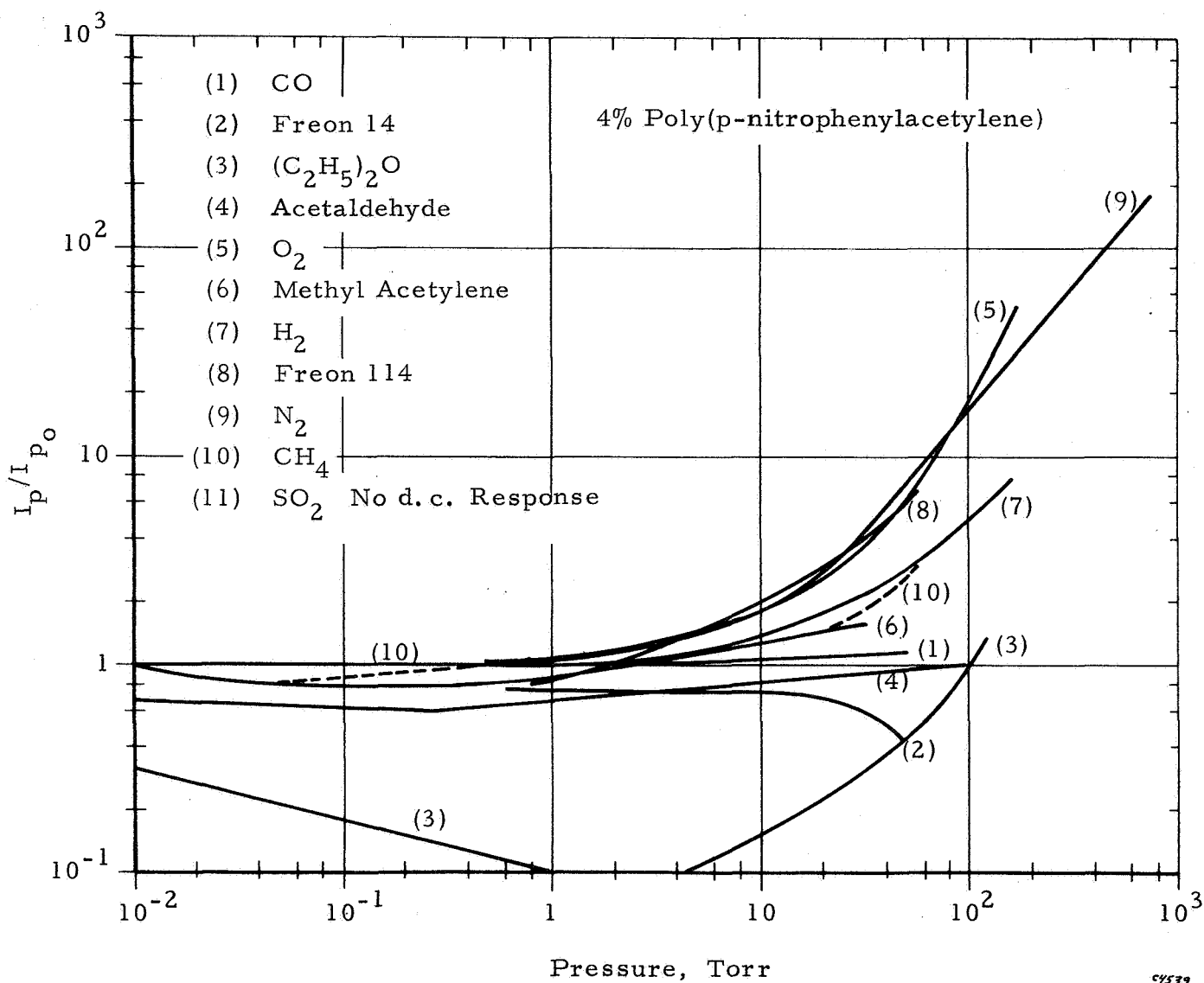


Figure 59. Response of Poly(p-nitrophenylacetylene) to Gases Above One Torr

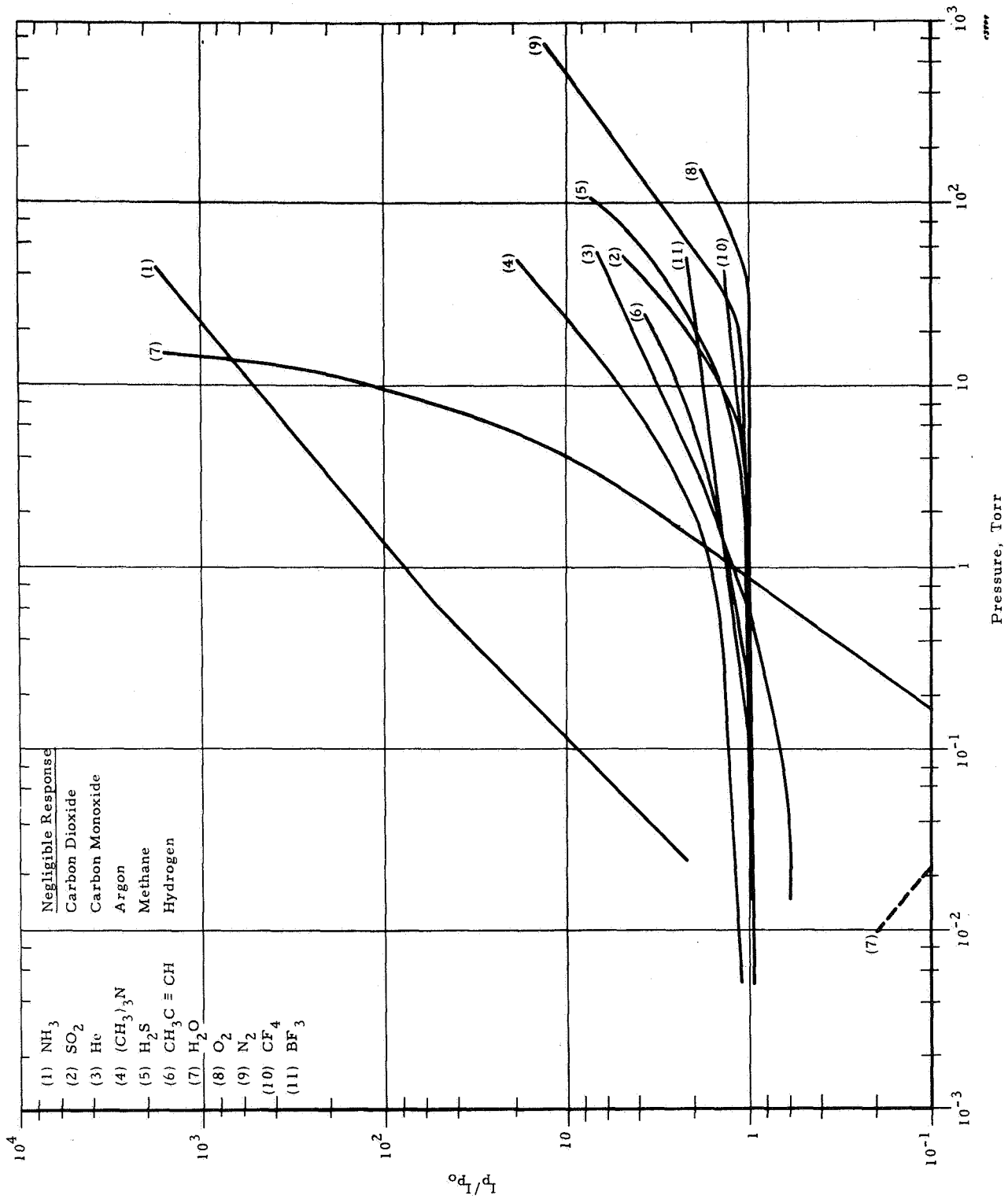


Figure 60. Response of Poly(p-formamidophenylacetylene) to Gas

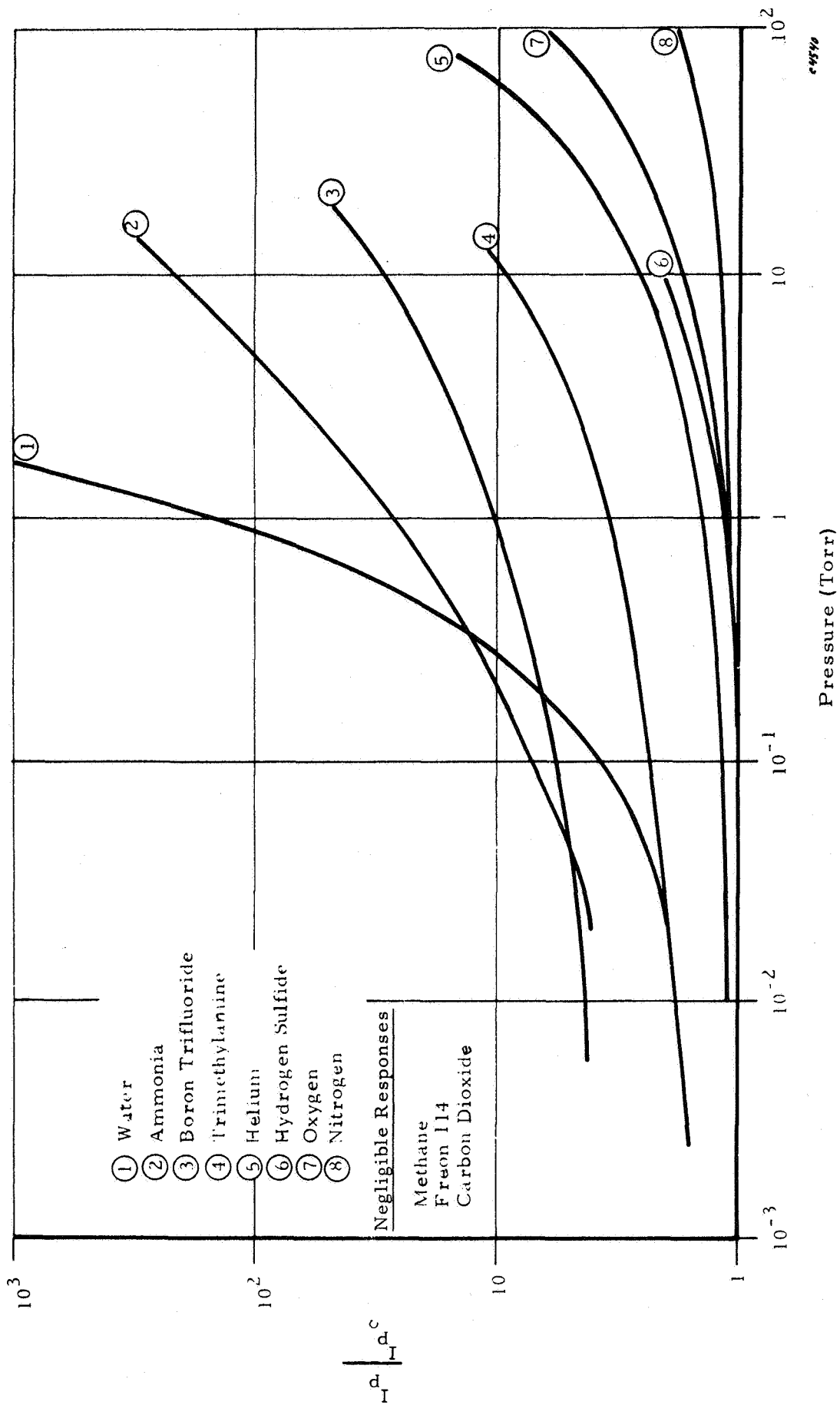
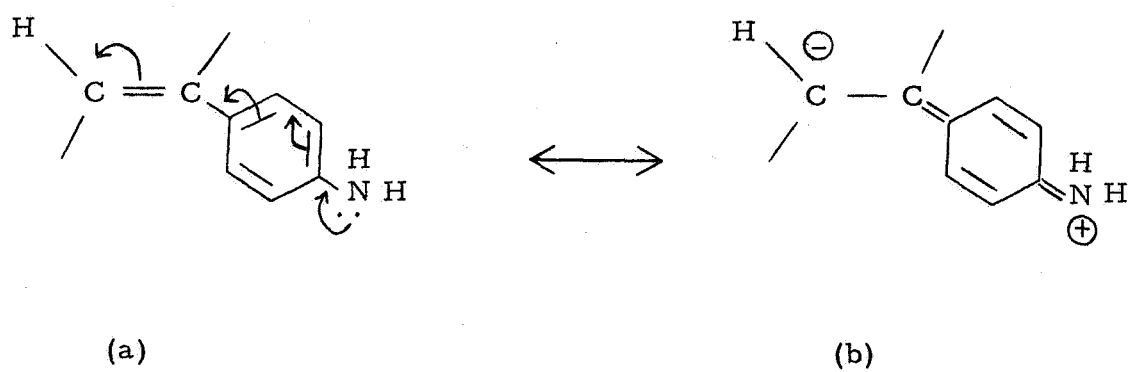


Figure 61. Response of Poly(p-aminophenylacetylene) to Various Gases



03907

Figure 62. Resonance Form of Polarized Poly(p-aminophenylacetylene)

that it has a protonated imino group. This must be related to the electron-donating tendency of the amino group. Therefore, since the ammonia is a proton-seeking substance, it is readily seen that a proton is available in the structure shown in Figure 62(b). The NH_4^+ ion that would result could migrate in an electric field, but slowly, since it would be diffusing through a solid; simultaneously, the electron could move freely along the polymer chain as well as from chain-to-chain, the polymer thereby showing enhanced conductivity after complexing with the ammonia.

In addition to ammonia, the boron trifluoride case with the amino polymer was also remarkable. When the BF_3 was introduced at 16 torr, the current increased, but the noise level also increased drastically. As it was incrementally removed, the noise decreased proportionately. This happened on repeated runs. The same situation did not prevail for the BF_3 /poly(phenylacetylene) system. In view of the fact that BF_3 is a strong electron-accepting gas, it could have been interacting, not only with the phenyl moiety, as it is wont to do in its capacity as a Lewis acid, but also with the NH_2 group. In fact, it is well-known that BF_3 forms strong complexes with amines and it is probable that the BF_3 could have induced a polarization of the aminophenyl moiety such that the electron density would have been highest around the amino group. This of course, would have been contrary to the normal tendency of the amino group to feed electrons into the ring and it is this interaction between the amino moiety and the BF_3 that could have generated a salt-like species which would increase the electrical noise in the system. It is also of interest to note the difference in responsiveness of the amino polymer to BF_3 versus that of the poly(phenylacetylene) (Figure 57). The extrapolation of the curve in Figure 61 shows a high degree of selectivity of the amino polymer to BF_3 in that it could potentially be detectable in the low parts per billion range. This further strengthens the argument for the concept surrounding this program; namely, more than one polymer may react with the same gas, but the more electronegative (or electropositive) species will more strongly interact with the corresponding conjugate structure. Subsequently, when the various responses are computerized, the multiple sensor detector will read back which gas is responsible for the particular interaction with which sensor. This is presumably analogous to the animal's multiple

sensor system and its relation to the brain which tells the animal which gas (or gases) it is smelling.

Thus, it is not the intent to use one sensor for all gases, but rather have a multiplicity of detectors such that one sensor is more preferentially activated by one gas than another. It may be, though, that other gases will activate the same sensor, but to a lesser degree. Furthermore, it is possible that two gases at different partial pressures may activate the same sensor to the same degree. However, in the ultimate device, there will be enough sensors such that although the probability exists of gas A and gas B affecting sensor 1 to the same extent (even though at different partial pressures), it is unlikely that the same mixture would have the same effect on sensor 2. Thus, if sensor 1 is more specific to gas A and less so to gas B, and if sensor 2 is more specific to gas B, it is not too likely sensor 2 would have the same interaction effect with A that sensor 1 has with B. Then, if the system has been calibrated and subjected to a computerized pattern recognition program, the resultant output would establish the identity of a number of gaseous components dependent upon the number of sensors present. For the moment, it suffices that the four polymers presently being used have satisfactorily shown excellent sensitivity as well as specificity to a few gases.

The primary objective of this program has been to gather information about gas/polymer interactions for the purpose of developing a practical gas detection device. Data gathering for the purpose of theoretical analysis has been secondary. Nevertheless, enough information has been obtained to allow at least a semi-quantitative evaluation of some of the outstanding theories of solid/gas interactions. Some of the areas investigated have been:

1. Charge-transfer complex formation (see Appendix A)
2. Pressure effects
3. Dielectric effects
4. Carrier traps and space charges

Of the four, only the pressure effect would be expected to be equivalent for all gases on the same polymer; it would, of course, be different for the same gas with different polymers. Accordingly, if one can find a way to determine the

pressure-conductivity relationship in the absence of the other effects, it should be possible to use a pressure-conductivity curve as a base line; the deviation from which would be a measure of the other effects, i. e., dielectric constant, donor-acceptor interactions and space charges.

Pohl,⁽⁵²⁾ Rembaum and Moacanin⁽⁵³⁾ and Pohl, Rembaum and Henry,⁽⁵⁴⁾ among others, have studied pressure-conductivity relationship in polymers using hydraulic presses with pressures in the kilobar range. They found that pressure changed the activation energy of mobility, μ , where μ is defined in Equation (8) as

$$\sigma = n |e| \mu \quad (8)$$

and σ is the conductivity, n is the number of carriers and e is the electronic charge. An equation was derived⁽⁵⁴⁾ that expresses the relation between the conductivity and the pressure in long chain polymers

$$\sigma = |e| \left[M_o \exp \frac{-E_g}{2kT} \right] \left\{ \frac{Ld}{3h} \exp \left[\frac{P^{1/2}}{kT} (b''T + b_o) \right] \right\} \quad (9)$$

where

- σ = conductivity
- e = electronic charge
- M_o = carrier concentration at infinite temperature
- E_g = activation energy for carriers
- L = length of polymer chains
- d = half length of a hop
- h = Planck's constant
- P = pressure
- b'', b_o = deformability constants
- k = Boltzmann's constant
- T = absolute temperature

If the temperature is held constant, and the various constants gathered together, Equation (9) can be reduced to

$$\sigma = \sigma_o \exp (BP^{1/2}) \quad (10)$$

The constant B is different for each polymer, and the value of σ_0 is determined at zero pressure. Taking logarithms of Equation (10), we get

$$\ln \frac{\sigma}{\sigma_0} = BP^{1/2} \quad \text{or} \quad \log_{10} \frac{\sigma}{\sigma_0} = 2.303 BP^{1/2} \quad (11)$$

Figure 63 is a semilog plot of σ/σ_0 versus $P^{1/2}$ for the amino polymer with three gases — a very active (BF_3), an inert (He) and a semiactive (O_2) gas. It is seen that helium and oxygen generate straight lines of differing slopes, whereas the boron trifluoride appears to show a double curvature. If it is assumed that helium is inert, then its curve might be taken to represent the base line from which to determine the empirical coefficients for gas/polymer interactions. Thus, based upon the fact that oxygen generates a straight line with a different slope than that for helium, its interaction parameter might be considered to be a multiplier for the constant B in Equation (10); while for the boron trifluoride case, the development of curvature in the plot could indicate its interaction parameter to involve the exponent of P. In that case, Equation (10) should be rewritten as

$$\sigma = \sigma_0 \exp \left[k_1 B(P^{1/2})^{k_2} \right] \quad (12)$$

Where k_1 and k_2 are the empirically determined gas interaction parameters, and B is a constant related to a particular polymer. The k_1 measures the deviation of the slope from that of an "ideal" gas, i. e., non-interacting gas, and k_2 establishes the deviation from linearity of the slope of an interacting gas. At present, there are no established values for k_1 and k_2 .

If, on the other hand, one examines Figure 64, which is a plot of the pressure effect of helium and argon on the nitro polymer, there is some doubt cast on the method of determining a base line curve for a pressure effect only. The argon line is fairly linear to about 36 torr, at which point it departs radically from linearity. Helium also shows a linear plot, and interestingly with the same slope as for argon, but it departs from linearity below one torr. Aside from experimental error, which may account for some of the deviation from linearity, particularly for helium, there may also be some interaction effects.

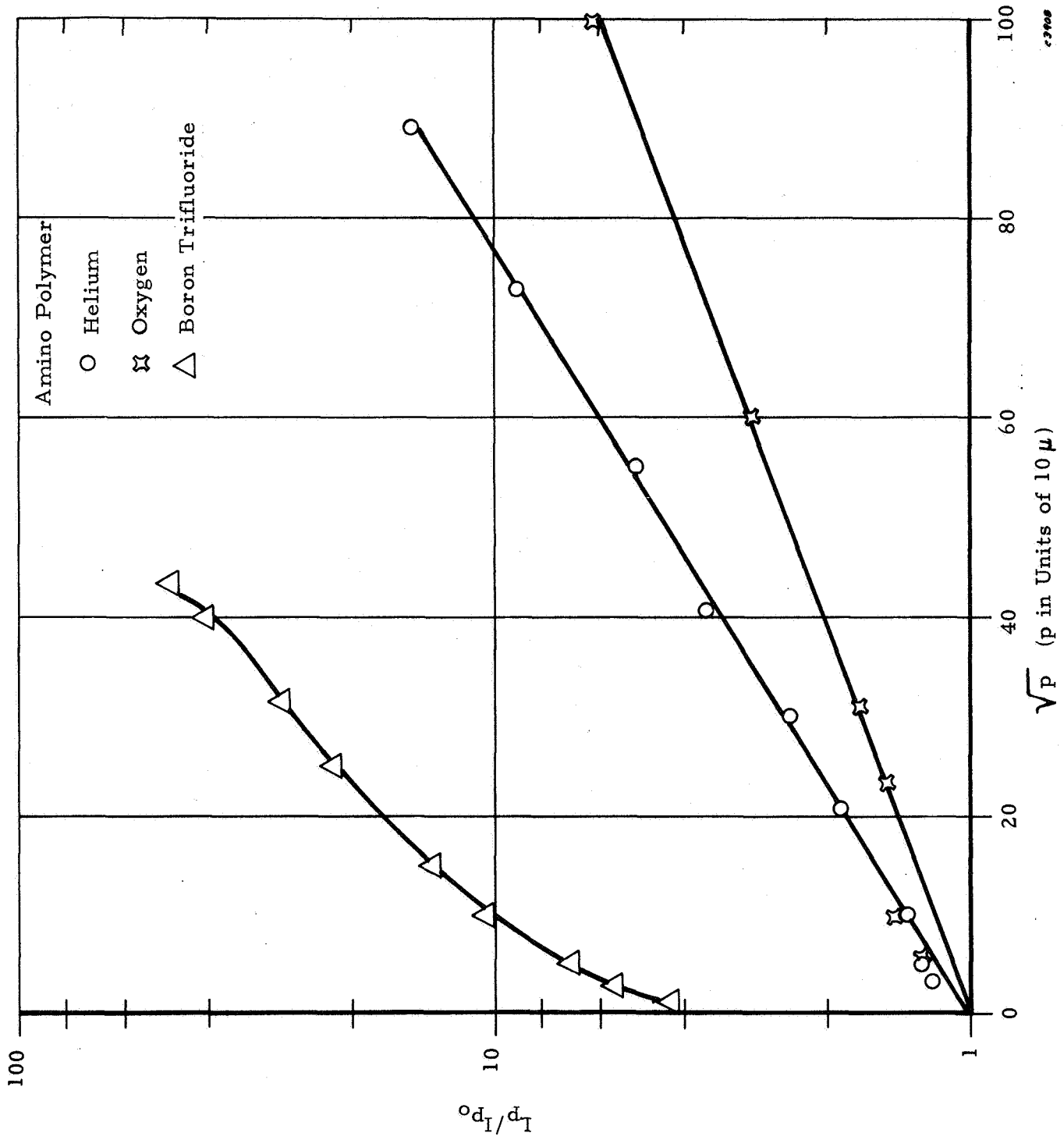


Figure 63. Effect of Pressure on Conductance of Poly(p-aminophenylacetylene)

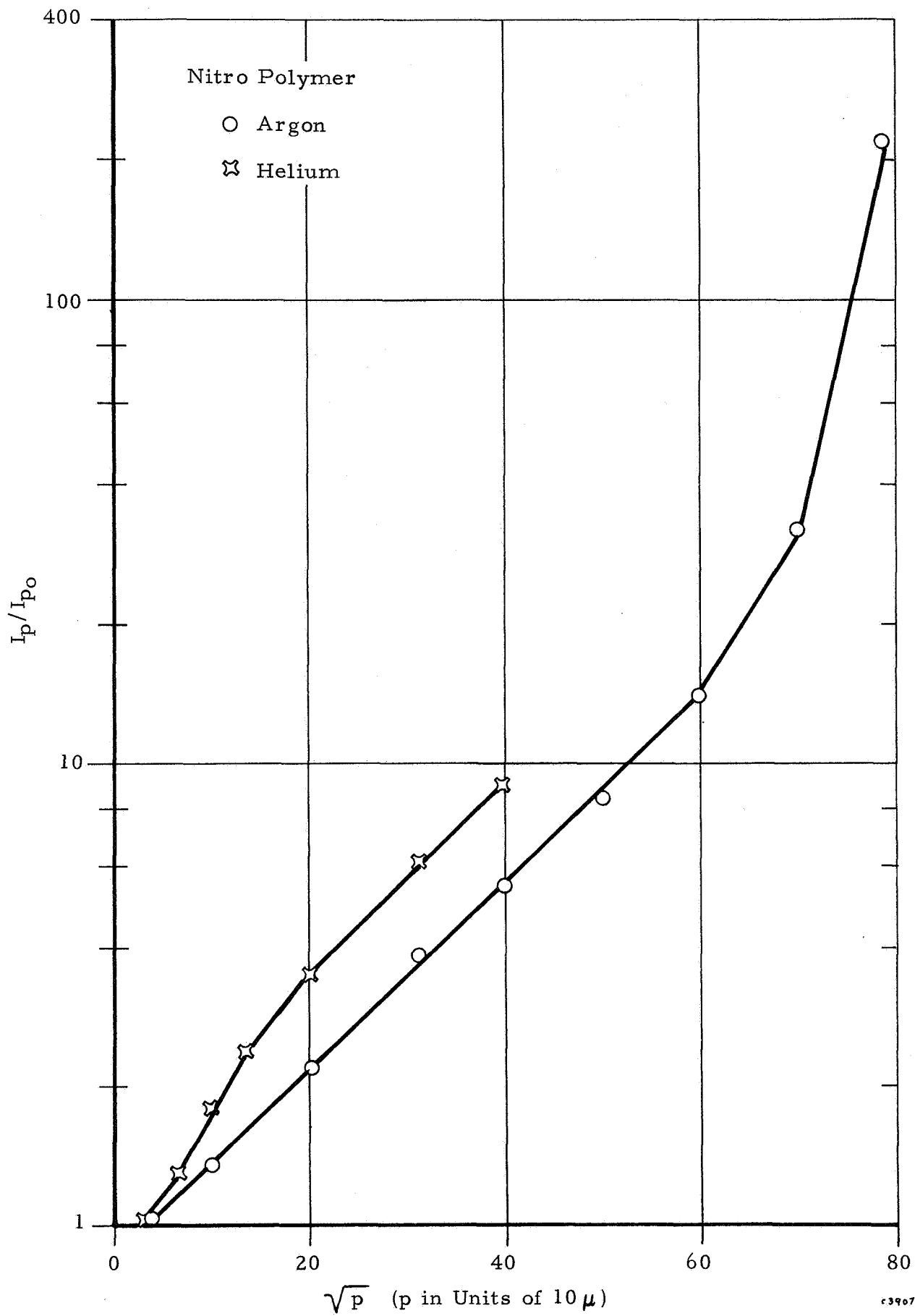


Figure 64. Effect Pressure in Conductance of Poly(p-nitrophenylacetylene)

In addition, as mentioned above, the constant B (the deformability parameter) is different for each polymer. This, in conjunction with the fact that it had earlier been stated that the nitro polymer may be a more electronically active substance, e.g., analogous to the DPPH case,⁽⁵¹⁾ can all lead to possibilities for deviation from linearity. However, the results, to date, point up the fact that some contribution from pressure exists, although other factors may be contributing, as well. Some of these factors, such as the dielectric effect and the space charge effects, will be discussed next.

In the course of making gas/conductivity response measurements on the formamido polymer, two identical sensors were used. They were placed in the same environment and one was connected to a Booton 75 C capacitor bridge while the other was connected to the Keithley 610B electrometer. Then, at each gas pressure level two measurements were made simultaneously — a capacitance and a dc conductance; the former being related to a change in the dielectric constant of the system. It was noted that the capacitance changed each time the conductance changed, although the conductance did not always change when the capacitance did. The change in capacitance was only on the order of 0.02 to 0.2%. Only a few points were checked by this method, but they were sufficient to point up the possibility of using a capacitance measurement for detecting gases that might be more sensitive than the conductivity method. A possible mechanism for gas/polymer interactions involving dielectric changes is, therefore, put forward that appears to fit the data.

It is well known^(55, 56) that the ionization potential of an impurity in a crystalline lattice is lowered by the permittivity of the lattice. The permittivity reduces the interaction potential between a carrier and its parent nucleus such that its wave function spreads out over many lattice constants. It is then easily excited into the conduction band of the crystal by thermal energy. It seems reasonable, therefore, that the wave functions of electrons in a conjugated polyene chain would be expanded by a dielectric medium, with a similar effect on the activation energy, and consequently on the conductivity.

The force between an electron and an ionized atom (or molecule), separated by a distance r , is given by⁽⁵⁷⁾

$$F = -eE \quad (13)$$

where $E = \frac{q}{4\pi\epsilon r^2}$, which is the electric field of a molecule with charge q in a dielectric medium of permittivity ϵ . The work to remove the electron to a distance r , is then given by

$$w = \int_0^r F dr = \frac{-eq}{4\pi\epsilon} \int_0^r \frac{dr}{r^2} \quad (14)$$

Integrating, and letting $q = e$, we get

$$w = \frac{e^2}{4\pi\epsilon r} \quad (15)$$

If w_1 is the work involved when the medium has a permittivity ϵ_1 and w_2 is the work for permittivity ϵ_2 , the difference, $w_1 - w_2$ is

$$w_1 - w_2 = \frac{e^2}{4\pi r} \left(\frac{1}{\epsilon_1} - \frac{1}{\epsilon_2} \right) \quad (16)$$

The energy required to move an electron from one molecule to another may be expressed in terms of the difference between the ionization energy, I , of the first molecule and the electron affinity, A , of the second, reduced by the work done on the electric field, as calculated in (15). This gives the activation energy of the carrier population, E_a ^(58, 59) as

$$E_a = (I - A) - w \quad (17)$$

The term $(I - A)$ is constant, regardless of the nature of the medium. The activation energy of a substance, after a change in permittivity of the medium develops, may then be written

$$\begin{aligned}
E_{a2} &= E_{a1} - (w_1 - w_2) \\
E_{a2} &= E_{a1} - \frac{e^2}{4\pi r} \left(\frac{1}{\epsilon_1} - \frac{1}{\epsilon_2} \right) \quad \text{or,} \\
E_{a2} &= E_{a1} - \frac{e^2}{4\pi r} \left(\frac{\epsilon_2 - \epsilon_1}{\epsilon_2 \epsilon_1} \right)
\end{aligned} \tag{18}$$

If the change in ϵ is small, Equation (18) may be rewritten to

$$E_{a2} = E_{a1} - \frac{e^2}{4\pi r} \left(\frac{\Delta\epsilon}{\epsilon^2} \right) \tag{19}$$

When the medium is between the plates of a capacitor, as in the lock-and-key sensor, changes in the permittivity of the medium may be recorded as changes in the capacitance. Since $C = D\epsilon$, where D is a geometric constant, then

$$D \frac{C_1 - C_2}{C_1^2} = \frac{\Delta\epsilon}{\epsilon^2} \tag{20}$$

may be substituted in Equation (19).

Assuming that the mobility of carriers remains constant, the conductivity equation may now be written as

$$\sigma_2 = \sigma_1 \exp \left[E_{a1} - \frac{e^2 D}{4\pi r} \left(\frac{C_1 - C_2}{C_1^2} \right) \right] \tag{21}$$

and taking logarithms,

$$\log_{10} \frac{\sigma_2}{\sigma_1} = \frac{1}{2.303} \left[E_{a1} - \frac{e^2 D}{4\pi r} \left(\frac{C_1 - C_2}{C_1^2} \right) \right] \tag{22}$$

Therefore, a plot of Equation (22) on semilog paper should give a straight line of slope $\frac{1}{2.303} \frac{e^2 D}{4\pi r}$ and the y-intercept $\left(y = \log \frac{\sigma_2}{\sigma_1} \right)$ is $\frac{1}{2.303} E_{a1}$, assuming no other interactions.

Although, as mentioned earlier, the experimental change in capacitance was found to be very small, leading to the possibility of errors, a definite correlation was found to exist between the conductivity and permittivity, as shown in Figures 65 - 67, and it appears to be roughly in the nature of that predicted by Equation (21).

Since a relationship has been shown to exist between the pressure and the conductivity, as well as between the dielectric effects and the conductivity, it is believed that the curves shown in Figures 63 and 64, and Figures 65 - 67 would show effects such that the dielectric would affect the pressure-conductivity curve and the pressure would be making a contribution to the dielectric curve. Thus, it is difficult to completely eliminate the other parameter from each set of curves, although they have been minimized.

Another way of qualitatively demonstrating the effects of a changed permittivity on the conductivity is shown in Tables VII - X. It may be assumed that gases, whose molecules are polar, will have a greater effect on the permittivity of a medium into which they are absorbed than those that are non-polar. Tables VII - X list the gases, to which each polymer was exposed, in decreasing order of their effect on the conductivity at a pressure of 10 torr. Column 1 lists the gases, column 2 the generally-accepted acid-base type for the gas, and column 3 indicates the symmetry or polarity of the gas molecule. It can be seen that the general trend indicates the dielectric effect to be most pronounced. In other words, the more acidic polymer would show more pronounced interactions with basic gases, and conversely with the basic polymer; or, in keeping with the concept of electronegativities, the more electronegative polymer should interact most strongly with basic gases.

Still another parameter may be involved in the operation of the sensors, viz., a space charge effect. It has been observed that a large space charge is developed in the lock-and-key sensor which may be explained in terms of carrier traps. Thus, when a voltage is first applied to a sensor, a current is developed that slowly decays to an equilibrium value. An explanation for this is that traps exist in the polymer, just below the conduction band, that capture carriers injected from the electrodes. The concentration of these

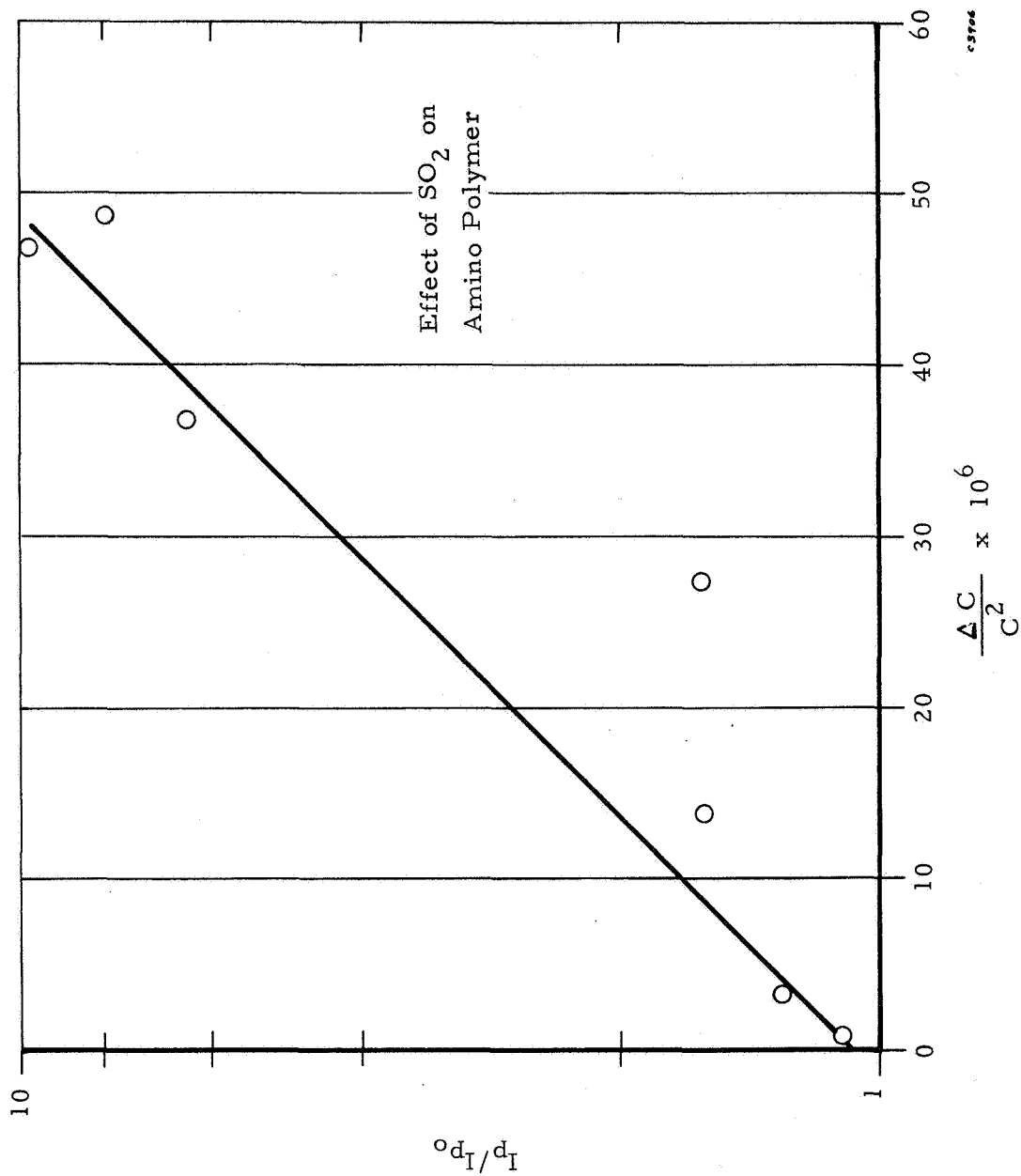


Figure 65. Relation Between Permittivity and Conductance of Poly(p-aminophenylacetylene)

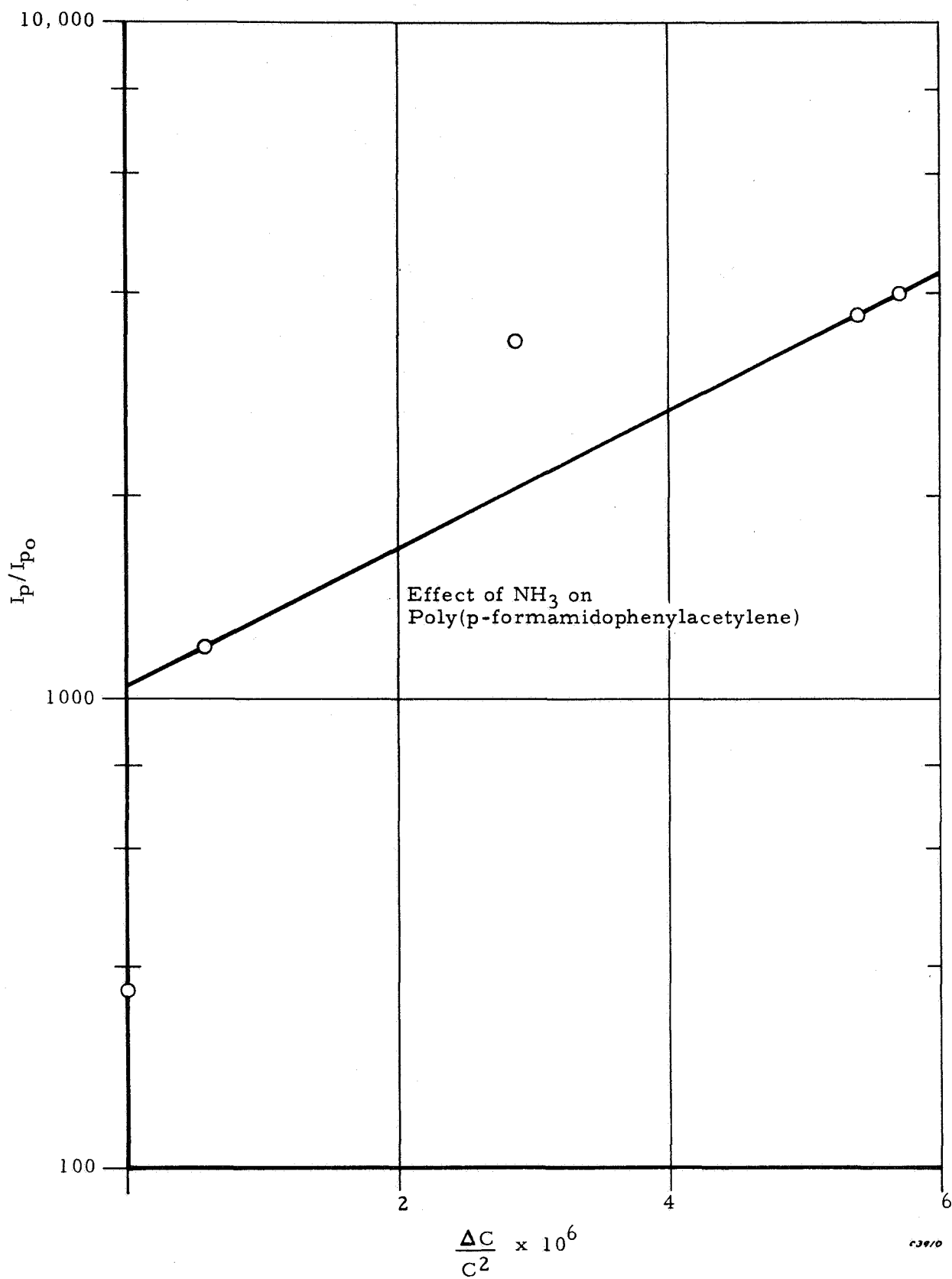


Figure 66. Relation Between Permittivity and Conductance of Poly(p-formamidophenylacetylene) in Presence of NH_3

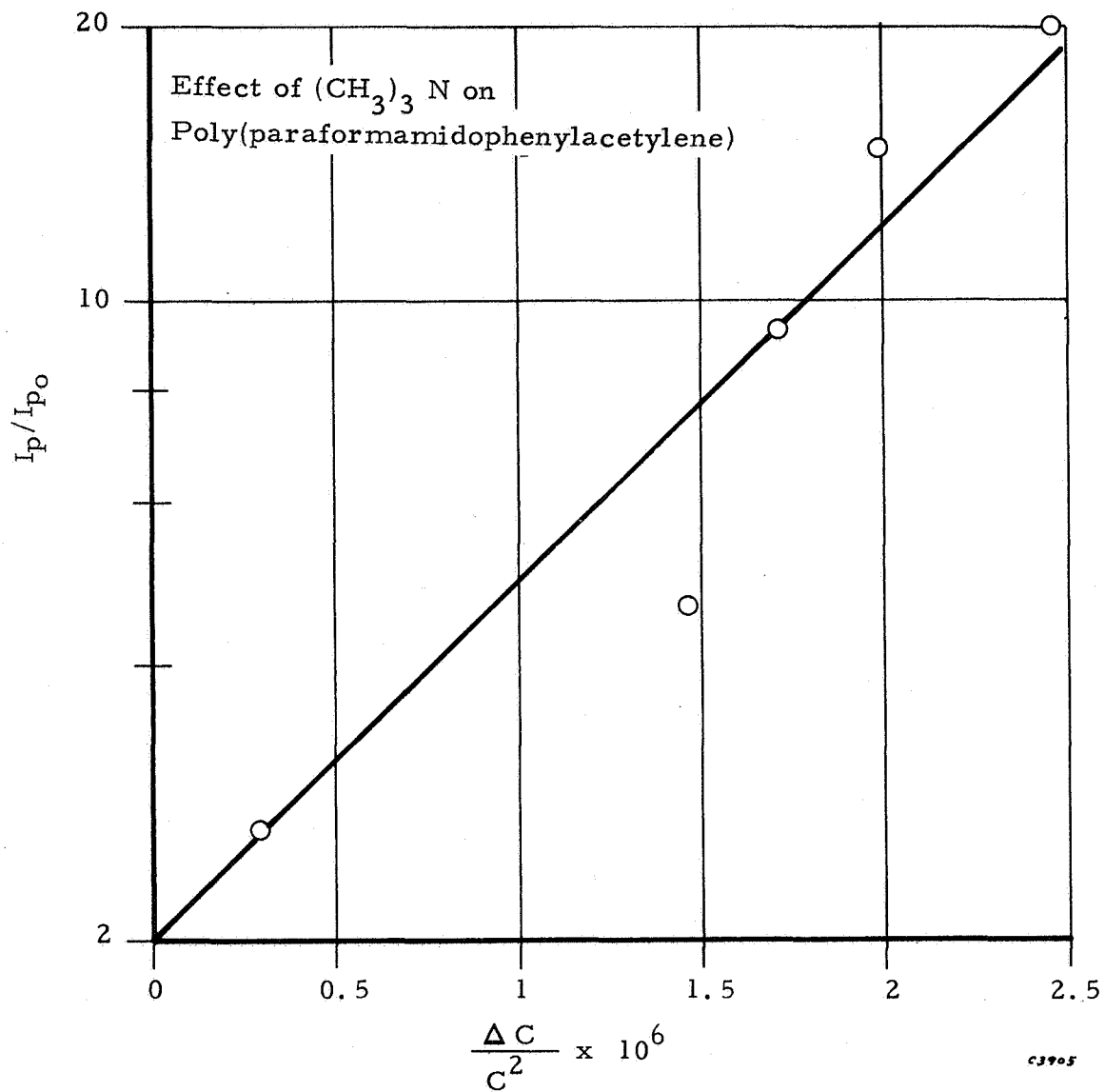


Figure 67. Relation Between Permittivity and Conductance of Poly(p-formamidophenylacetylene) in Presence of $(\text{CH}_3)_3\text{N}$

TABLE VII

GAS EFFECTS ON POLY(PHENYLACETYLENE) (AMPHOTERIC)


<u>Gas</u>	<u>Acidity or Basicity</u>	<u>Polarity (Symmetry)</u>	
H ₂ O	neutral	polar	
BF ₃	acid	polar	
NH ₃	base	polar	
He	neutral	symmetrical	 <p>Decreasing Order of Response</p>
H ₂ S	base	polar	
(CH ₃) ₃ N	base	polar	
CO ₂	acid	linear symmetrical	
(C ₂ H ₅) ₃ N	base	polar	
N ₂	base	linear symmetrical	
acetaldehyde	acid	polar	
O ₂	acid	linear symmetrical	
Freon F14	neutral	symmetrical	
(C ₂ H ₅) ₂ O	base	polar	

TABLE VIII
GAS EFFECTS ON POLY(P-NITROPHENYLACETYLENE)
(ACID-TYPE)

<u>Gas</u>	<u>Acidity or Basicity</u>	<u>Polarity (Symmetry)</u>	
H ₂ O	neutral	polar	
NH ₃	base	polar	
(CH ₃) ₃ N	base	polar	
He	neutral	symmetrical	↓ Decreasing Order of Response
CO ₂	acid	linear symmetrical	
Ar	neutral	symmetrical	
Freon F114	neutral	linear symmetrical	
O ₂	acid	linear symmetrical	
N ₂	base	linear symmetrical	
H ₂ S	acid	polar	
H ₂	acid	linear symmetrical	
(C ₂ H ₅) ₃ N	base	polar	
methyl acetylene	base	polar	
CO	base	polar	
acetaldehyde	acid	polar	
BF ₃	acid	polar	
Freon F14	neutral	symmetrical	


TABLE IX

GAS EFFECTS ON POLY(P-FORMAMIDOPHENYLACETYLENE)
(WEAK ACID-TYPE)

<u>Gas</u>	<u>Acidity or Basicity</u>	<u>Polarity (Symmetry)</u>	
NH ₃	base	polar	
H ₂ O	neutral	polar	
(CH ₃) ₃ N	base	polar	
He	neutral	symmetrical	↓ Decreasing Order of Response
methyl acetylene	base	polar	
BF ₃	acid	polar	
H ₂ S	acid	polar	
SO ₂	acid	linear symmetrical	
Freon F14	neutral	symmetrical	
N ₂	neutral	linear symmetrical	
O ₂	neutral	linear symmetrical	
CO ₂	neutral	linear symmetrical	
CO	base	polar	
Ar	neutral	symmetrical	
CH ₄	neutral	symmetrical	
H ₂	neutral	linear symmetrical	

TABLE X

GAS EFFECTS ON POLY(P-AMINOPHENYLACETYLENE)
(BASIC-TYPE)

<u>Gas</u>	<u>Acidity or Basicity</u>	<u>Polarity (Symmetry)</u>	
H ₂ O	neutral	polar	
NH ₃	base	polar	
BF ₃	acid	polar	
(CH ₃) ₃ N	base	polar	
SO ₂	acid	linear symmetrical	 <p>Decreasing Order of Response</p>
He	neutral	symmetrical	
H ₂ S	acid	polar	
O ₂	acid	linear symmetrical	
N ₂	base	linear symmetrical	
CH ₄	neutral	symmetrical	
Freon F114	neutral	linear symmetrical	
CO ₂	acid	linear symmetrical	
CO	base	polar	

trapped carriers is such that their net electric potential opposes the applied potential. Eventually, however, nearly all the traps will be filled and the net electric potential across the sample will reach some equilibrium value that determines the current flow.

When the initial applied voltage is 100 volts, the initial current is given by $I_1 = \frac{100}{R}$, where R is the resistance of the polymers. Then, when the traps are filled, the net electric potential will be $E_{\text{net}} = 100 - E_T$ where E_T is the trap potential, and the current will be $I_2 = \frac{100 - E_T}{R}$. As $E_T \rightarrow 100$ volts, the current will be reduced considerably. E_T , though, is dependent on the number of trapped charges, and this number, in turn, is dependent on the activation energy of the traps, with the trap energy distribution being quite broad — from deep to shallow.

Since the activation energy is related to the permittivity of the medium, then increasing the permittivity by addition of a gas will lower the activation energy of many of the shallow traps, thereby releasing a number of carriers. This will have two effects. First, a current surge will be noted due to the released carriers. Second, a new equilibrium current will result because of the decreased value of E_T caused by the liberation of the trapped carriers. The response obtained with the nitro polymer, as shown in Figure 53, may be related, not only to the earlier discussed sorption effect, but also to the electrical response upon liberation of trapped carriers after gas was introduced.

It is also well-established from energy band theory of semiconductors, that the bands may be pictured as bending up or down at the surface resulting in a space charge region variously known as the double layer, barrier layer or boundary layer. In the case of a clean silicon surface, for example, the space charge is a result of "dangling" covalent bonds that may act as electron traps, taking electrons from the bulk to a depth dependent on the number of surface states (number of unsatisfied bonds), and the density of carriers in the bulk.⁽⁶⁰⁾ If the surface has a layer of oxide, electrons may be trapped in the oxide, drawing holes to the oxide-silicon interface from a depth dependent on the same parameters, mentioned above. This depth is known

as the barrier width, and it serves to define the thickness of what shall be described as the "electrical surface" of a material as opposed to its physical surface. The "electrical surface" exhibits electrical properties that are usually different from those in the bulk, often including higher conductivity and a different type of carrier.

The question as to whether or not this behavior has been exhibited in the thin polymer films on the lock-and-key electrode has been given some consideration. Therefore, if there is an "electrical surface" and a bulk region, both parallel to the current path, which is responsible for conduction? Also, which is responsible for gas effects? By calculating the barrier width, and comparing it to the polymer film thickness, some insight may be gained as to whether these considerations are of some concern.

Bardeen⁽⁶¹⁾ gives the electrostatic potential across a barrier layer as

$$\psi = \frac{2\pi e}{\epsilon} Nw^2$$

from which

$$w = \sqrt{\frac{\psi \epsilon}{2\pi e N}} \quad (23)$$

Where ψ = electrostatic potential, e = electronic charge, ϵ = permittivity, N = density of carriers in the bulk and w = barrier width. In order to calculate the barrier width in the polymer, it is necessary to know N , the density of carriers. By assuming that at infinite temperature, each polymer chain contributes one carrier, and from the density, average molecular weight and activation energy (all of which have been determined), an estimate of N for the nitro polymer is $7.1 \times 10^{12} \text{ cm}^{-3}$. Since the dielectric constant for this polymer is 2.54, the barrier width is found from Equation (23) to be $w = \sqrt{\psi} (5.7 \times 10^{-4}) \text{ cm}$. If ψ is in the usual range of from 0.1 to 1 volt, then $1.8 \times 10^{-5} \text{ cm} < w < 5.7 \times 10^{-4} \text{ cm}$. This represents a calculated value for w . However, when a rough drift mobility measurement was made on a pellet of the nitro polymer, it was found that N had an experimental value of $22 \times 10^{-2} \text{ cm}^{-3}$, and this gave a value of $w \approx \sqrt{\psi} 5.7 \times 10^2 \text{ cm}$. Therefore, it is

obvious that a more exact value for N is necessary in order to reduce the discrepancy between the calculated and the experimental value for w.

It was stated earlier that the polymer film thickness for the nitro polymer in the lock-and-key electrode was found, interferometrically, to be 2.4×10^{-5} cm. Comparison with the values of w, shown above, would indicate that the polymer film may be regarded as all "electrical surface" (not to be confused with physical surface). On the basis of these considerations, therefore, it seems best to regard the polymer film as a homogeneous material with properties that may be related to the bulk material. When speaking of the physical surface, then, reference should be made only to the outermost monomolecular layer. It can be seen, from these results, that considerably more work needs to be done in order to pinpoint those characteristics that produce the observed results.

2.3 COMBINATION ORGANIC-INORGANIC DEVICES

Buck, Allen and Dalton ⁽²⁵⁾ have indicated that the change in surface conductivity of an inorganic semiconductor, as detected by the reverse leakage current of a p-n junction diode, could be used for detecting gases. The conductivity changes referred to were claimed to be inside the surface of the semiconductor, but are induced by a charge on the surface. Thus, adsorbed species were presumed to act as electron donors or acceptors thereby making the surface more strongly n-type or more strongly p-type than the bulk material. Then, if the bulk is quite pure (high resistivity and having few donors or acceptors), the relative conductance changes may be quite large, and electrically active adsorbed atoms may be detected with considerable sensitivity. With this concept in mind, and using high resistivity p-n junctions in an n-p-n configuration, they were able to detect ammonia at a concentration as low as $1/10^8$. However, it appears that their system was irreversible. It was believed that by using a similar device coated with conjugated polyenes one could get the gas/polymer interaction to inject carriers into this substrate and thereby obtain both the desired specificity as well as sensitivity.

A promising configuration that utilizes and amplifies the capacitive variations in the film rather than the resistivity changes, is obtained by using the films in combination with metal-oxide-silicon field effect transistors (MOS device). In this case, the capacitive changes in the film are utilized to modulate the source-drain current of the field effect transistor. This concept appears to be quite worthwhile because of the high gain characteristics of the MOSFET.

In a standard MOS field effect transistor, as typified by Figure 68 (excepting that the aluminum gate which is over the silicon dioxide insulating region is generally thicker), the properties of the "channel" region are governed by the SiO_2 and the aluminum gate. In order to demonstrate that the polymer must be in direct contact with the SiO_2 for it to affect the "channel" region, a transistor, such as shown in Figure 68, was coated with poly(p-nitrophenylacetylene) and exposed to 0.5 torr of ammonia. No effect was noted.

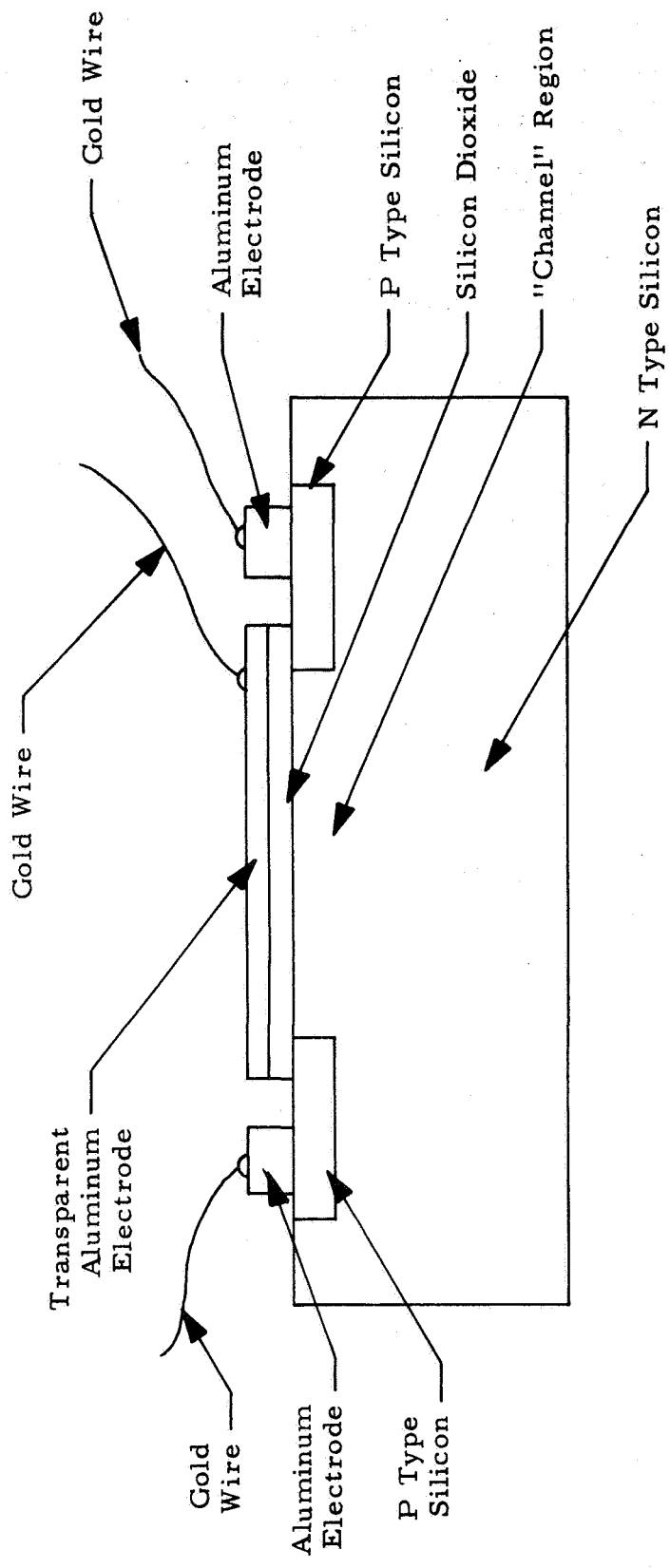
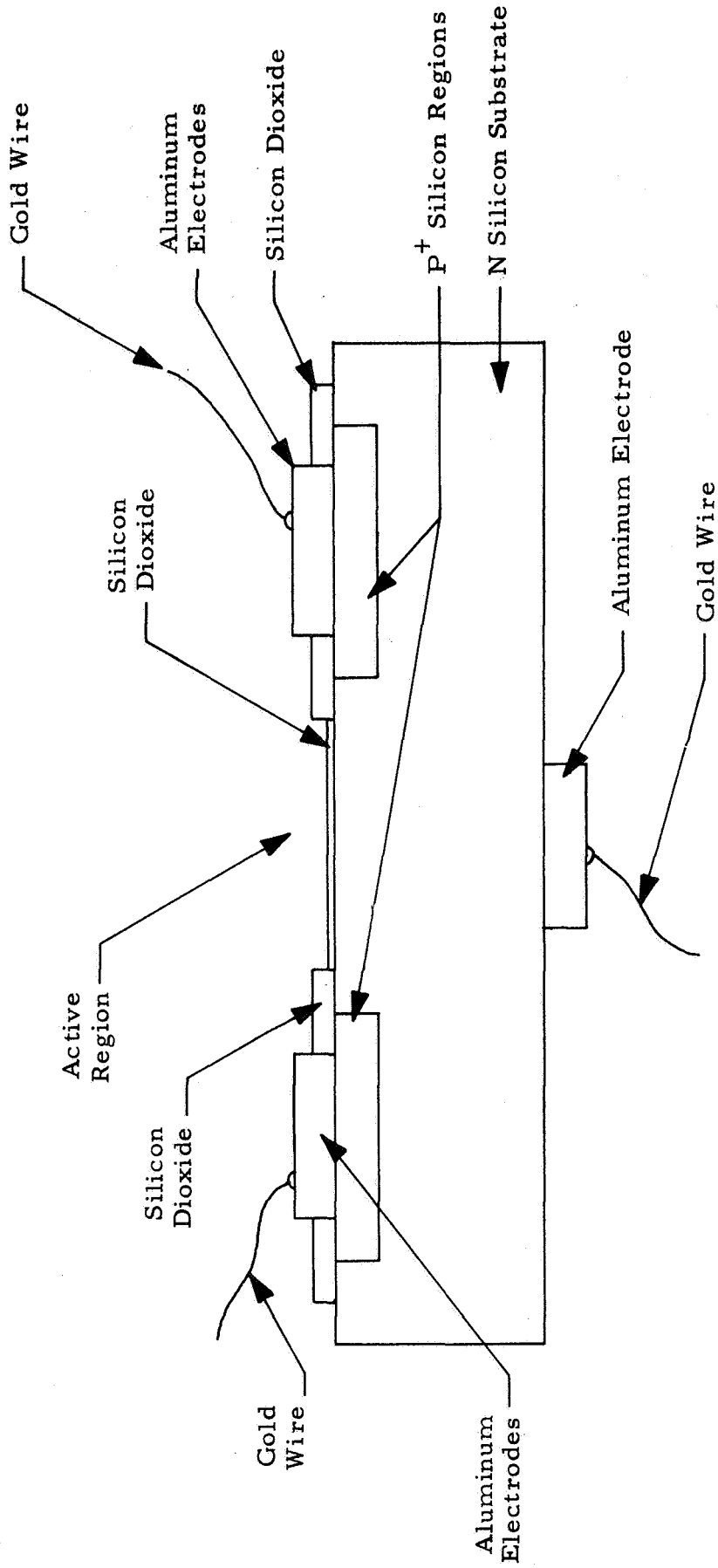


Figure 68. MOS Device but with a Thin Aluminum Gate

The next approach was to fabricate an MOS FET device by producing two heavily doped p regions on an n-type silicon wafer, but this time the gate was left off leaving the channel bare except for a thin layer of SiO_2 (Figure 69). Leads were attached to each p region and to the substrate. The behavior of the device was determined by monitoring the current through the channel when one p-n junction was reverse biased. Figure 70 depicts the circuitry involved. The wafer was mounted in a transistor case with leads attached in the same manner as in a commercial transistor. No cap was placed on the base to allow access for coating with polymers and exposure to a gas.

One device was left uncoated, evacuated to 10^{-5} torr and exposed to 0.5 torr of ammonia. Before evacuation, the reverse current dropped three orders of magnitude. However, there appeared to be some amines left in the vacuum chamber from previous runs and this first drop could probably be related to their presence. After complete evacuation, the current went up slightly. Subsequent exposure to ammonia caused a slight change to develop in the current, but the system appeared to have suffered some irreversible change since it did not regenerate either upon evacuation or further exposure to ammonia. Figure 71 is a plot of the response of this $p^+ n p^+$ uncoated device.

Another device was coated with poly(phenylacetylene), evacuated in the vacuum chamber to 10^{-5} torr and exposed to 0.5 torr of NH_3 . It was continuously cycled by exposure to gas, evacuation and re-exposure. Figure 72 depicts the response characteristics of this coated device. The initial current (before exposure) was 1.65×10^{-5} amps. Initial exposure caused the current to drop to 1.8×10^{-8} amps and evacuation only partially reversed it. However, it was reversible enough to permit the cycling behavior shown in Figure 72. Figure 73 is a reproduction of the current response of the same device tested one week later. This time the ammonia pressure was one torr. (Note the different scale used in this plot when comparing with Figure 72.) After the first exposure to NH_3 and subsequent evacuation, the n (substrate) lead was disconnected from the p lead. This resulted in a reduction in current, but a useful response characteristic was still observed.



63771

Figure 69. MOS-FET (P⁺ - n - p⁺) Device Used Without the Gate

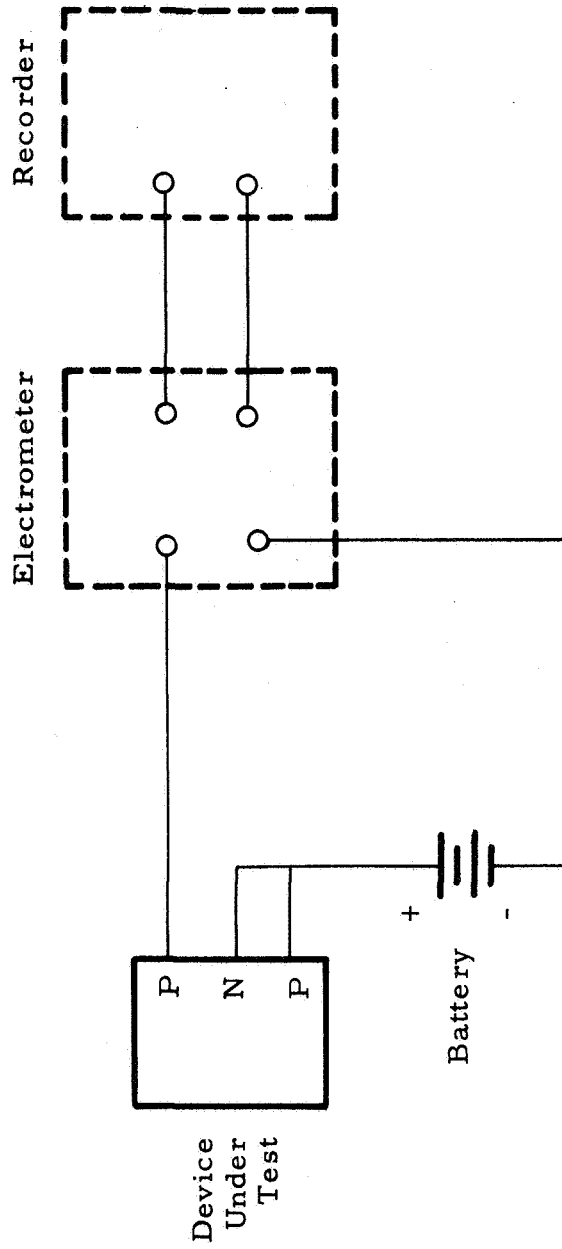
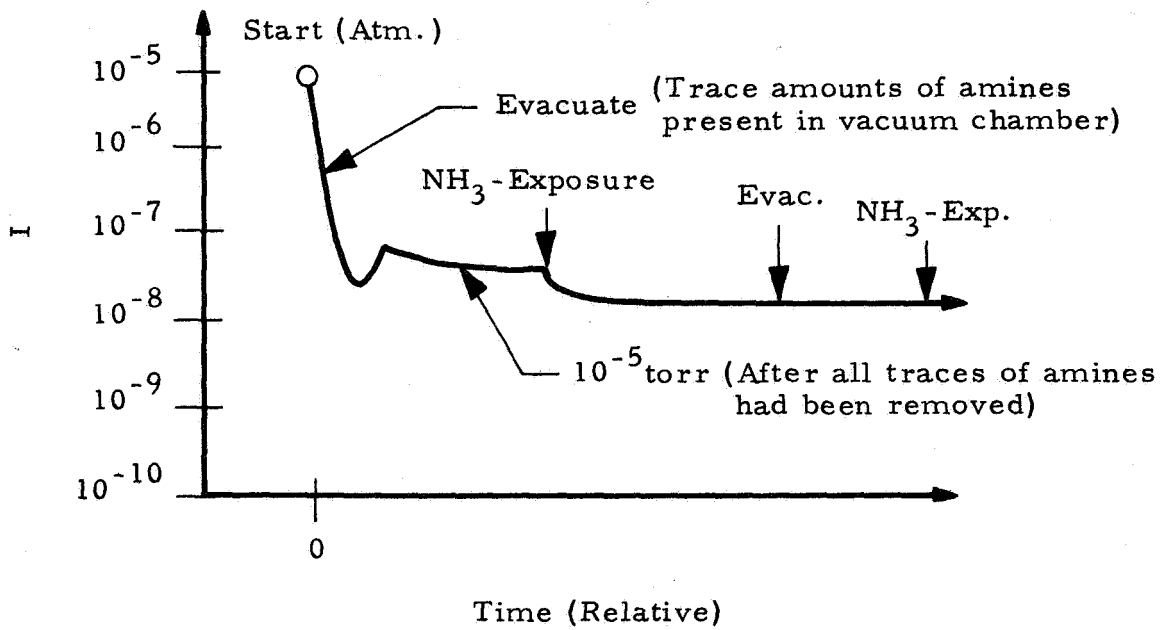
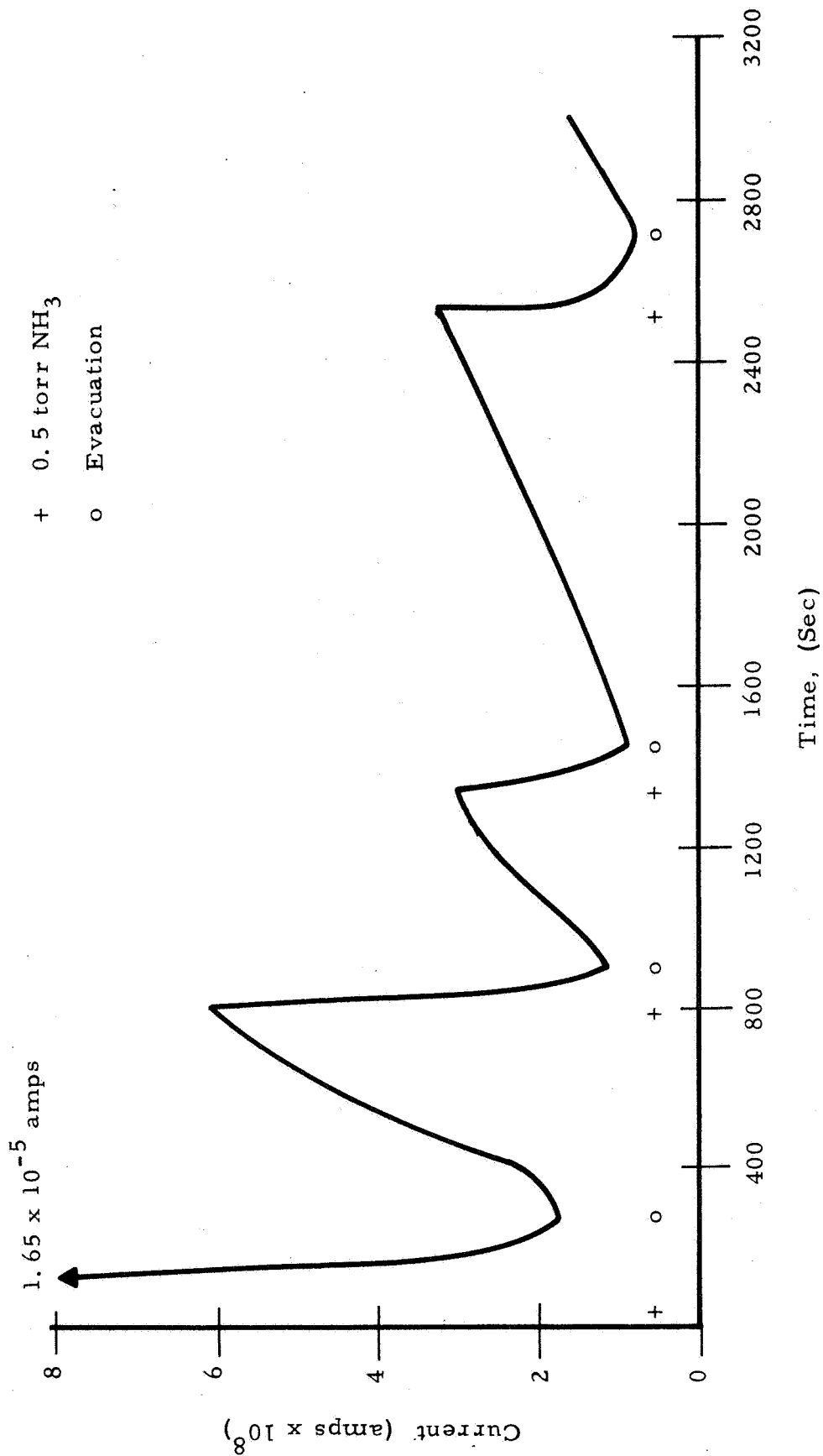


Figure 70. Circuitry for Measuring the Characteristics of P⁺N P⁺



63734

Figure 71. Gas Response of Uncoated Planar $p^+ n p^+$ Device



2779

Figure 72. Leakage Current Through p⁺n⁺p⁺ Silicon Sensor Coated With Poly(phenylacetylene) and Exposed to Ammonia Followed by Regeneration and Re-exposure (9 Volts Applied)

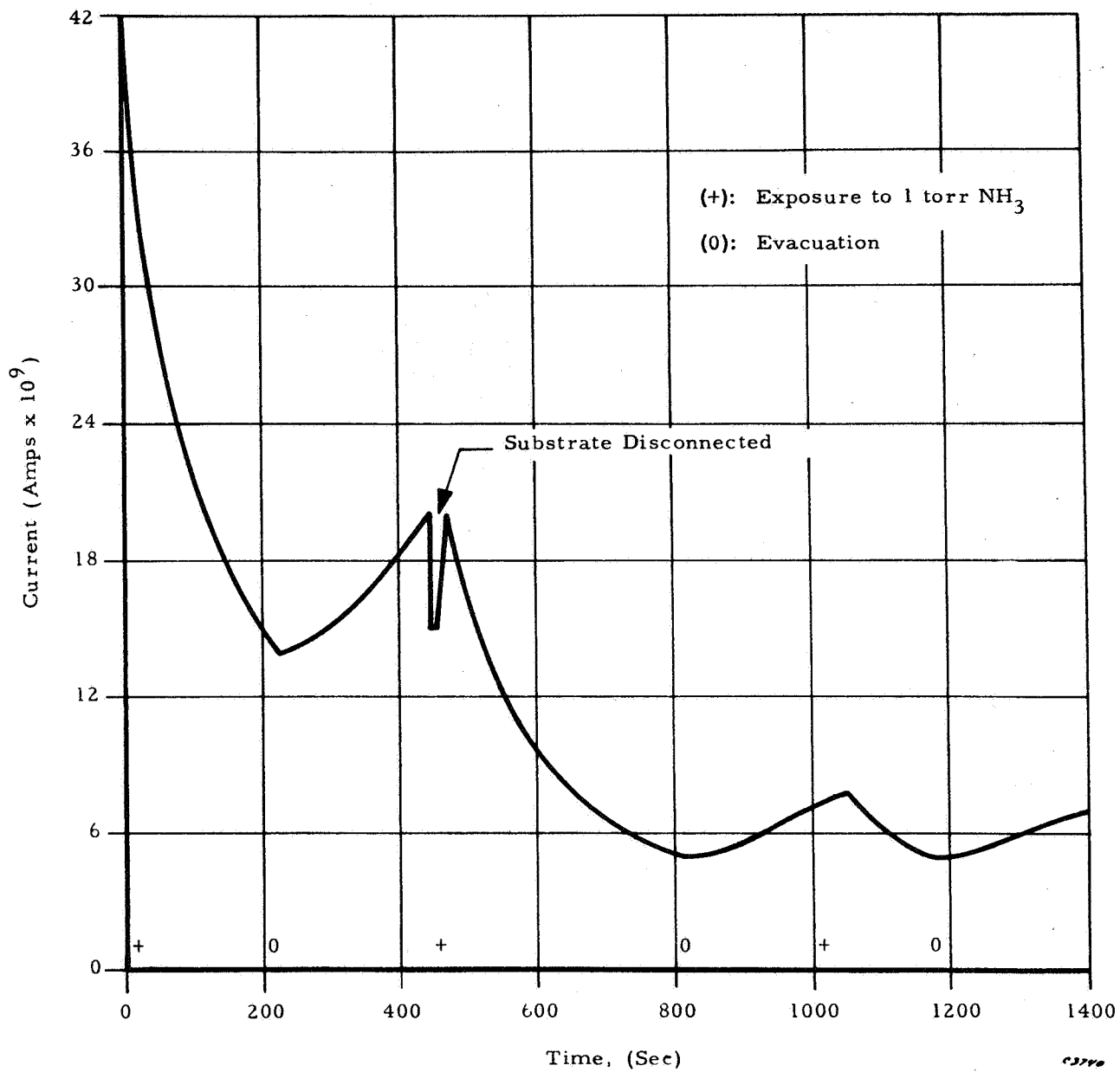


Figure 73. The $p^+ n p^+$ Sensor Coated with Poly(phenylacetylene) and Left Standing for One Week

A third device was coated with poly(p-nitrophenylacetylene) and tested in the same manner. Its response to different pressures of ammonia is depicted in Figure 74. The first injection of ammonia (0.5 torr) brought the current down from 2.6×10^{-4} amps to about 1.5×10^{-8} amps. Repeated evacuations and gas injections subsequently showed fairly good reproducibility — even to the good response at 0.09 torr.

Once again, as in the lock-and-key sensor, the nitro polymer shows the greater sensitivity to NH_3 over poly(phenylacetylene). This further supports the concept of electronegativity interactions between gases and polymeric substrates.

Some of the advantages of the silicon transistor-polymer combination are, as follows:

A higher current level is available (10^{-9} amps as opposed to 10^{-12} - 10^{-14} in the present glass substrate system). A higher current gives greater freedom from noise and less susceptibility to leakage currents caused by contamination. Another possible advantage is the ability to correct the device for long term dc drift by using an aluminum electrode as part of the active area thereby permitting application of a bias voltage as in a standard field-effect transistor. It was for this reason the FET with the transparent aluminum electrode was fabricated. However, a more feasible way would be to put the polymer on the silicon wafer before coating it with aluminum. A possible disadvantage to this method is that the polymer may be partly masked from the incoming gas. To get around this, the aluminum may be put on part of the channel area. This might sacrifice part of the control capability of the device, but there would be increased usefulness and availability of the polymer. A further advantage to this system is the lower voltage requirements to drive it (9 volts applied versus 100 volts for the glass-based substrate). Although the mechanism of its action is not completely understood, the most promising of the devices is a combination of organic polymer with the $p^+ - n - p^+$ silicon system. Appendix B gives a theoretical analysis of its action.

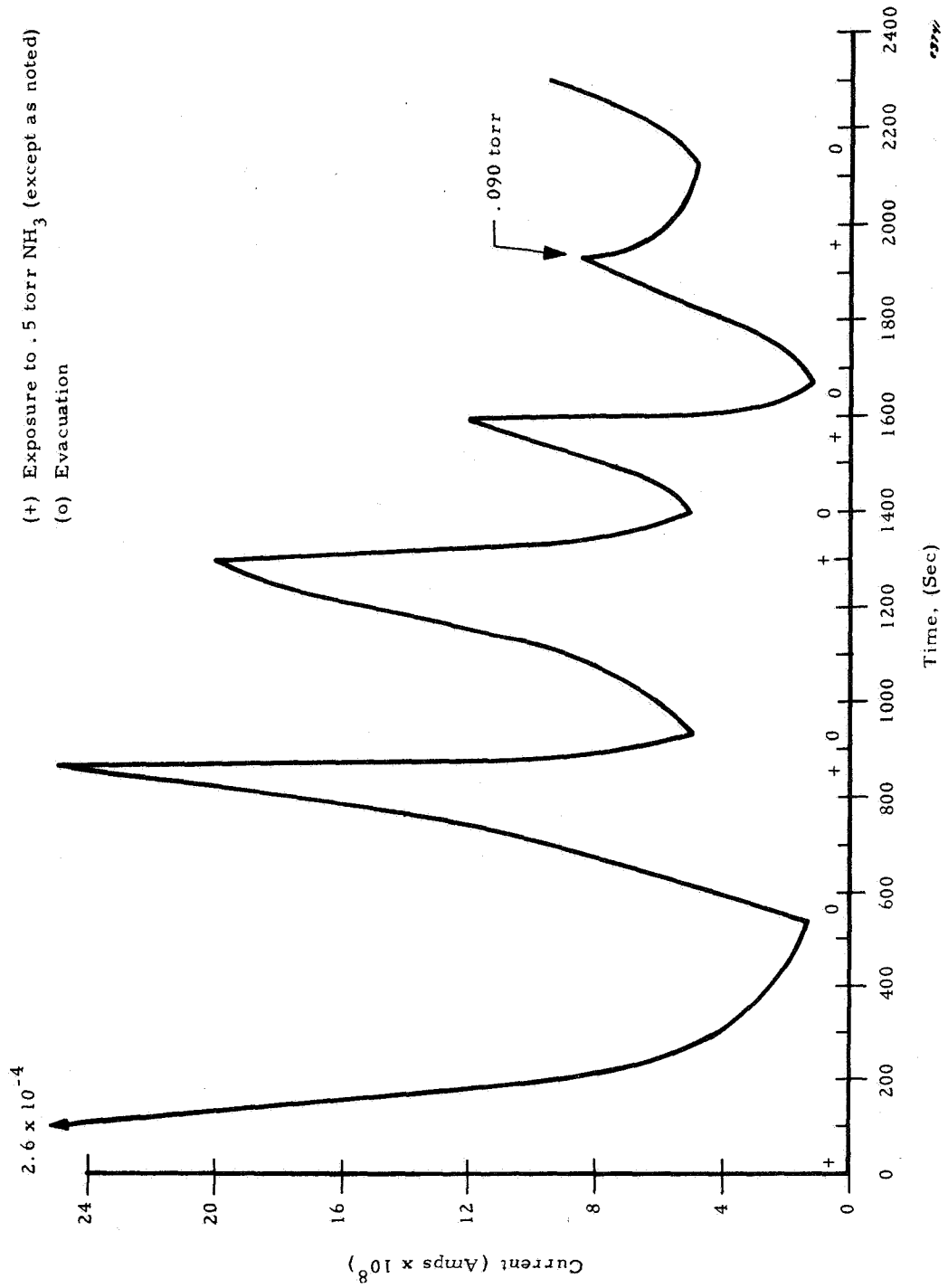


Figure 74. Response of a p⁺ n p⁺ Sensor Coated with Poly(p-nitrophenylacetylene) and Exposed to Ammonia.

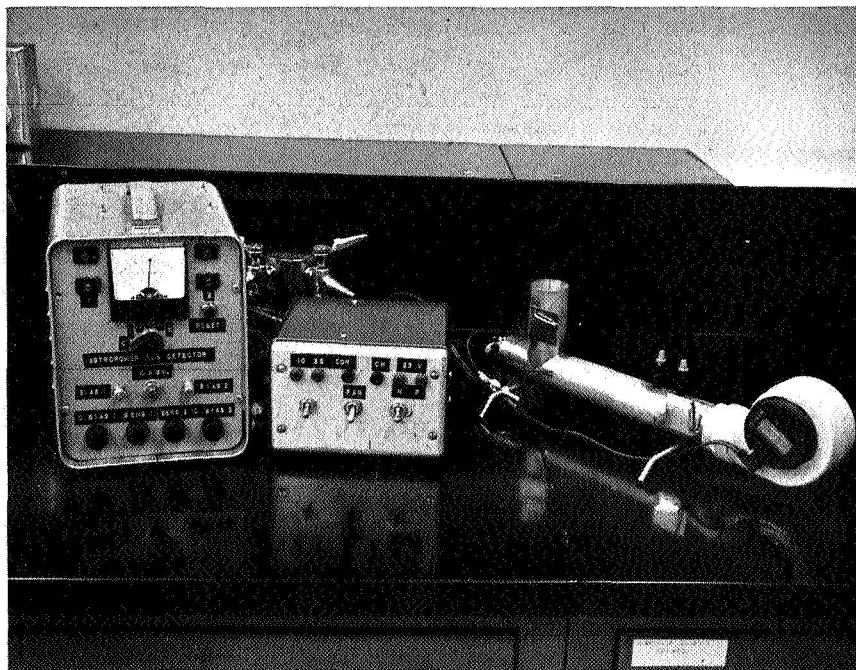
Silicon devices are very small and many may be put into a small space. Several gas detectors, each with a different polymer, and the associated control and amplification circuitry could be built into a few transistor cans, or on a single silicon wafer. A box the size of a cigarette package could probably contain the entire gas detector including the analog to digital conversion for computer input, but exclusive of power source. The results, to date, are encouraging.

2.4 PROTOTYPE PORTABLE GAS DETECTOR

A two sensor gas detector has been built. It uses poly (p-nitrophenylacetylene) and poly (p-aminophenylacetylene) as the sensing polymers, cast as thin films on the lock-and-key electrode geometry described earlier (Figure 30).

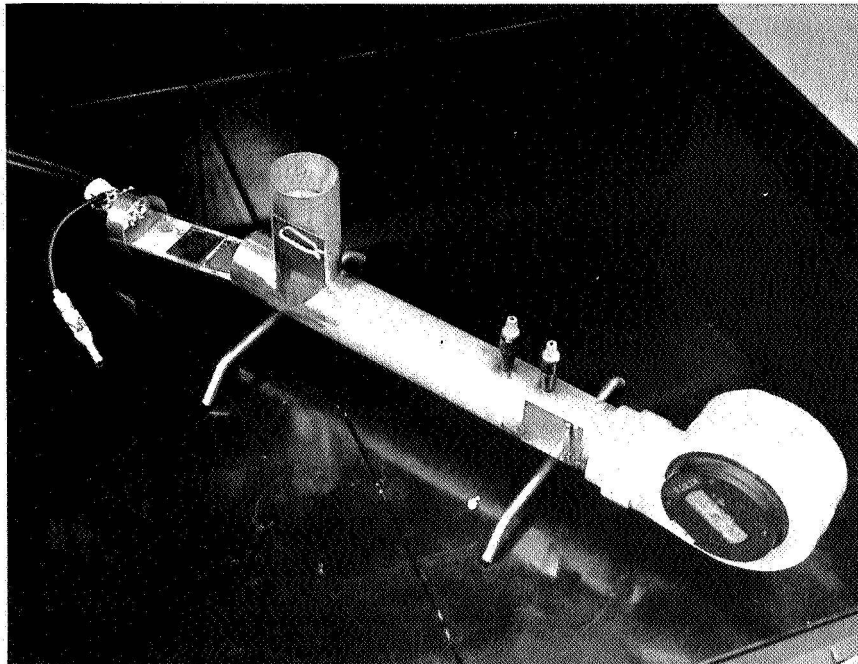
Figures 75-77 show the Astropower Gas Detector first, in an overall view of the entire package (Figure 75); second, the sensor housing chamber showing the sensors partly pulled out (Figure 76); and third, the actual sensors removed from the chamber (Figure 77). Figure 78 is a schematic of the input stage and Figure 79 is a block diagram of the entire unit. Appendix C gives a more detailed description of the operation of the input stage. Following, is a general description of the design of the detector plus some data on its response characteristics.

One sensor is connected to each side of a differential amplifier, and a voltage applied to the sensor. The amplifier detects the currents flowing through the sensors, and under standard atmosphere conditions the differential output is adjusted to zero. When a contaminant is present in the atmosphere, each sensor responds according to the extent of its interaction with the contaminant. The response is sensed by amplifying changes in current flowing through the sensors. Since it operates on a differential basis, the difference of the changes appears at the output as either a positive or negative voltage - the polarity depending on which sensor changes the most. A zero center panel meter, which serves as an indicator, is connected across the output, and the amplitude of the output voltage is dependent on the relative magnitude of the changes. The unit also incorporates a simple adjustable threshold logic circuit that turns on one of a pair of lights when the differential output exceeds



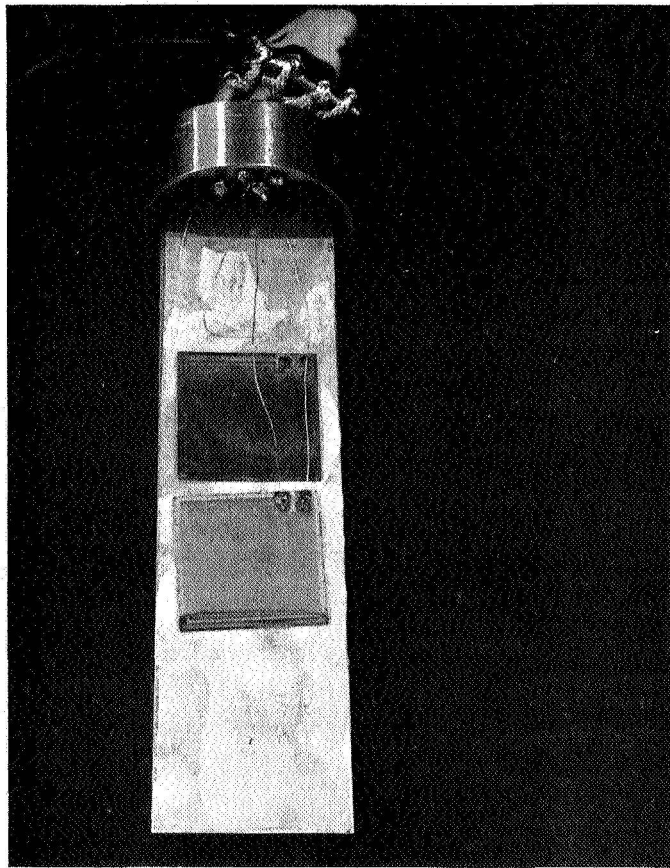
c30/3

Figure 75. Astropower Gas Detector Showing Detector Chamber and Attached Electronic Gear



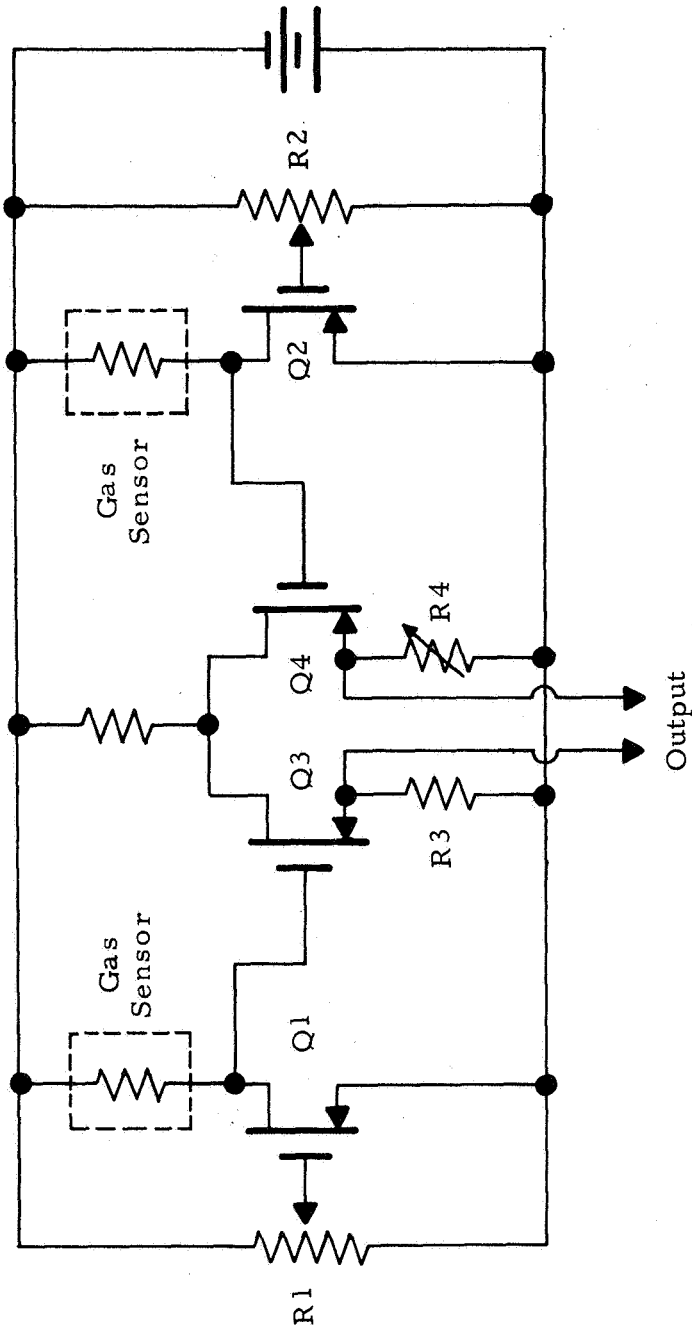
c 38/2

Figure 76. Detector Chamber with Sensors Partly Pulled Out



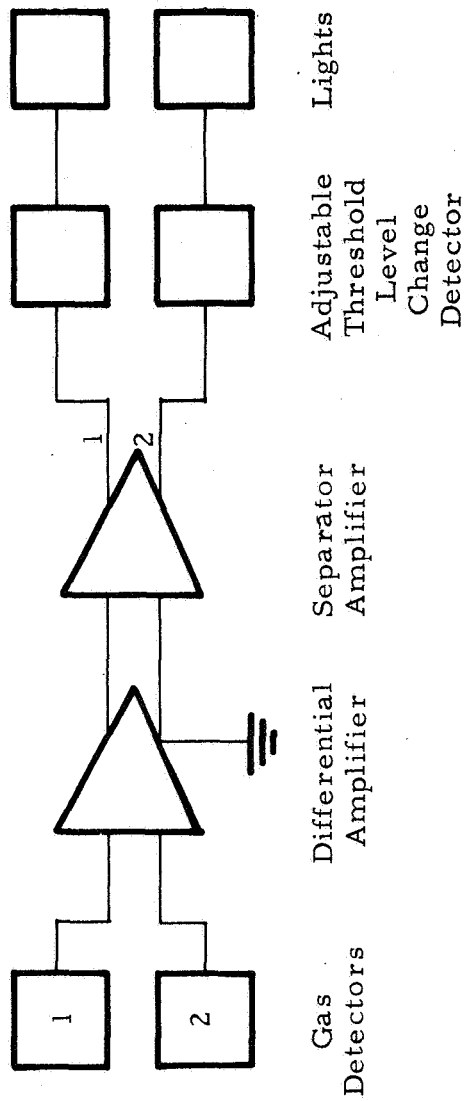
03814

Figure 77. Detector Sensors



63744

Figure 78. Circuit Schematic, Portable Gas Detector Differential Amplifier



238/8

Figure 79. Block Diagram of Differential Gas Detector (Prototype)

a predetermined level. The light that is on indicates which sensor has responded to the gas introduced.

This first generation prototype gas detector has been tested under laboratory atmosphere conditions mostly with ammonia (to which the nitro polymer responds) and sulfur dioxide (to which the amino polymer responds). In a quantitative reliability test, these gases were alternately injected into the sensor chamber with a gas hypodermic syringe. For 20 tests with each gas, the corresponding polymer responded to the gas to which it was sensitive with no response from the other polymer. Concentrations as low as 10 ppm were used with SO_2 and 5 ppm with NH_2 , with no failure to respond. The threshold of sensitivity was approximately 2 ppm. In one instance, when the sensor chamber had been left open, it detected a small leak in a sulfur dioxide bottle six feet away which was undetected by a person sitting next to the bottle. It is claimed (62) that the lower limit of SO_2 detectability by humans is 0.3-1ppm, and readily so at 3 ppm. Similar behavior was observed with the nitro polymer. By opening a bottle of ammonium hydroxide at varying distances from the inlet duct it was found that the sensor would respond as anticipated.

Other qualitative tests were also performed with various gases in order to assess the detector's capabilities. Table XI lists some of the gases used and which polymer responded.

One curious response was noticed with the nitro polymer. It appeared to be sensitive to some odor from the human body. Placing the hand near the inlet duct produced an immediate response that cannot be readily traced to water vapor or some foreign component on the hand. However, whatever the nature of the contaminant, it invariably caused the nitro polymer to respond. This characteristic need not destroy the detector's usefulness in a spacecraft or other inhabited area since a pattern recognition device used to sound alarms in the presence of harmful gases can also be educated to ignore a harmless gas.

TABLE XI
QUALITATIVE RESPONSE BEHAVIOR OF
ASTROPOWER GAS DETECTOR

<u>Gas</u>	<u>Polymer Responding</u>
CO ₂	Nitro
Diethyl ether	Nitro
BF ₃	Amino
Triethylamine	Amino
H ₂ S	Nitro

Section 3

CONCLUSIONS

The work clearly shows the fact that a solid state gas detector can be developed to operate successfully. Its operation is based on the use of polymeric organic semiconductors of varying electronegativity. It shows optimum response between electron attracting polymers and electron donating gases, and vice versa. Thus, poly (p-nidrophenylacetylene) is a sensitive, specific detector for ammonia while poly(p-aminophenylacetylene) shows strong responses with BF_3 and SO_2 .

It appears that many factors are involved in the generation of a response signal when a particular gas and a polymer interact. Th question of pressure effects, dielectric changes in the medium, charge-transfer effects, electrode geometry and polymer structure, among others, all appear to make some contribution to the system.

Measurements show that a bulk, rather than a surface, phenomenon prevails in the conduction mechanism, although a distinction has to be made between an "electrical surface" and a physical surface. That is, the "electrical surface" may extend throughout the bulk of the film. In the use of a combination organic-inorganic semiconductor device, signal amplification has been attained that may be related to band bending at the interface and inversion phenomena. Considerable further work is necessary to elucidate the mechanism of behavior of this system. However, with only an organic semiconductor on the lock-and-key electrode, it has been possible to build a prototype gas detector. Based upon a number of reliability tests with SO_2 and NH_3 in the presence of an amino polymer and a nitro polymer, both in the same chamber, it is shown that a multiple sensor gas detector is possible. That is, the ammonia was detected in a laboratory ambience by the nitro polymer and the SO_2 was detected by the amino polymer; each at concentrations as low as 3 ppm.

It has been demonstrated that a polymer-coated lock-and-key electrode geometry shows a faster response time than the finger electrode. This can be attributed to the fact that the incoming gas "sees" the maximum field more quickly in the former system; whereas in the latter there is a diffusion dependant characteristic. In addition, excellent sensitivities have been attained, and some specificity has been established for a number of gases on the various polymers used, e. g., NH_3 on the nitro polymer, and helium and BF_3 on the amino polymer. The greatest sensitivities, though, have been between limits of 2 ppm for NH_3 on the nitro polymer and about 2 ppm for BF_3 on the amino polymer. This has amply borne out the concept of electro-negativity effects as applied to a solid state gas detector.

Response and recovery times are in the order of seconds on the organic semiconductor while voltage requirements, although high for the organic semiconductors, are reasonably low for the combination organic-inorganic devices. However, before a piece of commercial hardware can be made available, each of the problem areas described, viz., type of polymer to be used optimization of organic-inorganic device and prototype gas detector, has to be further investigated in detail. It is notable that the prototype detector has been operated only with the organic semiconductor, alone. It has not been tried with the combination device. In order to try this, the organic-inorganic system has to be explored in greater depth. For example, it is not known to what extent the presence or absence of the gate over the polymer would affect its response to gases. Nor is it known whether an n-p-n device would be better than the p-n-p device used. Equally uncertain is what type of polymer can effect the maximum change in response. With respect to the polymer structure, therefore, it is of interest to ascertain whether an n-type polymeric organic semiconductor can be prepared; and how it would respond to gases. For the prototype detector, the question of ambience and circuitry are critical factors.

REFERENCES

1. Conference on Surface Effects in Detection, ed. by J. I. Bregman and A. Dravnieks, Spartan Books, Inc., Washington, D. C. (1965).
2. Byrd, N. R., Space Cabin Atmosphere Contaminant Measurement Techniques, Quarterly Progress Report, SM-48446-Q1, Contract NAS 12-15, September 1965.
3. Byrd, N. R., Space Cabin Atmosphere Contaminant Measurement Techniques, Quarterly Progress Report SM-48446-Q6, Contract NAS 12-15, April 1967.
4. Saunders, R. A., "Analysis of the Spacecraft Atmosphere," NRL Report 5816, October 23, 1965.
5. Shaffer, A., "Analytical Methods for Space Vehicle Atmospheric Control Processes," ASD Tech. Report 61-162, Part I, December 1961.
6. Johnson, J. E., Umstead, M. E. and Smith, W. D., "Nuclear Submarine Atmospheres, Part 2 - Development of a Total Hydrocarbon Analyzer," NRL Report 6064, January 30, 1964.
7. Piatt, V. R. and White, J. E., "The Present Status of Chemical Research in Atmosphere Purification and Control on Nuclear-Powered Submarines," AD 284576, August 29, 1962.
8. McKee, H. C., Rhoades, J. W., Wheeler, R. J. and Burchfield, H. P., "Gas Chromatographic Measurements of Trace Contaminants in a Simulated Space Cabin," NASA Technical Note D-1825, March 1963.
9. "Investigation of the Man-Machine Environmental Interface in the Closed Ecological System," Douglas Aircraft Company, Inc., MSSD, Proposal, January 26, 1965.
10. Coe, C. S., Rousseau, J. and Shaffer, A., "Analytical Methods for Space Vehicle Atmosphere Control Processes," ASD Tech. Report TR-61-162, Part II, p. 489, November 1962.

11. Olewinski, W. J., Rapier, G., Slawecki, T. K. and Warner, H., "Investigation of Toxic Properties of Materials Used in Space Vehicles," Aerospace Medical Research Labs. Report AMRL-TDR No. 63-99, December, 1963.
12. London, S. A. and West, A., "Gaseous Exchange in a Closed Ecological System," AMRL-TDR-62-139, December 1962.
13. Hoenig, S. A. and Eisenstadt, M. M., "Detection Techniques for Tenuous Planetary Atmospheres," NASA Grants and Research Contracts Office, Code SC, First Semiannual Report, June 1962 - Jan. 1, 1964.
14. Zisman, W. A., "Fundamental Factors in Detecting Chemicals as Adsorbed Films," NRL Report 6168, October 29, 1964.
15. Zisman, W. A., in Conference on Surface Effects in Detection, ed. by J. I. Bregman and A. Dravnieks, Spartan Books, Inc., Washington, D. C. (1965), p. 1.
16. Zisman, W. A., Bewig, K. W. and Timmons, C. O., Ibid., 53.
17. Labes, M. M. and Rudyj, O. N., J. Am. Chem. Soc. 85, 2055 (1963).
18. Reucroft, P. J., Rudyj, O. N. and Labes, M. M., Ibid, 2059 (1963).
19. Terenin, A., Proc. Chem. Soc., 1961, 321.
20. Weiss, D. E. and Bolto, B. A., in Physics and Chemistry of the Organic Solid State, Vol. II, ed. by D. Fox, M. M. Labes and A. Weisberger, Interscience Publishers, New York (1965) p. 67.
21. Jacobson, M. G., "Semiconductor Diode Construction for Use in Gas Detection," U.S. 2, 940, 041, June 7, 1960.
22. Jacobson, M. G., "Detection of Ambient Components by Semiconductors," U. S. 2, 965, 842, December 20, 1960.
23. Jacobson, M. G., "Semiconductor Diodes for Gas Detection," U.S. 2, 975, 362, March 14, 1961.
24. Jacobson, M. G., "Means and Methods for Gas Detection," U. S. 3, 039, 053, June 12, 1962.
25. Buck, T. M., Allen, F. G. and Dalton, J. V., in Conference on Surface Effects in Detection, ed. by J. I. Bregman and A. Dravnieks, Spartan Books, Inc., Washington, D. C. (1965) p. 147.
26. Dewar, M. J. S. and Talati, A. M., J. Am. Chem. Soc., 85, 1874 (1963).

27. Bohrer, J. J., Trans. New York Acad. of Sci. 20, 367 (1958).
28. Marvel, C. S., Jones, G. D., Mastin, T. W. and Schertz, G. L., J. Am. Chem. Soc., 64, 2358 (1942).
29. Alfrey, T., Jr., Haas, H. C. and Lewis, C. W., Ibid 73, 2851 (1951).
30. Okamoto, Y., Gordon, A., Movsovicus, F., Hellman, H. and Brenner, W., Chem. and Ind. 1961, 2004.
31. Liu, Yu-Ch'eng, Wu, Hsuan-Ch'ih, Lai, Szu-Ts'ung and Yu, Yu-Chen, Ko Fen Tzu T'ung Hsun 6 (6), 446-52 (1964); cf., C.A. 63, 16475c (1965).
32. Bawn, C. E. H., Lee, B. E. and North, A. M., Polymer Letters 2, 263 (1964).
33. Kambara, S. and Noguchi, H., Makromol. Chem. 73, 244 (1964).
34. Liu, Yu-Ch'eng, Wu, Hsuan-Ch'ih, Chung, Chin-Ts'ang and Shih, Chung-Hsiao, Ko Fen Tzu T'ung Hsun 6 (6), 477-480 (1964); cf., C.A. 63, 16475c (1965).
35. Noguchi, H. and Kambara, S., Polymer Letters 1, 553 (1964).
36. Byrd, N. R., Space Cabin Atmosphere Contaminant Measurement Techniques, Quarterly Progress Report SM-48446-Q2, Contract NAS 12-15, December 1965.
37. Roth, J. P., Rempp, P. and Parrod, J., J. Polymer Sci., Part C, No. 4, 1347 (1964).
38. Labes, M. M., Polymer Preprints, American Chemical Society Meeting in Los Angeles, California, April 1964, Vol. 4, No. 1, p. 202.
39. Byrd, N. R., Space Cabin Atmosphere Contaminant Measurement Techniques, Quarterly Progress Report SM-48446-Q3, Contract NAS 12-15, March 1966.
40. Byrd, N. R., Space Cabin Atmosphere Contaminant Measurement Techniques, Quarterly Progress Report, SM-48446-Q4, Contract NAS 12-15, June 1966.
41. Byrd, N. R., Space Cabin Atmosphere Contaminant Measurement Techniques, Quarterly Progress Report SM-48446-Q5, Contract NAS 12-15, Sept. 1966.
42. Statz, H., DeMors, G. A., Davis, L., Jr. and Adams, A., Jr., in Semiconductor Surface Physics, ed. by Kingston, R. H., Univ. of Penna. Press, Philadelphia (1957) pp. 143-144.

43. Weisz, P. B., in Semiconductor Surface Physics, ed. by Kingston, R. H., University of Pennsylvania Press, Philadelphia, Pa., (1957), p. 252.
44. Ibid. pp. 249, 251.
45. Bewig, K. W. and Zisman, W. A., in Solid Surfaces and the Gas-Solid Interface, Advances in Chemistry Series No. 33, A. C. S., Washington, D. C. (1961), p. 101.
46. Sears, F. W., Optics, Addison-Wesley Publ. Co., Inc., Reading, Mass., 3rd Edition (1958), p. 203.
47. Daniels, F., Mathews, J. H., Williams, J. W., Bender, P., Murphy, G. W. and Alberty, R. A., Experimental Physical Chemistry, McGraw-Hill Book Co., Inc., New York (1949), p. 276.
48. Weyl, W. A., A New Approach to Surface Chemistry and Heterogeneous Catalysis, Penn. State College Bulletin, XLV, No. 25, p. 31 (1951).
49. Pustinger, J. V., Jr., Hodgson, F. N. and Ross, W. D., Identification of Volatile Contaminants of Space Cabin Materials, Aerospace Medical Division, Air Force Systems Command, Wright-Patterson Air Force Base, Ohio, AMRL-TR-66-53, June 1966.
50. Byrd, N. R., Space Cabin Atmosphere Contaminant Measurement Techniques, Quarterly Progress Report SM-48446-Q7, Contract NAS 12-15, Aug. 1967.
51. Eley, D. D. and Inokuchi, H., Z. Elektrochem. 63, 29 (1959).
52. Pohl, H. A. and Chartoff, R. P., J. Polymer Sci., Part A, 2, 2787 (1964).
53. Rembaum, A. and Moacanin, J., Polymeric Semiconductors, Jet Propulsion Laboratory, Pasadena, Calif., 1964.
54. Pohl, H. A., Rembaum, A. and Henry, A., J. Am. Chem. Soc. 84, 2699 (1962).
55. Ioffe, A. F., Physics of Semiconductors, Academic Press, Inc., New York (1960) pp. 121 and 252.
56. Schockley, W., Electrons and Holes in Semiconductors, D. Van Nostrand, Co., Inc., Princeton, N. J. (1950), p. 223, et seq.
57. Alonso, M. and Finn, E. J., Fundamental University Physics, Vol. II, Addison-Wesley Publishing Co., Reading, Mass. (1967), p. 438.
58. Gutmann, F. and Lyons, L. E., Organic Semiconductors, John Wiley and Sons, Inc., New York (1967), p. 495.

59. Rosenberg, B., J. Chem. Phys. 36, 816 (1962).
60. Progress in Semiconductors, ed. by Gibson, A. F., John Wiley and Sons, Inc., New York (1960), Vol. 5, p. 3.
61. Bardeen, J. in Handbook of Physics, ed. by Condon, E. and Odishaw, H., McGraw-Hill Book Co., New York (1958), p. 8-61.
62. Sax, N.I., Dangerous Properties of Industrial Materials, Reinhold Publishing Corp., New York, 1967, pp 1146-1147.



APPENDIX A

CHARGE-TRANSFER COMPLEXES

Appendix A
CHARGE-TRANSFER COMPLEXES

It is one thing for a polymer to have a high degree of conjugation for conduction along the backbone; however, this type of conductivity, especially for inter-chain effects, can be considerably enhanced with charge-transfer complexes. By-and-large, the greatest number of investigations in organic semi-conductors has been with charge-transfer-complexes — either simple organic or polymeric^(A1-A4).

In conjugated polyenes, the electron and/or hole migration in an electric field, i. e., the charge carrier, is an intrinsic property of the molecule. In charge transfer complexes, this is not the case. These systems are comprised of mixtures of compounds that are separately insulators, but when combined in a particular ratio demonstrate enhanced conductivity due to an induced delocalization and increased mobility of electrons. For example, anthracene-iodine, p-phenylenediamine-chloranil, quinoline (as the quinolinium ion)-tetracyanoquinodimethan (TCNQ) complexes, and others are representative of the simple organic type of charge-transfer complex, and whose electrical conductivities are as much as six to nine orders of magnitude higher than those of the organic compounds from which they were derived. In all instances, they have involved the combination of compounds that are electron donors and electron acceptors. Among the types of molecular electron acceptors exhibiting the greatest complexing behavior are two similar materials — tetracyanoethylene (TCNE) and the aforementioned TCNQ.

For weak donors and acceptors, the molecular complex AD is formed by ion bonding van der Waals type forces and is, at first approximation, a singlet state with a slight admixture of a state in which electron transfer takes place giving rise to an ionic compound of the type A^-D^+ . The adduct AD has

a characteristic optical absorption spectrum which is found in neither the donor nor acceptor molecule alone. The electron transfer process is assumed to be responsible for the optical absorption which leads to the first excited level in which the contribution of the ionic state is greater. In a case where the molecules in the complex AD have sufficient donating and accepting power, electron transfer can take place in the ground state. Then the system, besides having characteristic optical absorption, will show paramagnetic behavior and free radical characteristics.

In quantum mechanical terms ^(A5) the wave function of the ground state of the molecular compound AD can be written as

$$\Psi_T = a \Psi_0 + b \Psi_1 + \dots \quad (1)$$

where Ψ_0 is a non-bond wave function $\Psi(A, B)$ which has the form $\Psi_0 = \Psi(A, B) = \alpha \Psi_A \Psi_B$ and is antisymmetric in all the electrons.

The wave function Ψ_1 corresponds to the electron transfer from B to A in the complex such as $\Psi_1 = \Psi(A^-, B^+) + \dots$. The $+$ sign indicates additional terms in $c \Psi_2 + \dots$. However, here the Ψ_T will be approximated by the first two terms alone.

By normalizing Ψ_T so that $\int \Psi_T^2 dv = 1$, the coefficients a and b can be related by

$$a^2 + 2ab S + b^2 = 1 \quad (2)$$

where

$$S = \int \Psi_0 \Psi_1 dv$$

For loose complexes, second-order perturbation theory gives a good approximation. Thus,

$$W_T = \int \Psi_T H \Psi_T dv$$

$$\approx W_0 - \frac{(H_{01} - SW_0)^2}{(W_1 - W_0)} + \dots \quad (3)$$

where

$$W_0 \equiv \int \Psi_0 H \Psi_0 \, dv; \quad W_1 \equiv \int \Psi_1 H \Psi_1 \, dv$$

and $H_{01} \equiv \int \Psi_0 H \Psi_1 \, dv$

H is the exact Hamiltonian operator for the nuclei and electrons in the system.

W_0 is equal to the sum of separate energies of A and B, modified by any energy of attraction arising from the interaction of A and B molecules. W_1 includes the attraction energy of ionic and covalent bonding.

Then the energy of formation, Q , of the AB complex is given by

$$Q = (W_A + W_B) - W_T = (W_A + W_B - W_0) + (W_0 - W_T) \quad (4)$$

Assuming that there will be an excited state, the appropriate wave function will be

$$\Psi_E = a^* \Psi_1 - b^* \Psi_0 + \dots$$

$$a^* \approx a; \quad b^* \approx b \quad (5)$$

and $a^{*2} - 2a^*b^*S + b^{*2} = 1 \quad (6)$

and using the approximation of the second-order perturbation theory

$$W_E = W_1 + \frac{(H_{01} - SW_1)^2}{(W_1 - W_0)} + \dots \quad (7)$$

The frequency of the absorption for the molecular complex is given by

$$h\nu = W_E - W_T = W_1 - W_0 + \frac{(H_{01} - SW_1)^2 + (H_{01} - SW_0)^2}{(W_1 - W_0)} \quad (8)$$

Then the strong absorption spectrum can be assigned to the $\Psi_T \rightarrow \Psi_E$ transition.

Further, one can write

$$W_1 - W_0 = I_B - E_A - (e^2/r) + C_{AB} \quad (9)$$

where I_B is the ionization energy of molecule B, E_A is the electron affinity of the A and e^2/r is the coulomb energy of the excited state with a separation of charge equal to r, and C_{AB} is the difference in energy in the non-bond and ionic bond forms.

The frequencies of the absorption spectrum for several molecular complexes have been found to be in good agreement with the predicted values according to the above theory.

In the case of very strong acceptors, complete electron transfer could occur, and the system becomes paramagnetic in its ground electronic state. For the system in the solid state, charge-transfer interactions are extensive and provide an electron conduction mechanism.

One of the most interesting features of these organic charge-transfer complexes is the semiconduction characteristics found in several systems; the hydrocarbon-halogen complexes ^(A6) are representative of these systems. These systems are good semiconductors and show strong electron paramagnetic resonance absorption. A detailed study of the EPR characteristics resulted in a complete elucidation of the electronic structure of the complexes and also a correlation between the electrical and magnetic properties. For example, the agreement between the activation energies of spin concentration and conduction for the hydrocarbon-halogen systems

indicated that the unpaired electrons (responsible for the EPR absorption) are the charge carriers in these semiconductors. It has been shown rather clearly that EPR techniques are very useful in studying these systems.

In the case of hydrocarbon-halogen systems, a delocalized π electron from the hydrocarbon goes over to a vacant antibonding orbital in the halogen (iodine) molecule. This charge transfer results in the formation of two radical molecular ions. Since these species show EPR absorption, one can perform a detailed study on these systems and hopefully understand the electrical and magnetic properties. Stamires^(A7, A8) has done an extensive amount of work in the area of charge-transfer complexes using EPR techniques. In some cases, a hyperfine structure was resolved and radical ions completely characterized, i. e., triphenylamine (donor) - I₂ (acceptor), or other amines such as diazabicyclo (2.2.2) octane (N(CH₂CH₂)₃N) with other acceptors, such as, halogens, tetracyanoethylene or chloranil. It appears to be a logical continuation of these types of measurements, therefore, that one studies electron transfer reactions between various type of amines and unsaturated conjugated polymeric systems. Amines, in general, are considered good donors.

REFERENCES

- A1. Kronick, P. L. and Labes, M. M., in Organic Semiconductors, ed. by Brophy, J. S. and Buttrey, J. W., The Macmillan Co., New York (1962), p. 36.
- A2. Kepler, R. G., Bierstedt, P. E. and Merrifield, R. E., Ibid., p 45.
- A3. Menefree, E. and Pao, Yoh-Han, Ibid., p. 49.
- A4. Sehr, R., Labes, M. M., Bose M., Ur, H. and Wilhelm, F., in Symposium on Electrical Conductivity in Organic Solids, ed. by Kallmann, H. and Silver, M., Interscience Publishers, New York (1961), p. 309.
- A5. Mulliken, R. S., J. Am. Chem. Soc. 74, 811 (1952).
- A6. Singer, L. S. and Kommandeur, J., J. Chem. Phys. 34, 133 (1961).
- A7. Stamires, D. N. and Turkevich, J., J. Am. Chem. Soc. 85, 2557 (1961).
- A8. Ibid., 86, 749 (1964).

APPENDIX B

ORGANIC SEMICONDUCTORS WITH PN-JUNCTION
DEVICES FOR GAS DETECTION

Appendix B
ORGANIC SEMICONDUCTORS WITH PN-JUNCTION
DEVICES FOR GAS DETECTION

B.1 INTRODUCTION

The detection and identification of ambient gas phases in closed environments, by a sensitive means is an acute and pressing technological problem. Of particular importance are the detection and identification of toxic gas components in crew compartments of aerospace vehicles, and of gaseous byproducts of undesired chemical reactions indicating malfunctioning power plants or fuel containers.

A promising approach to gas detection and identification, which could lead to a sensitive and compact device, has been investigated. The method relies on the reversible and specific adsorption of gas on thin films of organic solids and the consequent change in the density of electronic charge carriers (electrons or holes). This effect results from the electronic interaction (i. e. charge transfer) between the gas phases and the surface of the solid. It can serve as the basis for a device in two different ways: (1) The variation of charge carrier density as a source of current change (when a voltage is applied) allows one to detect gas phases by means of current readings, and (2) the variation of charge density as cause of capacity change allows gas detection by means of capacity readings.

However, direct capacitance or current measurements on the organic films are either inaccurate or difficult in practice because of the low dielectric constant and high resistivity of these substances. To overcome these difficulties, the films must be used in a device that allows amplification of the variations in charge resulting from the reversible gas adsorption.

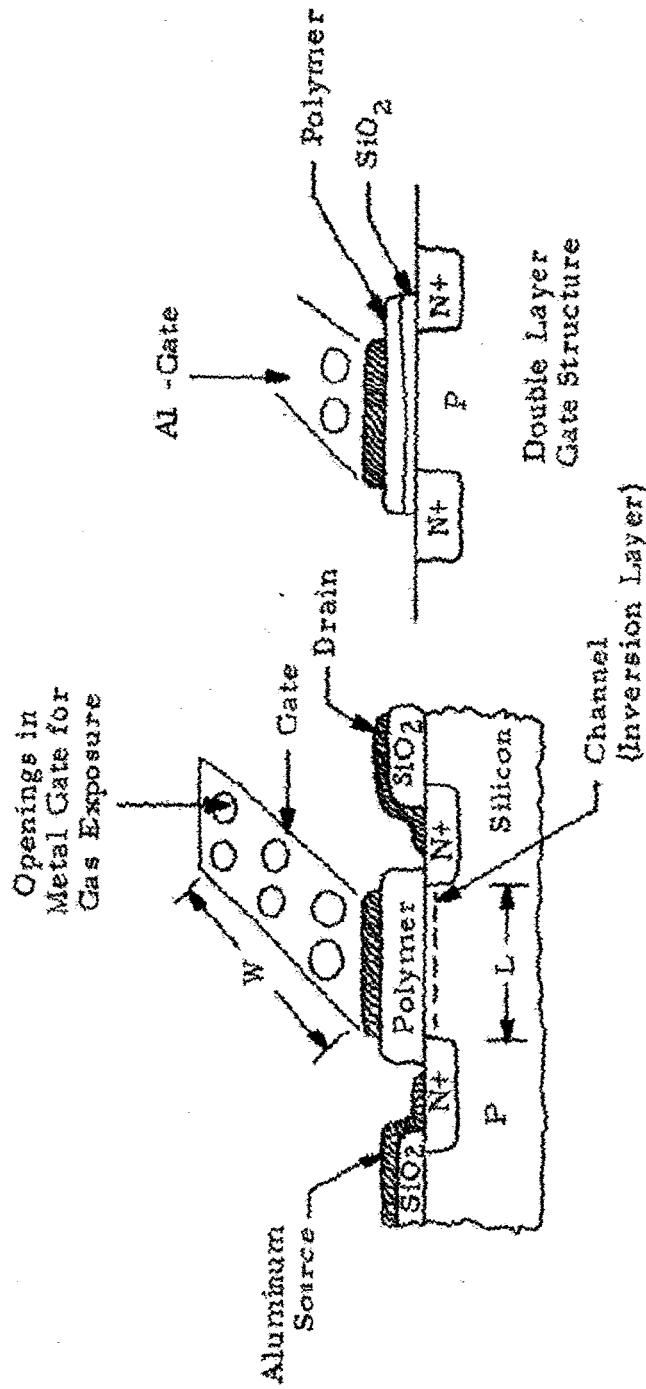
One possibility is the combination of organic film and p-n junction of a silicon diode with the diode biased in reverse. In this arrangement the high resistance reverse current path of the diode is paralleled by the more or less conductive sheet of the adsorbing organic film. Another configuration, utilizing and amplifying the capacitive variations in the film rather than the resistivity changes, is obtained by using the films in combination with metal oxide silicon field effect transistors. In this case the capacitive changes in the film are utilized to modulate the source-drain current of the field effect transistor. This concept appears to be very promising because of its high gain characteristics.

B.2 METAL-ORGANIC-SILICON FIELD EFFECT TRANSISTOR – A NEW APPROACH TO GAS DETECTORS

Employing the metal-polymer-oxide-semiconductor properties, a new device was conceived which should be very sensitive as a gas sensor. This device makes use of the surface conduction in an inversion layer of the semiconductor which can be controlled by altering the charge density in the polymer. No current passage is required in the polymer to enhance the current flow in the surface inversion layer. The basic structure of this device is that of a metal-oxide-transistor (MOST), where the dielectric gate is substituted by the polymer (Figure B-1). A double layer structure is advantageous with oxide and polymer insulating layer to prevent chemisorption effects. The PN-junctions are used here to terminate and confine the channel to the area $W \times L$.

The voltage-current characteristics of the insulated-gate field effect gas sensor device can be readily derived from standard MOST theory. The output current of the device is given by

$$I_D = \frac{\mu C_H W}{2 L T} (V_T - V_G)^2 \quad (1)$$



4582/

Figure B-1. Polymer-Modified Form of Basic MOST Device

where

- μ_{ch} = channel mobility
- W = channel width
- L = length
- T = thickness of insulator (polymer)

and

$$V_T = \frac{f N_{sst}}{E_p E_o} \quad (2)$$

where

- f = electron charge
- N_{ss} = surface states/cm²
- E_p = dielectric constant of polymer

If the applied voltage $V_G = 0$ and V_T is positive, which requires negative charges in the semiconductor and positive charges in the polymer, then the quiescent and steady state current is equal to

$$I_{Do} = \frac{\mu_{CH} W}{2 L t} V_T^2 \quad (3)$$

Inserting (2) into (3) yields

$$I_{Do} = \frac{\mu_{CH} W q^2 t N_{ss}^2}{2 L (E_p E_o)^2} \quad (4)$$

Equation (4) indicates that the proposed device is active and has a gain, since by changing N_{ss} by 10, a current variation of 100 is produced. From normal conductivity modulation one would expect no gain, since

$$I \propto \sigma = q N_{ss} \mu \quad (5)$$

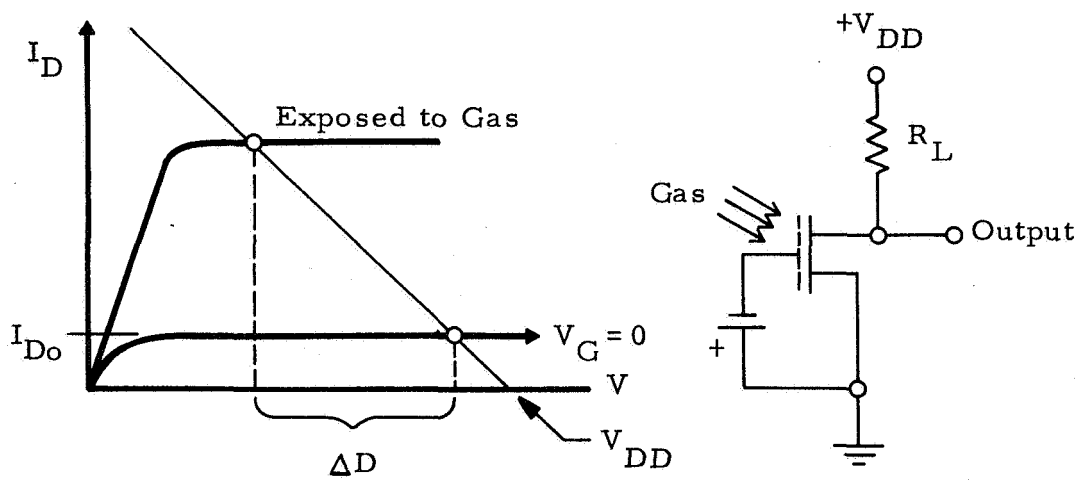
In addition, it is of advantage that the device can be operated as a voltage amplifier with a gain of

$$A_v = g_m R_L \quad (6)$$

where the transconductance

$$g_m = \frac{d I_D}{d V_G} \quad (7)$$

Gain is then provided, if the condition $R > \frac{1}{g_m}$ can be met. The device characteristics with load line and the amplifier circuit is shown in Figure B-2.



3822

Figure B-2. MOST Device Characteristics with Load Line and Amplifier Circuit

APPENDIX C

ANALYSIS OF THE PORTABLE GAS DETECTOR

Appendix C
ANALYSIS OF THE PORTABLE GAS DETECTOR

In the development of a portable gas detector, based upon an organic semiconductor as a sensor, there are many factors involved in its modus operandi. Most important of these are the resistivity of the polymeric semiconductor and the circuitry used to amplify the response. At present, there is little that can be done to increase the conductivity other than to develop a new series of polymers. However, working with poly(phenylacetylene) and its derivatives, e. g., the nitro, formamido and amino polymers, the high resistivity materials can be accommodated by modifying the amplifying circuitry.

Looking at the input stage of the portable gas detector, as shown in Figure C-1, it is found to consist of two identical amplifier stages connected for a differential output. The transistors are General Instrument MEM520, metal oxide silicon insulated gate field effect transistors (IGFET). They were selected because of their resistance specifications, i. e., R_{GS} , the resistance from gate-to-source, and R_{DSS} , the resistance from drain-to-source with no voltage applied to the gate; both values are chosen as high as possible.

Figure C-2 is an equivalent circuit for the input to one half of the differential amplifier. The relationship between the voltage drop, E_S , across the gas sensor, the input voltage, E_i , the resistance of the gas sensor, R_S , and the equivalent resistance of R_i , of R_{DSS} and R_{GS} in parallel is given, by Ohm's Law:

$$\frac{E_S}{E_i} = \frac{R_S}{R_i} \quad \text{where } R_i = \frac{(R_{GS})(R_{DSS})}{R_{GS} + R_{DSS}} \quad (1)$$

For the MEM520, $R_{GS} \approx 10^{15}$ ohms and $R_{DSS} \approx 4 \times 10^{10}$ ohms, and since R_{GS} is much larger than R_{DSS} it may be neglected.

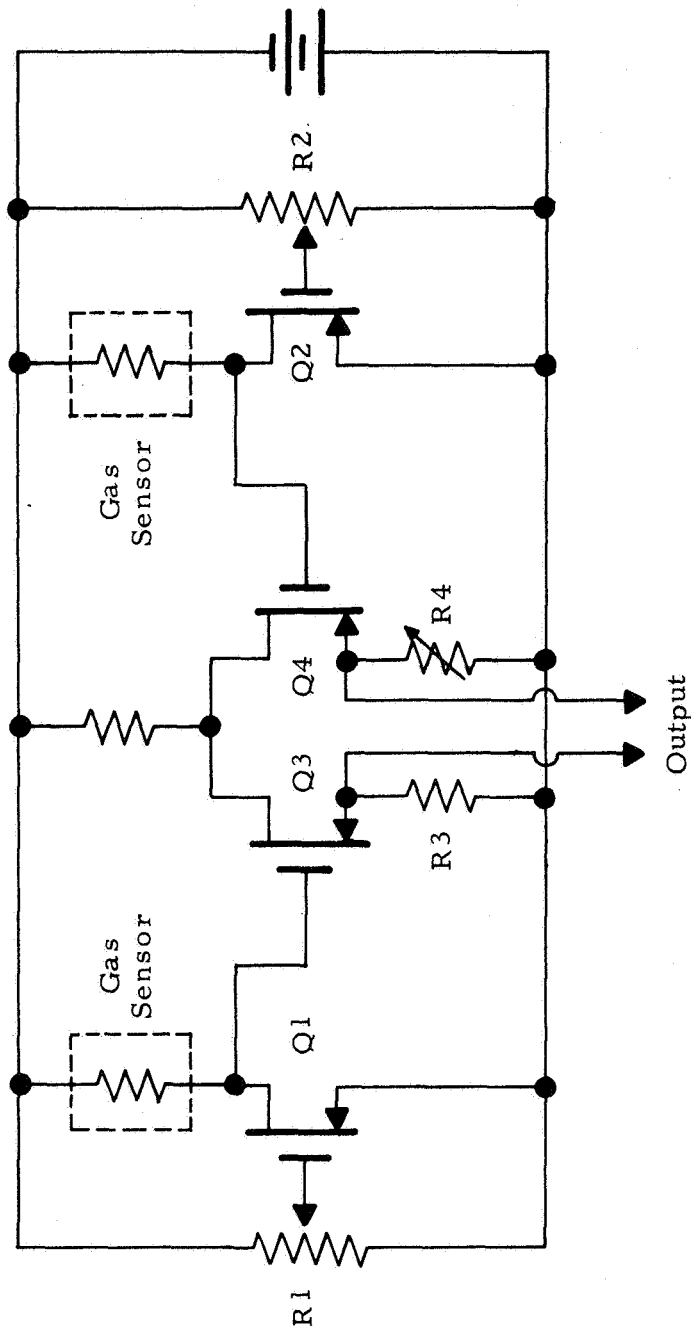
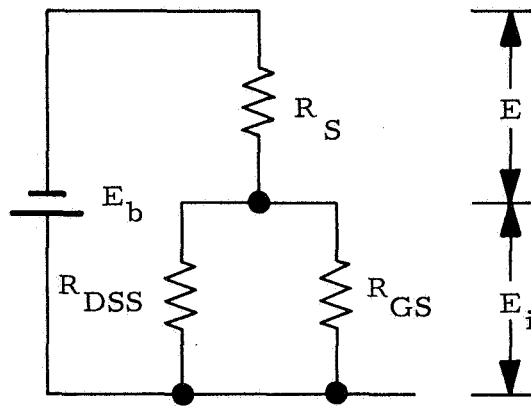


Figure C-1. Circuitry Schematic of the Differential Amplifier and Gas Detector

C3777

R_S = Resistance of Sensor



c3823

Figure C-2. Equivalent Circuit For the Input Stage to One Half of the Differential Amplifier

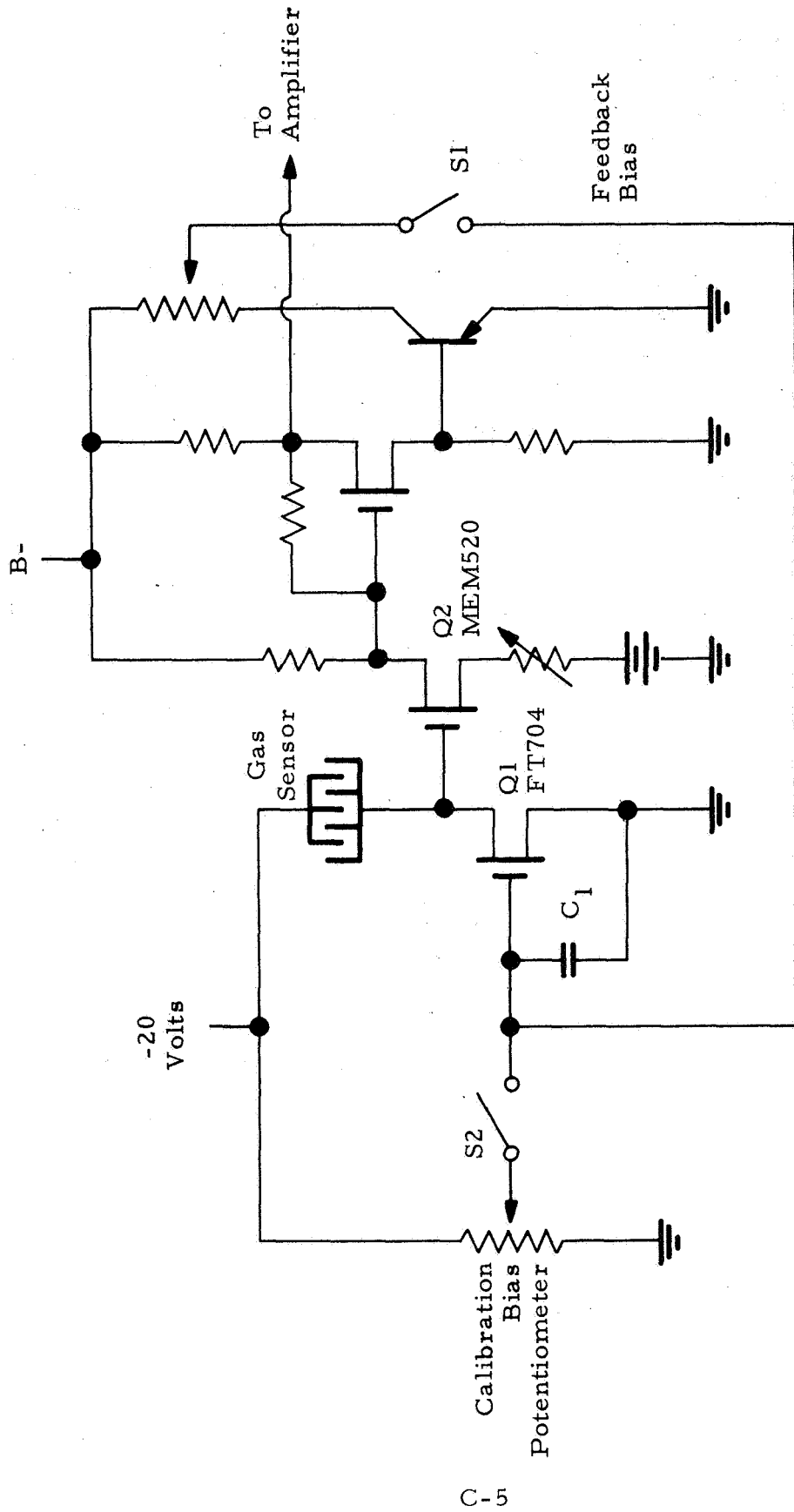
The amplifier was designed to operate at a gate potential of 10 volts, and the power supply applies 20 volts across the network. Thus, the value of R_S may be determined as follows:

$$R_S = R_i \frac{E_S}{E_i} = 4 \times 10^{10} \times \frac{20 - 10}{10} = 4 \times 10^{10} \text{ ohms} \quad (2)$$

This, therefore, gives the maximum resistance the sensor may have using an MEM520 for Q1. R_{DSS} is controlled by the voltage on its gate and may take smaller values, but the upper limit is determined by the geometry of the device.

As mentioned earlier, the resistivities of most of the polymers presently being considered are either too high or are borderline values. However, it has been observed that water vapor does effect a pronounced change in the resistivity of the polymer. When the polymers were being evaluated for their gas response characteristics, under vacuum conditions, an electrometer was used to measure these responses. In the portable gas detector, an electrometer was not used. Thus, to bring the polymer's resistivity into a region where it could be measured in this device, the signal amplification was a necessary factor in the design. However, since the portable detector was being operated in a laboratory ambience, the moisture normally present in the atmosphere could make a contribution to bringing the resistivity down to a level where it could be measured by the instrumentation of the portable detector. Even under these circumstances, though, the poly(phenylacetylene) did not come down to a measurable value. The amino polymer is well within the region of the instrument's capability, but for the nitro polymer, if the relative humidity was below 40%, the resistance was above the maximum allowable value. Therefore, in order to use all the polymers prepared, under all conditions, it is necessary to raise the maximum usable value of R_S . This can be done in one of two ways: (1) raise the value of E_S/E_i , or (2) raise the value of R_{DSS} .

Redesign of the amplifier permits the use of gate potentials on the order of 0.1 volt, as shown in Figure C-3. A new IGFET, the FT704, is being produced by Fairchild Semiconductor that offers an R_{DSS} of 1.5×10^{12} ohms.



C3219

Figure C-3. Schematic for Input Stage of Second Generation Portable Gas Detector

Substituting these values into Equation (2) gives $R_S \approx 3 \times 10^{14}$ ohms. However, if only the transistor were changed, and the present circuitry used, i. e., replacing Q1 with an FT704, then R_S will have a maximum value of 1.4×10^{12} ohms. Thus, even this value of R_S , which is two orders of magnitude better than is possible in the present design of the detector (see Equation 2), will be sufficient to demonstrate the feasibility of using the organic polymers to build a practical gas detector. Of course, it should be borne in mind that using a combination MOS-organic polymer device as a sensor would greatly increase the sensitivity of the system.

APPENDIX D

NEW TECHNOLOGY DISCLOSURE
GAS DETECTION DEVICES

Appendix D
NEW TECHNOLOGY DISCLOSURE
GAS DETECTION DEVICES

A gas detection device has been reported in contractor's docket No. R-3569 and will be found described in pages 132-142 and 164-168.